nature chemistry

SUPPLEMENTARY INFORMATION

https://doi.org/10.1038/s41557-020-0487-3

In the format provided by the authors and unedited.

Synthesis and characterization of crystalline niobium and tantalum carbonyl complexes at room temperature

W. Unkrig, M. Schmitt, D. Kratzert, D. Himmel and I. Krossing ✉

Institut für Anorganische und Analytische Chemie, Albert-Ludwigs-Universität Freiburg, Freiburg, Germany. ✉e-mail: krossing@uni-freiburg.de

Supplementary Materials for

Synthesis and characterization of crystalline niobium and tantalum carbonyl complexes at room temperature

Authors: W. Unkrig, M. Schmitt, D. Himmel, D. Kratzert, I. Krossing*

* Correspondence to: krossing@uni-freiburg.de

This PDF file includes:

Figs. 1 to 43 and Tables 1 to 17

1 Abbreviations 3

2 Material and Methods 4

Techniques and Instruments 4

Vibrational Spectroscopy 4

NMR-Spectroscopy 5

Single Crystal X-ray Diffraction 6

UV/Vis Spectroscopy 6

Computational Details 7

3 Detailed Synthesis of Compounds 1, 2, 4, 5 and 6 8

Discussions of the Yields Compounds 1, 2, 4 and 5 11

4 Structural Discussions of Compounds 1 - 6 13

$[M(CO)_7]^+[Al(OC(CF_3)_3)_4]^-$ (M = Nb (**1**), Ta (**2**)) 13

$[Ag_6\{Nb(CO)_6\}_4]^{2+}$ 2$[Al(OC(CF_3)_3)_4]^-$ (**3**) 16

$[(o\text{-dfb})M(CO)_4]^+[Al(OC(CF_3)_3)_4]^-$ (M = Nb (**4**), Ta (**5**)) 18

$Ta_2(CO)_{12}$ (**6**) 19

5 Detailed Vibrational Analysis 24

IR and Raman Data of $[M(CO)_7]^+[Al\{OC(CF_3)_3\}_4]^-$ (M = Nb (**1**), Ta (**2**)) 24

IR and Raman Data of $[(o\text{-dfb})M(CO)_4]^+[Al\{OC(CF_3)_3\}_4]^-$ (M = Nb (**4**), Ta (**5**)) 27

6 ^{93}Nb NMR Spectra of the Temperature and CO Pressure Dependent Equilibrium of $[Nb(CO)_7]^+[Al\{OC(CF_3)_3\}_4]^-$ (1) and $[(o\text{-dfb})Nb(CO)_4]^+[Al\{OC(CF_3)_3\}_4]^-$ (4) 33

7 Computational Details on Relaxed Potential Energy Scan Along $C_{3v} \rightarrow C_{2v} \rightarrow C_{3v}$ Path with Varying Point Charges 0 - –0.7 *e* 34

8 UV/VIS Spectra of 2, 4 and 5 36

9 Single-Crystal Diffraction Results for Compounds 1 - 6 37

10 Full Details to the Single-Crystal Structure Determinations 39

11 Full NMR Characterization of 1, 2, 4, 5 47

12 Computational Details to the Structure Determination 57

13 Computational Details on Gas Phase DFT Studies 59

14 References to the Supporting Materials 83

1 Abbreviations

o-dfb = *ortho*-difluorobenzene, 1,2-$F_2C_6H_4$

4FB = 1,2,3,4-tetrafluorobenzene, 1,2,3,4-$F_4C_6H_2$

$[Al(OR^F)_4]^-$ = $[Al\{OC(CF_3)_4\}_4]^-$

FWHM = full width half maximum (NMR spectroscopy)

TMCC = transition metal carbonyl cation

WCA = weakly coordinating anion

Compounds:

1 $[Nb(CO)_7]^+[Al(OR^F)_4]^-$; **1**$^+$ $[Nb(CO)_7]^+$

2 $[Ta(CO)_7]^+[Al(OR^F)_4]^-$; **2**$^+$ $[Ta(CO)_7]^+$

3 $[Ag_6\{Nb(CO)_6\}_4]^{2+}[Al(OR^F)_4]^-_2$; **3**$^{2+}$ $[Ag_6\{Nb(CO)_6\}_4]^{2+}$

4 $[(o\text{-dfb})Nb(CO)_4]^+[Al(OR^F)_4]^-$; **4**$^+$ $[(o\text{-dfb})Nb(CO)_4]^+$

5 $[(o\text{-dfb})Ta(CO)_4]^+[Al(OR^F)_4]^-$; **5**$^+$ $[(o\text{-dfb})Ta(CO)_4]^+$

6 $Ta_2(CO)_{12}$

2 Material and Methods

The methods and techniques established in our group were used [29,56]. Due to minor deviations, however, these were described again in detail here.

Techniques and Instruments

All reactions were carried out in an inert atmosphere using standard vacuum and Schlenk techniques and a glovebox filled with Ar. Special double-Schlenk flasks [57] separated by a G3 or G4 frit and sealed with grease-free teflon or glass valves and Rettberg NMR tubes were used for most of the manipulations. Pentane was dried using a conventional MBraun Grubbs apparatus, while *ortho*-difluorobenzene ($F_2C_6H_4$, *o*-dfb, abcr) and 1,2,3,4-tetrafluorobenzene ($F_4C_6H_2$, 4FB, Fluorochem) were dried over CaH_2 and distilled afterwards. Besides the general practice, 4FB was stirred for 24h with $Ag[Al(OR^F)_4]$ at room temperature to remove traces of benzene and other fluorobenzenes and condensed subsequently. Consequently, the solvent was contaminated with $HOC(CF_3)_3$, but as the alcohol is formed in low quantity (<1 %) in each reaction anyway, it had no influence to the reaction. All solvents were degassed before used and stored over molecular sieves (4 Å). $[NEt_4]^+[M(CO)_6]^-$ (M = Nb, Ta) and $Ag[Al(OR^F)_4]$ (commercially available at www.iolitec.de) were synthesized according to literature [39,58].

Vibrational Spectroscopy

IR spectra (range: 4000-550 cm^{-1}, resolution: 2 cm^{-1}, 64 scans, r.t.) were recorded in the glovebox on a Bruker ALPHA FT-IR spectrometer equipped with an Eco-ZnSe-ATR module. FT Raman measurements (range: 4000-50 cm^{-1}, resolution: 4 cm^{-1}, r.t.) were recorded on a Bruker VERTEX 70 spectrometer equipped with a RAM II module (1064 nm exciting line of a Nd-YAG laser) by using a highly sensitive L-N_2 cooled Ge detector. The Bruker OPUS 7.5.18 software was used to collect, evaluate and edit the vibrational spectra. Unless otherwise noted, the spectra were baseline corrected (default parameters, 1 iteration). All IR and Raman spectra were normalized to 100 (%) and intensities are given as follows: vw = very weak (< 0.2), w = weak (< 0.4), m = medium (< 0.6), s = strong (< 0.8), vs = very strong (≥ 0.8), sh = shoulder, br = broad. Graphical representations were visualized with OPUS or OriginPro (version 9.2). Only bands that can be assigned to the desired products, the co-product or solvents were detected. Bands caused by the co-product $[NEt_4]^+[Al(OR^F)_4]^-$ or solvents are shown below. Raman bands of perfluoropolyalkylether oil in measured samples were indistinguishable from background.

$[NEt_4]^+[Al(OR^F)_4]^-$:

FTIR (ZnSe): ν [cm^{-1}] = 3018 (vw), 3012 (vw), 3000 (vw), 1487 (vw), 1458 (vw), 1444 (vw), 1399 (vw), 1352 (w), 1297 (w), 1272 (s), 1249 (m), 1240 (s), 1209 (vs), 1161 (s), 1068 (vw), 1052 (vw), 998 (vw), 969 (vs), 832 (w), 782 (vw), 756 (vw), 726 (vs), 636 (vw), 571 (vw), 561 (w).

FT Raman (3000 scans, 120 mW): ν [cm^{-1}] = 3003 (s), 2968 (s), 2952 (m), 2905 (vw), 2885 (vw), 2780 (vw), 2759 (vw), 2570 (vw), 1989 (vw), 1490 (vw), 1465 (s), 1396 (vw), 1368 (vw), 1300 (m), 1273 (w), 1235 (vw), 1214 (vw), 1173 (vw), 1140 (vw), 1117 (w), 1068 (vw), 999 (w), 977 (vw), 904 (vw), 891 (vw), 833 (vw), 798 (vs), 747 (vs), 672 (w), 571 (w), 562 (w), 538 (m), 447 (vw), 417 (s), 322 (s), 288 (w), 233 (w), 206 (vw), 170 (vw), 118 (w), 99 (w), 84 (w).

1,2,3,4-$F_4C_6H_2$:

FTIR (ZnSe): ν [cm^{-1}] = 3097 (vw), 2310 (vw), 1845 (vw), 1792 (vw), 1728 (vw), 1633 (vw), 1609 (vw), 1507 (vs), 1438 (vw), 1398 (vw), 1327 (w), 1313 (vw), 1266 (vw), 1236 (m), 1160 (w), 1093 (vw), 1045 (s), 982 (vs), 962 (w), 861 (vw), 800 (m), 745 (m), 729 (vw), 681 (m), 604 (vw), 593 (w).

1,2-$F_2C_6H_4$:

FTIR (ZnSe): ν [cm^{-1}] = 3077 (vw), 2030 (vw), 1943 (vw), 1902 (vw), 1776 (vw), 1618 (vw), 1603 (vw), 1581 (vw), 1556 (vw), 1526 (vw), 1503 (s), 1469 (vw), 1455 (vw), 1402 (vw), 1291 (vw), 1266 (s), 1205 (vw), 1194 (vw), 1152 (vw), 1101 (w), 1024 (vw), 931 (vw), 905 (vw), 855 (vw), 841 (vw), 745 (vs), 566 (vw).

NMR-Spectroscopy

NMR spectra were measured in NMR tubes with J. Young or Rettberg valves on a Bruker Avance II+ 400 MHz, on a Bruker Avance III HD 300 MHz or on a Bruker Avance 200 MHz spectrometer. All low temperature measurements started at –30 °C and were allowed to warm up stepwise to room temperature. The solvent used was either *ortho*-difluorobenzene ($F_2C_6H_4$, *o*-dfb, abcr) or 1,2,3,4-tetrafluorobenzene ($F_4C_6H_2$, 4FB, Fluorochem). All spectra were calibrated by using the ^1H signal of the solvent (*o*-dfb: δ = 6.97 ppm, rel. to TMS, 4FB: δ = 6.97 ppm, rel. to TMS). All spectra were measured under CO pressure slightly above atmospheric pressure due to stability particularly important for compounds **1** and **4**. Chemical shifts of the solvents, the co-product and impurities are listed below. The Bruker Topspin software package (version 3.5 or 4.0.6) was used for measuring and processing spectra. Typically very small impurities (<1 %) of $HOC(CF_3)_3$ were detected in the ^{19}F NMR at –76.8 ppm.

Chemical shifts of the solvents, the co-product and impurities

$[NEt_4]^+$:

^1H NMR (400.17 MHz, $F_4C_6H_2$, 298 K): δ = 3.77 (q, 8H, CH_2, $^3J_{HH}$ = 7.29 Hz), 1.85 (tt, 12H, CH_3, $^1J_{HH}$ = 1.85, $^3J_{HH}$ = 7.29 Hz) ppm.

^{13}C NMR (100.62 MHz, $F_4C_6H_2$, 298 K): δ = 54.3 (t, 4C, CH_2, $^1J_{CN}$ = 3.02 Hz), 7.98 (s, 4C, CH_3) ppm.

CO_{free}:

^{13}C NMR (100.62 MHz, $F_4C_6H_2$, 298 K): δ = 185.8 (s, CO) ppm.

1,2,3,4-$F_4C_6H_2$:

^{1}H NMR (400.17 MHz, TMS, 298 K): δ = 7.06 - 6.86 (m, 2H, CH) ppm.

^{19}F NMR (376.54 MHz, 298 K): δ = –141.5 - –141.8 (m, 2F, CF), –158.7 – 159.0 (m, 2F, CF) ppm.

^{13}C NMR (100.62 MHz, $F_4C_6H_2$, 298 K): δ = 151.0 - 150.5 (m, 2C, CF), 148.5 - 148.1 (m, 2C, CF), 112.5 - 111.9 (m, 2C, CH) ppm.

1,2-$F_2C_6H_4$:

^{1}H NMR (400.17 MHz, TMS, 298 K): δ = 7.03 - 6.85 (m, 4H, CH) ppm.

^{19}F NMR (376.54 MHz, 298 K): δ = –139.3 - –139.5 (m, 2F, CF) ppm.

Side products of **4**, probably caused by minor impurities of *o*-dfb:

^{93}Nb NMR (97.95 MHz, $F_4C_6H_2$, 298 K): δ = –1486.2 (s), –1547.1 (s) ppm.

Single Crystal X-ray Diffraction

Structural analysis of single crystals were carried out on a Bruker SMART APEX II Quazar CCD area detector diffractometer using a D8 goniometer with an Incoatec Mo-Microfocus Source IμS with mirror-monochromated Mo-Kα radiation (λ = 0.71073 Å) and equipped with an Oxford Cryosystem 800 low temperature device at 100 K. All crystals were selected under perfluoropolyalkylether oil (AB128330, ABCR GmbH & Co. KG) at about –30 °C in a nitrogen gas stream using a custom-built device and mounted on 0.1, 0.2 or 0.3 mm micromounts (M1-L19-100/200/300). The data was processed with APEX v2018.1-2, structures were solved by using SHELXT [59,60], integrated with SAINT (V8.34A) and refined with SHELXL [61] in the GUI software ShelXle [62]. For empirical absorption correction SADABS 2016/2 [63] was used. Disordered fragments were modeled with the DSR-tool [64,65]. All graphics of crystal structures were plotted with OLEX2 (version 1.2.10) [66]. All structures can be found in The Cambridge Crystallographic Data Centre at https://www.ccdc.cam.ac.uk/structures/ (CCDC 1909275 (**1**), CCDC 1909276 (**2**), CCDC 1909277 (**3a**), CCDC 1909279 (**3b**), CCDC 1909278 (**4**), CCDC 1909449 (**5**), CCDC 1909450 (**6a**), CCDC 1909274 (**6b**)).

UV/Vis Spectroscopy

UV/Vis reflectance spectra were measured at room temperature in a special sample holder with a quartz window to protect the solid powdered air and moisture sensitive samples from decomposition. The data was recorded on a Thermoscientific Evolution 600 spectrometer equipped with an integration sphere. The baseline was measured against Spectralon®.

Computational Details

Quantum chemical calculations were performed with the TURBOMOLE [67,68] (version 7.2) or ORCA (version 4.0.1.2) [69] program packages. The investigated molecular structures were optimized at the density functional theory (DFT) level and were run in redundant internal coordinates using the B3LYP [70–72] functional with the resolution-of-identity (RI) approximation [73–75] together with the basis set def2-TZVPP [76] and with dispersion correction (DFT-D3(BJ)) [77,78]. A fine integration grid (m4) and the default SCF convergence criteria (10^{-6} a. u.) were used.

All optimized structures were checked for minima and imaginary frequencies with the implemented module AOFORCE [79] and for proper spin occupancies using the implemented module EIGER.

To account for relativistic effects for the heavy elements Nb and Ta the corresponding scalar relativistic pseudo potentials of the Stuttgart/Cologne group (ECP28MWB for Nb and ECP60MWB for Ta) were used [80].

Based on these structures, single point calculations at the CCSD(T)/triple-ζ (def2-TZVPP) level plus extrapolation of the correlation energy with MP2 from triple-ζ to quadruple-ζ basis sets (def2-QZVPPD) were performed [81,82]. This compound method approximates CCSD(T)/def2-QZPPPD energies by the following formula and was abbreviated by this notation: CCSD(T)/TZ→QZD.

$$E_{comp} = E_{CCSD(T)/def2\text{-}TZVPP} + E_{MP2/def2\text{-}QZVPPD} - E_{MP2/def2\text{-}TZVPP} \approx E_{CCSD(T)/def2\text{-}QZVPPD} \quad (1)$$

Thermal contributions to reaction energies were calculated at the B3LYP-D3(BJ)/def2-TZVPP level with the FREEH module for standard conditions (298.15 K, 0.1 MPa) by the following formula.

$$H° = E_{comp} + E_{vrt} + RT \quad (2)$$

$$G° = H° - T \bullet S° \quad (3)$$

(Where E_{vrt}= sum of translational, rotational, and vibrational energy incl. zero point vibrational energy)

Raman scattering cross sections were calculated with the integrated modules EGRAD [83,84] and INTENSE. IR and Raman spectra were calculated at the B3LYP-D3(BJ)/def2-TZVPP level of theory (scaling factor: 0.968 [48]) and simulated with an FWHM of 10 cm^{-1}.

All calculations containing point charges were carried out in Cartesian coordinates [85,86] with tighter SCF convergence criteria of 10^{-8} a. u. and the vibrational analyses was performed with the implemented module NUMFORCE.

The ORCA program system was used to perform the relaxed potential energy scans at (RI-)BP86 [85,86] -D3(BJ)/def2-SVP [76] or B3LYP-D3(BJ)/def2-TZVPP levels of theory.

3 Detailed Synthesis of Compounds 1, 2, 4, 5 and 6

*Synthesis of **1***: $[NEt_4]^+[Nb(CO)_6]^-$ (0.050 g, 0.128 mmol, 1 eq) and $Ag[Al(OR^F)_4]$ (0.275 g, 0.256 mmol, 2 eq) were weighed in the glovebox each in one side of a double-Schlenk flask and dissolved in *o*-dfb or 4FB (each ca. 5 ml). Argon was removed and the flask was flooded with CO (3 bar). The solution of $Ag[Al(OR^F)_4]$ was transferred to the other side through the frit at –40 °C. The dark red suspension was stirred for 2 h at –40 °C and then stored at –28 °C over night to let the Silver settle. The red solution was filtered through the frit, pentane (ca. 10 ml) was added to the Ag^0 precipitate under a reverse flow of Argon, which was removed and the flask was flooded with CO (slightly above 1 bar). After 5 days $[Nb(CO)_7]^+[Al(OR^F)_4]^-$ was obtained as dark red crystals and the co-product $[NEt_4]^+[Al(OR^F)_4]^-$ as colorless crystals. Due to the sensitivity of the material, no yield can be given.

FTIR (ZnSe): ν [cm^{-1}] = 2167 (vw), 2116 (vw), 2092 (w), 2059 (m), 2043 (m), 1398 (vw), 1352 (w), 1297 (m), 1274 (s), 1242 (s), 1212 (vs), 1161 (m), 971 (vs), 831 (w), 782 (vw), 756 (vw), 726 (vs), 571 (vw), 561 (w).

FT Raman (in perfluoropolyalkylether oil, 100 scans, 100 mW, individual baseline correction): ν [cm^{-1}] = 2168 (s), 2122 (vs), 2095 (w), 2064 (m), 2047 (m), 1308 (vw), 1299 (vw), 1286 (vw), 1276 (vw), 1237 (vw), 1170 (vw), 1134 (vw), 1115 (vw), 979 (vw), 830 (vw), 797 (w), 746 (w), 563 (vw), 538 (vw), 355 (w), 323 (w), 289 (vw), 262 (vw), 235 (vw), 109 (vs).

^{19}F NMR (376.54 MHz, $F_4C_6H_2$, 243 K): δ = –77.1 (s, 36F, $C(C\mathbf{F}_3)_3$) ppm.

^{27}Al NMR (104.27 MHz, $F_4C_6H_2$, 243 K): δ = 36.2 (s, $\mathbf{Al}(OR^F)_4$) ppm.

^{13}C NMR (100.62 MHz, $F_4C_6H_2$, 243 K): δ = 206.2 (bs, **C**O, FWHM = 360 Hz), 121.2 (q, 12C, **C**F_3, $^1J_{CF}$ = 293 Hz) ppm.

^{93}Nb NMR (97.95 MHz, $F_4C_6H_2$, 243 K): δ = –1425.6 (s, **Nb**C) ppm.

*Synthesis of **2***: $[NEt_4]^+[Ta(CO)_6]^-$ (0.060 g, 0.125 mmol, 1 eq) and $Ag[Al(OR^F)_4]$ (0.269 g, 0.250 mmol, 2 eq) were weighed in the glovebox each in one side of a double-Schlenk flask and dissolved in *o*-dfb or 4FB (each ca. 5 ml). Argon was removed and the flask was flooded with CO (3 bar). The solution of $Ag[Al(OR^F)_4]$ was transferred to the other side through the frit at –40 °C. The orange suspension was stirred for 1h at –40 °C and was then allowed to warm up slowly to room temperature. The suspension was stirred over night at room temperature and stored another night without stirring to let the Silver settle. The bright orange solution was filtered through the frit, pentane (ca. 20 ml) was added to the Ag^0 precipitate under a reverse flow of Argon, which was removed again and the flask was flooded with CO (1.2 bar). After 3 days $[Ta(CO)_7]^+[Al(OR^F)_4]^-$ was obtained as bright orange crystals and the co-product $[NEt_4]^+[Al(OR^F)_4]^-$ as colorless crystals (0.266 g, 0.109 mmol, 87%).

FTIR (dissolved in 4FB, ZnSe): ν [cm^{-1}] = 2169 (vw), 2112 (br), 2078 (sh), 2047 (vw), 1352 (vw), 1299 (w), 1277 (w), 1219 (s), 973 (vs), 831 (vw), 755 (vw), 727 (m), 571 (vw), 560 (vw).

FTIR (precipitated, ZnSe): ν [cm^{-1}] = 2169 (vw), 2121 (vw), 2080 (vw), 2059 (sh), 2045 (m), 1459 (vw), 1444 (vw), 1398 (vw), 1352 (w), 1297 (m), 1272 (s), 1240 (s), 1211 (vs), 1162 (m), 998 (vw), 970 (vs), 832 (w), 782 (vw), 756 (vw), 727 (vs), 571 (vw), 561 (w).

FTIR (crystallized at 293 K, ZnSe): ν [cm^{-1}] = 2168 (vw), 2105 (w), 2081 (m), 2054 (vs), 2030 (vs), 1509 (vw), 1398 (vw), 1353 (w), 1296 (m), 1272 (s), 1265 (s), 1239 (s), 1207 (vs), 1175 (s), 1161 (s), 965 (vs), 831 (w), 756 (w), 724 (vs), 569 (vw), 560 (w).

FTIR (crystallized at 303 K, ZnSe): ν [cm^{-1}] = 2168 (vw), 2102 (vw), 2081 (w), 2051 (s), 2044 (s), 1487 (vw), 1398 (vw), 1352 (w), 1296 (m), 1273 (s), 1241 (s), 1207 (vs), 1161 (s), 1054 (vw), 968 (vs), 831 (w), 800 (vw), 781 (vw), 756 (vw), 725 (vs), 560 (w).

FT Raman (10000 scans, 25 mW): ν [cm^{-1}] = 2168 (m), 2111 (m), 2061 (w), 2047 (w), 1489 (vw), 1397 (vw), 1299 (vw), 1275 (vw), 1234 (vw), 1213 (vw), 1141 (vw), 1117 (vw), 998 (vw), 977 (vw), 903 (vw), 829 (vw), 797 (w), 746 (w), 562 (vw), 538 (vw), 370 (w), 323 (vw), 288 (vw), 234 (vw), 168 (vw), 111 (vs).

^{19}F NMR (376.54 MHz, $F_4C_6H_2$, 298 K): δ = –76.9 (s, 36F, C(C**F**$_3$)$_3$) ppm.

^{27}Al NMR (104.27 MHz, $F_4C_6H_2$, 298 K): δ = 35.0 (s, **Al**(OR^F)$_4$) ppm.

^{13}C NMR (100.62 MHz, $F_4C_6H_2$, 298 K): δ = 202.6 (bs, **C**O, FWHM = 205 Hz), 121.3 (q, 12C, **C**F_3, $^1J_{CF}$ = 293 Hz) ppm.

UV-Vis (reflectance): $\lambda_{max.}$ [nm] = 392.

Synthesis of **4**: $[NEt_4]^+[Nb(CO)_6]^-$ (0.100 g, 0.256 mmol, 1 eq) and $Ag[Al(OR^F)_4]$ (0.550 g, 0.511 mmol, 2 eq) were weighed in the glovebox each in one side of a double-Schlenk flask and dissolved in *o*-dfb (each ca. 5 ml). Argon was removed and the flask was flooded with CO (3 bar). The solution of $Ag[Al(OR^F)_4]$ was transferred to the other side through the frit at –40 °C. The dark red suspension was stirred for 1h at –40 °C and was then allowed to warm up slowly to room temperature. The suspension was stirred overnight and stored another night to let the Silver settle. The red solution was filtered through the frit, pentane (ca. 20 ml) was added to the Ag^0 precipitate under a reverse flow of Argon, which was removed again and the flask was flooded with CO (1.2 bar). After 3 days $[(o\text{-dfb})Nb(CO)_4]^+[Al(OR^F)_4]^-$ was obtained as dark red crystals and the co-product $[NEt_4]^+[Al(OR^F)_4]^-$ as colorless crystals (0.475 g, 0.199 mmol, 78%).

FTIR (ZnSe): ν [cm^{-1}] = 3100 (vw), 2093 (m), 2024 (s), 1555 (vw), 1534 (vw), 1493 (vw), 1429 (vw), 1353 (w), 1297 (m), 1274 (s), 1240 (s), 1215 (vs), 1170 (w), 1084 (vw), 970 (vs), 886 (vw), 852 (vw), 831 (vw), 824 (vw), 759 (vw), 726 (vs), 561 (vw).

FT Raman (10000 scans, 80 mW): ν [cm^{-1}] = 3101 (vw), 2094 (m), 2044 (vs), 2027 (s), 1555 (vw), 1495 (vw), 1430 (vw), 1340 (vw), 1284 (vw), 1244 (vw), 1221 (vw), 1160 (vw), 1131 (vw), 1085 (vw), 1011 (vw), 990 (vw), 972 (vw), 887 (vw), 824 (vw), 797 (vw), 760 (vw), 746 (vw), 565 (vw), 538 (vw), 423 (vw), 367 (vw), 340 (w), 292 (vw), 262 (vw), 234 (vw), 180 (vw), 113 (s).

^{19}F NMR (282.45 MHz, $F_4C_6H_2$, 298 K): δ = –76.1 (s, 36F, C(C**F**$_3$)$_3$) ppm.

^{27}Al NMR (78.22 MHz, $F_4C_6H_2$, 298 K): δ = 34.4 (s, **Al**(OR^F)$_4$) ppm.

^{13}C NMR (100.62 MHz, $F_4C_6H_2$, 298 K): δ = 206.3 (bs, **C**O, FWHM = 205 Hz), 121.3 (q, 12C **C**F$_3$, $^1J_{CF}$ = 293 Hz) ppm.

^{93}Nb NMR (97.95 MHz, $F_4C_6H_2$, 298 K): δ = –1393.6 (s, **Nb**C) ppm.

UV-Vis (reflectance): $\lambda_{max.}$ [nm] = 399.

*Synthesis of **5***: $[NEt_4]^+[Ta(CO)_6]^-$ (0.060 g, 0.125 mmol, 1 eq) and Ag[Al(OR^F)$_4$] (0.269 g, 0.250 mmol, 2 eq) were weighed in the glovebox each in one side of a double-Schlenk flask and dissolved in *o*-dfb (each ca. 5 ml). Argon was removed and the flask was flooded with CO (3 bar). The solution of Ag[Al(OR^F)$_4$] was transferred to the other side through the frit at –40 °C. The dark red suspension was stirred for 1h at –40 °C and was then allowed to warm up slowly to room temperature. The suspension was stirred overnight and stored another night to let the Silver settle. The red solution was filtered through the frit, pentane (ca. 20 ml) was added to the Ag^0 precipitate under a reverse flow of Argon. After 3 days $[(o\text{-dfb})Ta(CO)_4]^+[Al(OR^F)_4]^-$ was obtained as dark red crystals and the co-product $[NEt_4]^+[Al(OR^F)_4]^-$ as colorless crystals (0.253 g, 0.103 mmol, 82%).

FTIR (ZnSe): ν [cm^{-1}] = 3102 (vw), 2111 (vw), 2089 (m), 2007 (vs), 1986 (sh), 1554 (vw), 1527 (vw), 1493 (vw), 1472 (vw), 1425 (vw), 1398 (vw), 1352 (w), 1296 (m), 1272 (s), 1238 (s), 1207 (vs), 1167 (s), 1081 (vw), 966 (vs), 886 (vw), 851 (vw), 828 (w), 782 (vw), 759 (vw), 725 (vs), 677 (vw), 571 (vw), 560 (w).

FT Raman (10000 scans, 50 mW, individual bk): ν [cm^{-1}] = 3101 (vw), 2938 (vw), 2909 (vw), 2757 (vw), 2091 (m), 2034 (vs), 2020 (s), 1282 (vw), 1010 (vw), 990 (vw), 887 (vw), 819 (vw), 798 (w), 761 (vw), 746 (w), 565 (vw), 538 (vw), 503 (vw), 381 (w), 351 (vw), 330 (vw), 323 (vw), 288 (vw), 260 (vw), 234 (vw), 171 (vw), 116 (s).

^{19}F NMR (376.54 MHz, $F_4C_6H_2$, 298 K): δ = –76.1 (s, 36F, C(C**F**$_3$)$_3$) ppm.

^{27}Al NMR (104.27 MHz, $F_4C_6H_2$, 298 K): δ = 34.3 (s, **Al**(OR^F)$_4$) ppm.

^{13}C NMR (100.62 MHz, $F_4C_6H_2$, 298 K): δ = 202.5 (bs, **C**O, FWHM = 376 Hz), 121.3 (q, 12C, **C**F$_3$, $^1J_{CF}$ = 293 Hz) ppm.

UV-Vis (reflectance): $\lambda_{max.}$ [nm] = 392.

*Synthesis of **6***:

a: $[NEt_4]^+[Ta(CO)_6]^-$ (0.060 g, 0.13 mmol, 2 eq) and Ag[Al(OR^F)$_4$] (0.14 g, 0.13 mmol, 2 eq) were weighed in the glovebox on the same side of a double-Schlenk flask. Pentane (ca. 5 ml) and one drop 4FB was added at –40 °C. Argon was removed and the flask was flooded with CO (3 bar). The suspension was stirred for 1h at room temperature, the red solution filtered through

the frit and stored at –30 °C. After 2 weeks $Ta_2(CO)_{12}$ was obtained as red crystals (orthorhombic space group *Pbca*).

b: $[NEt_4]^+[Ta(CO)_6]^-$ (0.029 g, 0.056 mmol, 1 eq) and $[Ta(CO)_7]^+[Al(OR^F)_4]^-$ (0.080 g, 0.056 mmol, 1 eq) were weighed in the glovebox on the same side of a double-Schlenk flask. Pentane (ca. 5 ml) was added at –40 °C. Argon was removed and the flask was flooded with CO (3 bar). The suspension was stirred for 1h at room temperature, the orange solution filtered through the frit and stored at –30 °C. After 2 weeks $Ta_2(CO)_{12}$ was obtained as red crystals (triclinic space group *P*-1). The yields could not be determined since the products were only stable under CO pressure.

FT Raman (5000 scans, 25 mW): ν [cm^{-1}] = 2097 (s), 2038 (vw), 1991 (s), 1975 (s), 1955 (m), 1939 (m), 1926 (m), 531 (vw), 497 (vw), 457 (vw), 443 (vw), 395 (w), 377 (w), 335 (vw), 109 (vs), 90 (vs).

Discussions of the Yields Compounds 1, 2, 4 and 5

As described in the main article, it should be noted that **1**, **2**, **4** and **5** could not be separated from the stoichiometric co-product $[NEt_4]^+[Al(OR^F)_4]^-$. The solubility and crystallization behavior of $[NEt_4]^+[Al(OR^F)_4]^-$ was very similar to that of the desired complexes, thus, no classical yields can be given. We note however that the isolated combined crystalline materials, consisting of product and co-product correspond to 87 % (**2**), 78 % (**4**) and 82 % (**5**) the expected amount for the mixture of both components. We emphasize that because the non-reactive, air- and water-stable $[NEt_4]^+[Al(OR^F)_4]^-$ has previously been characterized in details, all spectroscopic signatures could be assigned with certainty and the complexes **1**, **2** and **4**, **5** were unambiguously characterized.

In the following, we rationalize the problems of yield determination:

Despite many, many attempts we could not find the conditions, where only one or the other type of crystals precipitated and thus would allow for a purification by fractionated crystallisation. This is on the one hand due to the limited amount of solvents with which the metal carbonyl cations are compatible (essentially only ortho-difluorobenzene and tetrafluorobenzene. Crystallization was induced by gas phase diffusion of pentane into a ortho-difluorobenzene or tetrafluorobenzene solution) and on the other to the very comparable solubilities of the products $[NEt_4][Al(OR^F)_4]$ and $[M(CO)_7][Al(OR^F)_4]$ **that have to form** in a 1:1 stoichiometric ratio according to the reaction equation, e.g. for **1** and **2**:

$$2\ Ag^+[Al(OR^F)_4]^- + 1\ [NEt_4]^+[M(CO)_6]^- + CO \rightarrow 1\ [M(CO)_7][Al(OR^F)_4] + 1\ [NEt_4][Al(OR^F)_4] + 2\ Ag^0_{(s)}$$

Thus, although both do form separate crystal structures, they could not be separated. This is also meant to be shown by the picture inset in Figure 2, main text: You do see the red-orange $[Ta(CO)_7][Al(OR^F)_4]$ crystals embedded in the colourless $[NEt_4][Al(OR^F)_4]$ matrix. Due to the sensitivity of the $[M(CO)_7][Al(OR^F)_4]$ materials they can only be handled in a very clean glove box. Although some "crystal picking and removal" would in principle be possible, this is not honest and does not correspond to a true yield. Since the ammonium salt $[NEt_4][Al(OR^F)_4]$ is completely unreactive towards pretty much each and every follow up reaction one could think of, we decided to report the honest combined yields ($[NEt_4][Al(OR^F)_4]$ and $[M(CO)_7][Al(OR^F)_4]$).

However, it is even difficult to determine the complex-co-product ratio: There are simply no experimentally well founded observables to base this on. Thus, the anion is equal, no differentiation in IR/Raman/NMR whatsoever occurs (cf. S-Figure 11, S-Figure 30, 34). The

carbonyl cation does not contain protons, the integration of which in NMR spectra could be well done. The only common nucleus in both product cations (carbonyl and ammonium cation) is ^{13}C.

However, i) ^{13}C has a low sensitivity and ii) it is broadened in the ^{13}C-NMR spectra (Cf. S-Figures 30 and 34) and in addition for M = Nb couples to the quadrupolar ^{93}Nb nucleus. All of this makes an integration not more than a guess. Therefore decided, to leave it out.

But, the most substantial answers do come from the combined yields themselves, which are in the range 78 – 87 % of combined crystalline materials: The NMR investigations and the IR / Raman investigations clearly did prove that no other compound is included with the solids. This means that almost all of the products did crystallize and even if one assumes a – very unlikely – largely preferential precipitation tendency of the ammonium by-product of 100 %, the observed 87 % combined yield of **2** and $[NEt_4][Al(OR^F)_4]$ means that the mixture contains 76 % of the theoretically possible yield of only **2**. Thus, in a worst case scenario the molar ratio **2** : $[NEt_4][Al(OR^F)_4]$ = 1 : 1.3, close to the stoichiometrically expected 1:1 ratio.

Thus, we consider to give the combined yields of $[NEt_4][Al(OR^F)_4]$ and the complexes **1**, **2** and **4**, **5** the best approach.

However, we did find one other approach, to assess the product ratios: We used the ^{1}H and ^{19}F-NMR-signals of the solvent 4FB (tetrafluorobenzene) as a reference. Then we integrated the amount of anion (one signal for 36 equivalent F-atoms in $[Al(OR^F)_4]^-$) in relation to the 4FB solvent. The ^{1}H-NMR data of the NEt_4^+ cation of the $[NEt_4][Al(OR^F)_4]$ by product, was then set into relation to the ^{1}H-NMR signals of the solvent 4FB as well. Thereby we estimated the ratio of the $[Al(OR^F)_4]^-$ anion that belongs only to $[NEt_4][Al(OR^F)_4]$. The to 100 % anion missing amount, therefore, must be ion-paired with the target cations $\mathbf{1}^+$, $\mathbf{2}^+$, $\mathbf{4}^+$ or $\mathbf{5}^+$. The results of these analyses are given in the table below.

For comparison, we also did use the direct integration of the broader and low natural abundancy ^{13}C nucleus (1.1 % natural abundancy, noisier signals). The ^{13}C nucleus is present in the carbonyl-moieties of $\mathbf{1}^+$, $\mathbf{2}^+$, $\mathbf{4}^+$ or $\mathbf{5}^+$ as well as the NEt_4^+ cation of $[NEt_4][Al(OR^F)_4]$. For the reasons given above these ^{13}C-based data included in the table in italics are viewed as much less reliable. We used spectra with extra-long relaxation time delays (60 s) for maximum precision (and to actually be able to see the carbonyl ligands that else would not show up).

Table. Determination of the ratio between the cation $\mathbf{1}^+$, $\mathbf{2}^+$, $\mathbf{4}^+$ or $\mathbf{5}^+$ and the by-product cation NEt_4^+ in 4FB solution by integration with respect to the solvent 4FB (line ^{19}F-NMR, more reliable) as well as by direct integration of the ^{13}C-NMR signals of carbonyl to NEt_4^+ (line *^{13}C-NMR*, less reliable).

Ratio	$\mathbf{1}^+ : [NEt_4]^+$	$\mathbf{2}^+ : [NEt_4]^+$	$\mathbf{4}^+ : [NEt_4]^+$	$\mathbf{5}^+ : [NEt_4]^+$
^{19}F-NMR:	1.63 : 1	7.47 : 1	2.77 : 1	1.40 : 1
^{13}C-NMR:	*1.29 : 1*	*6.94 : 1*	*4.30 : 1*	*1.75 : 1*

But: For the preparation of the samples, from which these spectra were recorded, it was always attempted to load **more of the red-orange crystals** (i.e. the target products **1**, **2**, **4** and **5**) than the

colourless by-product $[NEt_4][Al(OR^F)_4]$ and the ratios given in the Table do reflect this but do not give the bulk composition of the crystalline material isolated.

Overall, we could produce samples that are enriched in the target cations, but always did contain by-product $[NEt_4][Al(OR^F)_4]$. Thus, to our conviction, the combined yields are the most honest to be given.

4 Structural Discussions of Compounds 1 - 6

$[M(CO)_7]^+[Al(OC(CF_3)_3)_4]^-$ (M = Nb (**1**), Ta (**2**))

The experimentally determined symmetry of $\mathbf{1}^+$ and $\mathbf{2}^+$ (Supplementary Figure 4) is almost C_{2v}. Bond lengths and angles were therefore compared with DFT calculations in this symmetry (Supplementary Table 1) even C_{3v} is slightly more stable (Supplementary Figure 1).

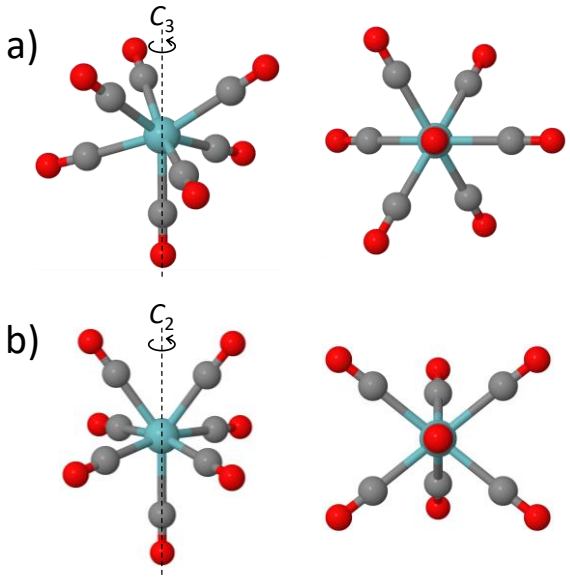

Supplementary Figure 1. Side and front view of calculated minimum structures of $M(CO)_7^+$ in C_{3v} (**a**) and C_{2v} (**b**), (RI-)B3LYP-D3(BJ)/def2-TZVPP.

The C_{2v} structure is a true transition state in the gas phase with one imaginary frequency of $-39.0\ cm^{-1}$ (BP86)/ $-34.1\ cm^{-1}$ (B3LYP). Increase of the convergence criteria (SCF convergence 10^{-9} a.u., energy change $\leq 10^{-9}$, cartesian gradient $\leq 10^{-7}$) and different integration grids (m4, m5, m7) have no effect on the value of the imaginary frequency. Small displacement along the imaginary frequency in both directions and subsequent geometry optimization leads to two equivalent C_{3v} structures with both methods. The imaginary frequency corresponds primarily to a distortion of the C1-Ta-C4 bond angle (Supplementary Figure 2, which is why the relaxed potential energy surface scans (Supplementary Figure 15) along this angle are a good approximation for the minimum energy pathway connecting the $C_{3v} \rightarrow C_{2v} \rightarrow C_{3v}$ structures. The

scans illustrate that the C_{2v} structure with a C1-Ta-C4 bond angle of 144° is the transition state between the two possible equivalent C_{3v} structures with a bond angle of 163° and 124°.

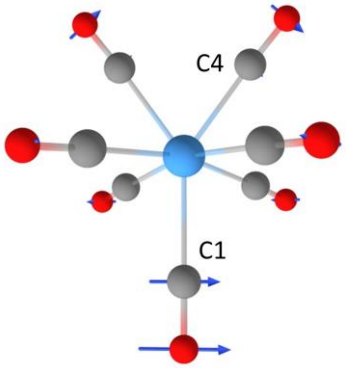

Supplementary Figure 2. Calculated C_{2v} structure of $[Ta(CO)_7]^+$ with scaled displacement vectors corresponding to the imaginary frequency at 39.0 cm^{-1} at (RI-)BP86-D3(BJ)/def2-SVP level of theory.

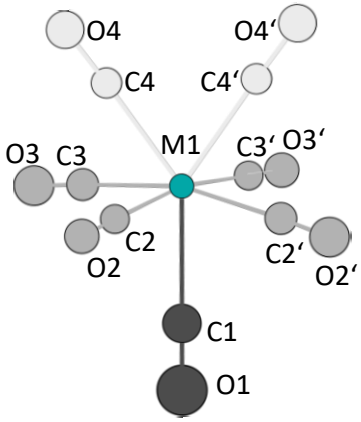

Supplementary Figure 3. Three sets of bond lengths of $\mathbf{1}^+$ or $\mathbf{2}^+$. The outer CO ligands with the shortest M-C bond lengths are shown in pale grey, the ligands on the plane with M1 are shown in middle grey and the longest M-C bond length in dark grey.

The bond lengths of $\mathbf{1}^+$ and $\mathbf{2}^+$ differ from the calculated ones by a deviation of maximum 3%. For the angles, the deviation is maximum 2% (Supplementary Table 1).

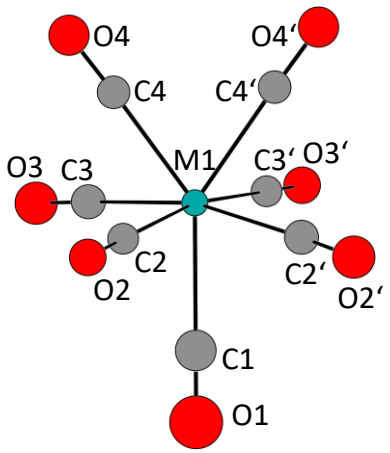

Supplementary Figure 4. Atom labels of $\mathbf{1}^+$ (M1 = Nb) or $\mathbf{2}^+$ (M1 = Ta) for the assignment of bond lengths and angles.

Supplementary Table 1. Bond length [Å] and angles [°] of structurally characterized and calculated cations $\mathbf{1}^+$ and $\mathbf{2}^+$. Distances and angles between atoms, which were generated according symmetry, are not displayed.

$[M(CO)_7]^+$	$\mathbf{1}^+$ (M = Nb)	C_{2v} calcd[a]	$\mathbf{2}^+$ (M = Ta)	C_{2v} calcd[a]
M-C1	2.270(5)	2.29242	2.236(9)	2.27722
M-C2	2.188(2)	2.20357	2.165(5)	2.20069
M-C3	2.206(3)	2.20357	2.200(7)	2.20077
M-C4	2.132(3)	2.14268	2.138(7)	2.15194
C1-O1	1.104(4)	1.12106	1.108(10)	1.12199
C2-O2	1.125(3)	1.12752	1.119(6)	1.12865
C3-O3	1.116(3)	1.12752	1.099(8)	1.12865
C4-O4	1.124(3)	1.13127	1.109(8)	1.13186
C1-M-C2	83.29(9)	83.577	82.72(17)	83.3062
C1-M-C3	85.23(9)	83.577	84.65(11)	83.2045
C1-M-C4	144.75(9)	144.432	144.22(19)	144.241
C2-M-C3	76.58(15)	77.0699	76.5(3)	77.0707
C2-M-C4	74.55(13)	74.2537	74.7(2)	74.3834
C3-M-C4	73.42(13)	74.2537	73.7(2)	74.4357
C2-M-C2‘	102.28(15)	101.463	102.1(3)	101.313
C3-M-C3‘	102.28(15)	101.463	102.1(3)	101.313
C4-M-C4‘	70.50(18)	71.1	71.6(4)	71.5

[a] Calculated at the (RI-)B3LYP-D3(BJ)/def2-TZVPP level, C_{2v}

The comparison of the calculated C_{3v} and C_{2v} symmetries to the experimental structure shows a very small difference. The largest angle between the two symmetries amounts to 11.9° (Supplementary Figure 5). In accordance, the largest ellipsoid in the experimental structure was obtained at this spot.

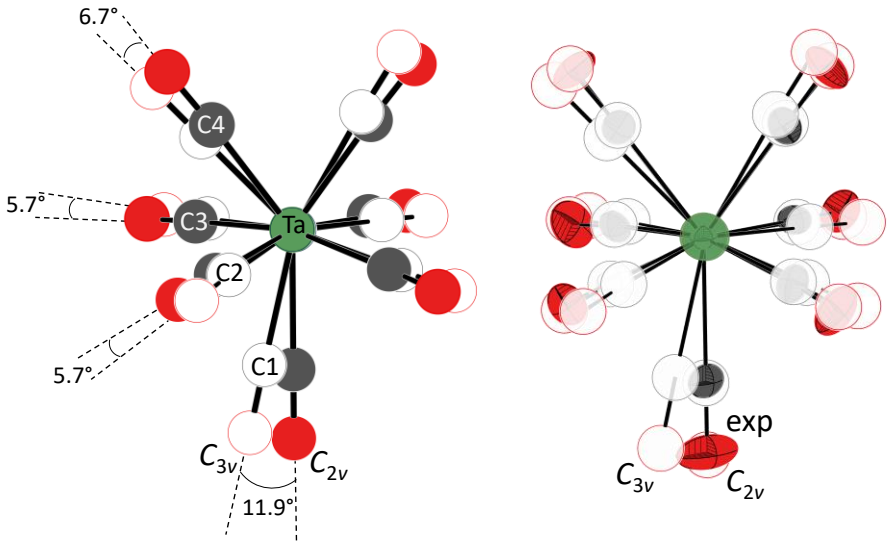

Supplementary Figure 5. Overlay generated by the program OLEX2 (v1.2.10) [66] of calculated C_{3v} and C_{2v} structures of $[Ta(CO)_7]^+$ (filled atoms).

$[Ag_6\{Nb(CO)_6\}_4]^{2+}$ $2[Al(OC(CF_3)_3)_4]^-$ **(3)**

On the way to **1** an heterobimetallic carbonyl cluster dication $[Ag_6\{Nb(CO)_6\}_4]^{2+}$ (**3**$^{2+}$), stabilized by two $[Al(OR^F)_4]^-$ and six *o*-dfb (**3a**) or 4FB (**3b**), was repeatedly isolated as red crystals after 2 days at −30 °C (Supplementary Figure 6). Four $Nb(CO)_6$ fragments cap an octahedron consisting of silver atoms on every other triangle face. In order to obtain the dication, 6 silver(I) cations and 4 niobium(-I) ions must formally be present. However, the charge cannot be assigned clearly.

The bond lengths between the silver atoms are 2.87 to 2.95 Å (mean value: 2.90 Å), which is similar to a bond in elemental metallic silver with 2.88 Å [87]. The bonds between silver and niobium are 2.97 to 3.02 Å, (mean value: 2.99 Å).

The attempt to synthesize **3** exclusively failed, which is why no other analytics could be done yet.

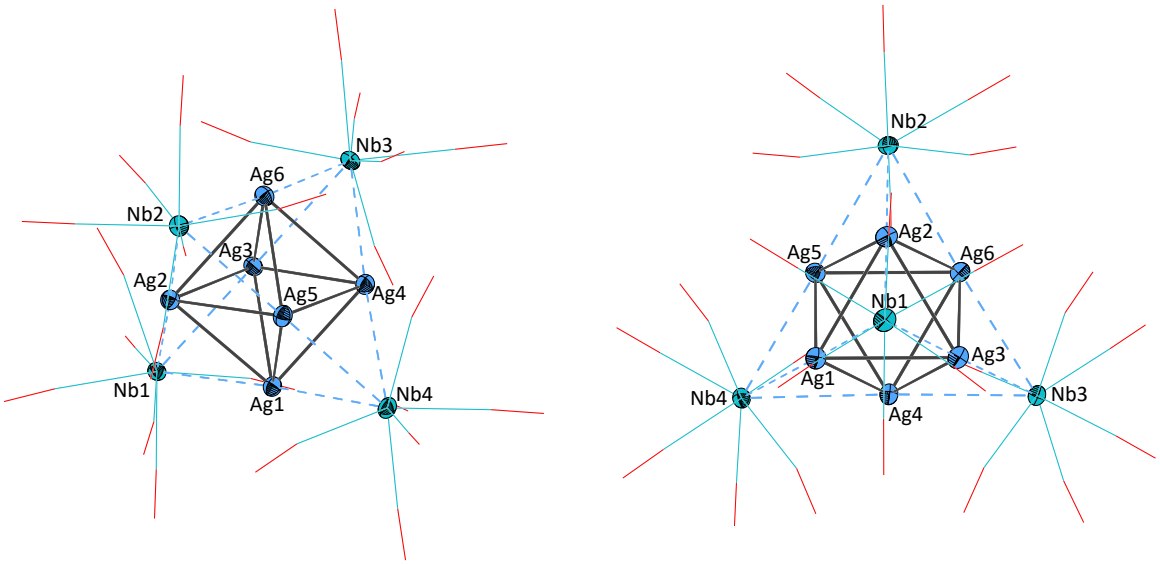

Supplementary Figure 6. Atom labels of $\mathbf{3}^{2+}$ (left: side view, right: front view) for the assignment of bond lengths and angles.

Supplementary Table 2. Mean values of bond length [Å] of $\mathbf{3}^{2+}$.

Average value	**3a^{2+} (*o*-dfb)**	**3b^{2+} (4FB)**	***T* calcd[a]**
Ag-Ag	2.8998	2.9011	2.9573
Ag-Nb	2.9939	2.9858	3.0387
Ag-C	2.640	2.634	2.4508
C-O	1.133	1.1280	1.1566
C_{Ag}-O	1.145	1.132	1.1664
C_{free}-O	1.121	1.124	1.1469
Nb-C	2.167	2.168	2.1717
Nb-C_{Ag}	2.142	2.158	2.1627
Nb-C_{free}	2.192	2.179	2.1807

[a] (RI-)BP86-D3(BJ)/def-SV(P).

[(*o*-dfb)M(CO)$_4$]$^+$[Al(OC(CF$_3$)$_3$)$_4$]$^-$ (M = Nb (**4**), Ta (**5**))

Single crystals of **4** and **5** could be obtained at room temperature. The bond lengths of **4** and **5** differ from the calculated ones by a deviation of maximum 3%. For the angles, the maximum deviation is 2%.

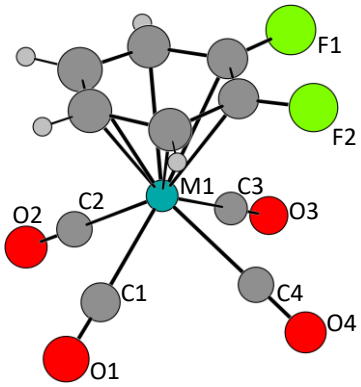

Supplementary Figure 7. Atom labels of **4**$^+$ (M1 = Nb) or **5**$^+$ (M1 = Ta) for bond lengths and angles in Table S3.

Supplementary Table 3. Bond lengths [Å] and angles [°] of structurally characterized cations **4**$^+$ and **5**$^+$ compared with calculated structures.

[(*o*-dfb)M(CO)$_4$]$^+$	**4$^+$ (M = Nb)**	***C*$_s$ calcd[a]**	**5$^+$ (M = Ta)**	***C*$_s$ calcd[a]**
M-C1	2.115(4)	2.11796	2.116(11)	2.11811
M-C2	2.109(4)	2.11796	2.090(12)	2.11811
M-C3	2.113(4)	2.11571	2.135(14)	2.12019
M-C4	2.116(3)	2.11571	2.079(9)	2.12019
M-*o*-dfb	2.0278(16)	2.09788	1.991(6)	2.08787
M-*o*-dfb$_{centroid}$	2.0279(16)	2.09813	1.992(6)	2.08814
C1-O1	1.142(5)	1.13409	1.119(12)	1.13582
C2-O2	1.142(5)	1.13409	1.122(13)	1.13582
C3-O3	1.123(5)	1.13458	1.103(13)	1.13532
C4-O4	1.128(5)	1.13458	1.140(11)	1.13532
C1-M-C2	73.33(14)	73.604	73.3(4)	73.0345
C1-M-C3	116.99(17)	116.42	115.4(4)	116.544
C1-M-C4	73.97(15)	73.9925	75.7(3)	74.1338
C2-M-C3	74.75(17)	73.9925	74.1(4)	74.1338
C2-M-C4	114.65(14)	116.42	117.9(4)	116.544
C3-M-C4	72.41(14)	73.9603	72.9(4)	73.4789

[a] Calculated at the (RI-)B3LYP-D3(BJ)/def2-TZVPP level.

$Ta_2(CO)_{12}$ **(6)**

Bond lengths of **6a** and **b** differ from calculated ones by a maximum of 2%. For the angles of **6a**, the deviation is <1%, whereas **6b** differs by a maximum of 5%. In accordance, **6a** deviates from the calculated transition state of C_2 symmetry by R = 0.07135 and from the global D_2 minimum by R = 0.09717. By contrast, **6b** deviates much more in both cases: with C_2 by R = 0.16182 and D_2 by R = 0.17773. The coordination sphere of each tantalum atom in both structures is almost C_{2v} symmetric. The deviation is listed for the fragments 1 and 2 (Supplementary Figure 8) in Supplementary Table 4.

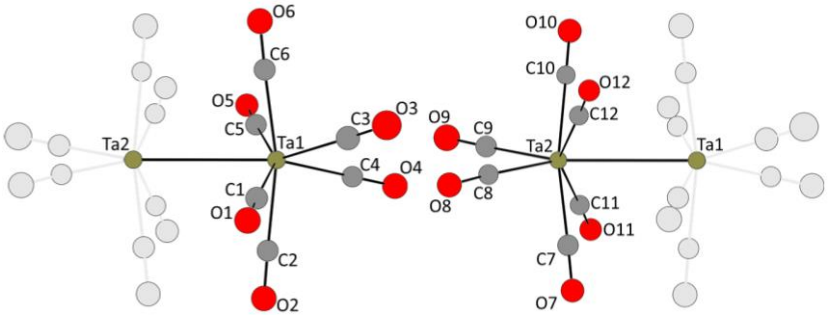

Supplementary Figure 8. Fragments 1 (left) and 2 (right) of **6** for the assignment of the coordination sphere of the Tantalum atoms.

Supplementary Table 4. Symmetry values of the fragments 1 and 2 of the **6a** and **b** determined with "Chemcraft".

	6a (*pbca*)		**6b ($P\bar{1}$)**	
Fragment	1	2	1	2
R (C_2)	0.13131	0.06079	0.13060	0.12291
R (C_{2v})	0.19612	0.18415	0.12719	0.25558

The program "Chemcraft" (Chemcraft - graphical software for visualization of quantum chemistry computations. https://www.chemcraftprog.com, 08/04/2019) was used to study the symmetry deviations. R is defined as a root-mean-square displacement of atomic coordinates. The lower the value, the smaller the deviation.

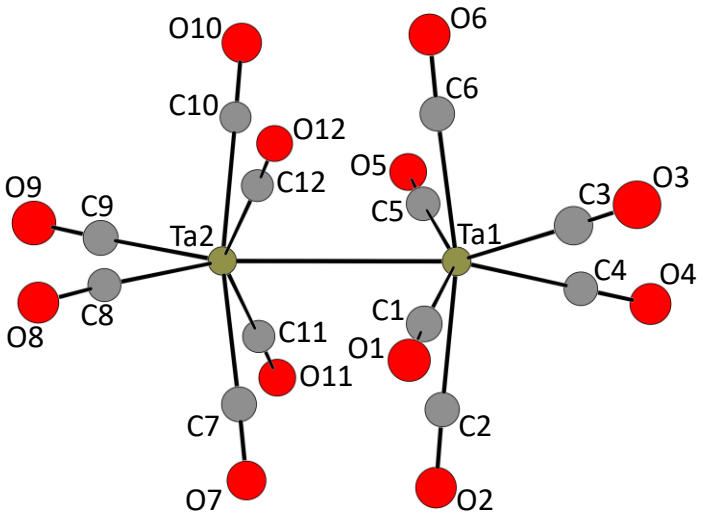

Supplementary Figure 9. Atom labels of **6** for the assignment of bond lengths and angles.

Supplementary Table 5. Mean values of bond length [Å] of **6** the calculated structure.

mean value	6a	D_2 calcd[a]	6b
Ta1-C	2.120	2.11870	2.130
Ta2-C	2.121	2.12297	2.123
Ta-C	2.121	2.12083	2.126
C-O	1.136	1.13532	1.140

[a] Calculated at the (RI-)B3LYP-D3(BJ)/def2-TZVPP level.

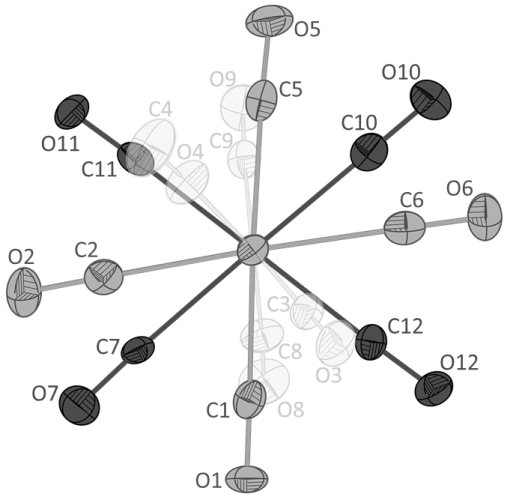

Supplementary Figure 10. View along the Ta-Ta bond of **6**. The outer CO ligands are shown in pale grey, the inner ligands around Ta1 are shown in middle grey and of Ta2 in dark grey.

Supplementary Table 6. Experimental and calculated bond length [Å] and angles [°] of **6** (**a**, *Pbca*; **b**, $P\bar{1}$).

	6a (M = Ta)	***D*$_2$ calcd**[a]	**6b (M = Ta)**
M1-M2	3.2878(5)	3.28774	3.3006(3)
M1-C1	2.135(8)	2.13856	2.136(3)
M1-C2	2.130(8)	2.1187	2.151(3)
M1-C3	2.079(8)	2.08	2.091(4)
M1-C4	2.097(9)	2.0997	2.089(4)
M1-C5	2.130(8)	2.13113	2.157(3)
M1-C6	2.149(8)	2.14408	2.153(3)
M2-C7	2.143(7)	2.15165	2.141(3)
M2-C8	2.094(8)	2.09408	2.092(4)
M2-C9	2.064(8)	2.06338	2.082(4)
M2-C10	2.134(8)	2.14147	2.140(3)
M2-C11	2.138(8)	2.13521	2.150(3)
M2-C12	2.154(8)	2.152	2.132(3)
C1-O1	1.134(9)	1.13136	1.134(4)
C2-O2	1.136(9)	1.15326	1.133(4)
C3-O3	1.142(9)	1.13881	1.144(4)
C4-O4	1.132(9)	1.12739	1.143(4)
C5-O5	1.130(9)	1.12523	1.134(4)
C6-O6	1.131(9)	1.14309	1.140(4)
C7-O7	1.129(8)	1.11336	1.134(4)
C8-O8	1.135(9)	1.13648	1.146(4)
C9-O9	1.168(9)	1.17091	1.150(4)
C10-O10	1.134(9)	1.11991	1.138(4)
C11-O11	1.135(9)	1.13835	1.139(4)
C12-O12	1.122(9)	1.12567	1.144(4)
C1-M1-M2	76.9(2)	76.8891	77.88(9)
C2-M1-M2	82.64(19)	82.6252	82.04(9)
C3-M1-M2	146.6(2)	146.682	142.61(9)
C4-M1-M2	141.7(2)	141.805	147.49(10)
C5-M1-M2	78.0(2)	78.0802	80.29(9)

C6-M1-M2	84.59(19)	84.565	81.18(9)
C7-M2-M1	85.23(19)	85.2746	85.45(9)
C8-M2-M1	144.9(2)	144.838	141.53(10)
C9-M2-M1	142.8(2)	142.778	145.12(10)
C10-M2-M1	83.5(2)	83.4708	85.40(9)
C11-M2-M1	76.41(18)	76.3832	76.21(9)
C12-M2-M1	76.50(19)	76.4598	76.18(9)
C1-M1-C2	77.2(3)	77.1872	75.30(12)
C1-M1-C3	78.1(3)	78.0796	78.47(13)
C1-M1-C4	126.8(3)	126.756	119.03(13)
C1-M1-C5	154.8(3)	154.892	157.90(13)
C1-M1-C6	97.9(3)	98.0097	101.04(12)
C2-M1-C3	112.8(3)	112.681	118.93(13)
C2-M1-C4	75.8(3)	75.8596	76.70(13)
C2-M1-C5	101.6(3)	101.531	98.39(12)
C2-M1-C6	167.1(3)	167.042	163.22(13)
C3-M1-C4	71.6(3)	71.4737	69.88(13)
C3-M1-C5	123.9(3)	123.901	122.09(13)
C3-M1-C6	77.4(3)	77.5178	75.44(13)
C4-M1-C5	75.8(3)	75.8498	78.83(14)
C4-M1-C6	116.0(3)	115.983	118.40(14)
C5-M1-C6	77.6(3)	77.6226	78.81(12)
C7-M2-C8	75.0(3)	74.8447	76.24(13)
C7-M2-C9	114.4(3)	114.455	110.89(13)
C7-M2-C10	168.7(3)	168.71	170.47(13)
C7-M2-C11	77.9(3)	77.9804	77.26(12)
C7-M2-C12	99.5(3)	99.4773	101.62(12)
C8-M2-C9	72.3(3)	72.3831	73.34(14)
C8-M2-C10	114.3(3)	114.416	112.81(13)
C8-M2-C11	125.4(3)	125.444	130.02(13)
C8-M2-C12	78.5(3)	78.5646	74.85(13)
C9-M2-C10	75.6(3)	75.5785	75.62(14)
C9-M2-C11	77.5(3)	77.4748	77.76(13)

C9-M2-C12	126.3(3)	126.38	126.58(13)
C10-M2-C11	100.2(3)	100.152	97.93(13)
C10-M2-C12	77.0(3)	77.0097	78.74(13)
C11-M2-C12	152.9(3)	152.841	152.37(13)
O1-C1-M1	177.8(6)	177.811	177.7(3)
O2-C2-M1	178.1(6)	177.872	179.4(3)
O3-C3-M1	178.0(7)	178.022	179.0(3)
O4-C4-M1	178.5(8)	178.923	178.1(3)
O5-C5-M1	177.1(7)	177.602	179.1(3)
O6-C6-M1	178.9(7)	178.862	178.9(3)
O7-C7-M2	177.5(7)	177.171	178.0(3)
O8-C8-M2	177.7(7)	177.657	178.7(3)
O9-C9-M2	177.3(6)	177.25	178.8(3)
O10-C10-M2	178.9(7)	178.843	178.0(3)
O11-C11-M2	178.1(6)	177.656	177.5(3)
O12-C12-M2	178.4(6)	177.799	175.6(3)

[a] Calculated at the (RI-)B3LYP-D3(BJ)/def2-TZVPP level.

5 Detailed Vibrational Analysis

IR and Raman Data of $[M(CO)_7]^+[Al\{OC(CF_3)_3\}_4]^-$ (M = Nb (**1**), Ta (**2**))

Supplementary Table 7. Experimental (grey shaded) and calculated IR and Raman frequencies ν(CO) [cm^{-1}] of $[M(CO)_7]^+$ $\mathbf{1}^+$ (M = Nb) and $\mathbf{2}^+$ (M = Ta); br: broad, v: very, s: strong, m: medium, w: weak, sh: shoulder.

IR			Raman	calcd[a]	
$Nb(CO)_7^+$(g)[d]	**1**[c]		**1**[c]	C_{3v} (IR/Ra) [sym]	C_{2v} (IR/Ra) [sym]
2169 (vw)	2167 (vw)		2168 (s)	2168 (5/27 %) [A_1], ν_s	2173 (9/54 %) [A_1], ν_s
					2134 (14/59 %) [A_1], ν_s
2125 (m)	2116 (vw)		2122 (s)	2114 (37/84 %) [E], ν_{as}	
2100 (m)	2092 (w)		2095 (w)	2092 (61/4 %) [A_1], ν_{as}	2093 (0/100 %)* [A_2], ν_{as}
					2087 (52/10 %) [B_2], ν_{as}
2075 (s)			2069 (sh, m)	2073 (100/31 %) [E], ν_{as}	2083 (100/7 %) [B_1], ν_{as}
			2064 (m)		2066 (62/30 %) [A_1], ν_s
2057 (w)	2059 (m)		2047 (m)	2061 (56/18 %) [A_1], ν_s	2064 (42/33 %) [B_2], ν_{as}
	2043 (m)				
$Ta(CO)_7^+$(g)[d]	**2**[b]	**2**[c]	**2**[c]	C_{3v} [sym]	C_{2v} [sym]
2168 (vw)	2169 (vw)	2168 (vw)	2168 (m)	2166 (4/28 %) [A_1], ν_s	2170 (7/48 %) [A_1], ν_s
2113 (m)	2121 (br, vw)	2105 (br, w)	2111 (m)	2104 (37/100 %) [E], ν_{as}	2126 (17/62 %) [A_1], ν_s
2089 (m)	2080 (vw)	2081 (w)	2085 (w)	2083 (65/4 %) [A_1], ν_{as}	2083 (0/100 %)* [A_2], ν_{as}
					2078 (52/10 %) [B_2], ν_{as}
					2074 (100/7 %) [B_1], ν_{as}
2067 (s)	2059 (sh, m)	2054 (vs)	2061 (m)	2067 (100/35 %) [E], ν_{as}	2062 (62/32 %) [A_1], ν_s
2056 (w)			2047 (m)	2057 (53/22 %) [A_1], ν_s	2060 (42/36 %) [B_2], ν_{as}
	2045 (m)				
		2030 (vs)			

[a] calculated at (RI-)B3LYP-D3(BJ)/def2-TZVPP level, scale factor 0.968 [48], all vibrations are IR and Raman active, with the exception of the IR inactive C_{2v} stretches at 2093 (Nb), 2083 cm^{-1} (Ta; marked with a '*'); [b] precipitated, C_{3v} predominant; [c] crystallized at 293 K, C_{2v} predominant; [d] gas phase; band intensities were estimated from [26].

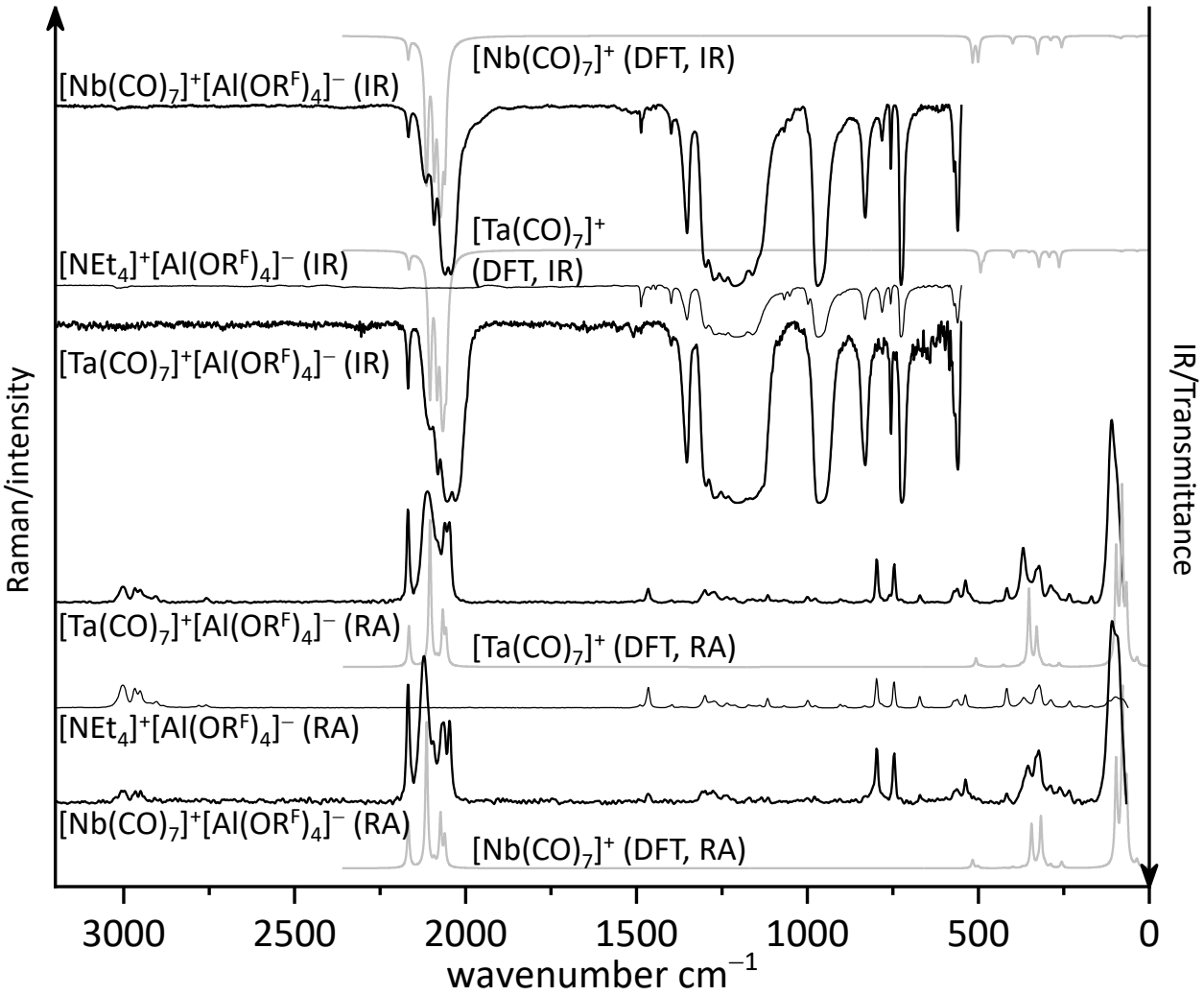

Supplementary Figure 11. Experimental and calculated (C_{3v}, (RI-)B3LYP-D3(BJ)/def2-TZVPP) IR and Raman spectra of **1**, **2** and co product $[NEt_4]^+[Al(OR^F)_4]^-$. The frequencies and intensities are listed in Supplemental Table 7 as well as given in the section "Detailed Synthesis of Compounds 1, 2, 4, 5 and 6" on p. 8-10.

Supplementary Table 8. Calculated stretching vibrations *v*(CO) of $M(CO)_7^+$ (M = Nb, *Ta*). All vibrations with the exception of 2093, *2083* cm^{-1} (IR inactive, marked with a star) are IR and Raman active.

C_{2v} calcd[a]	sym		C_{3v} calcd[a]	sym	
2173 (vw), *2170 (vw)*	A_1, ν_s	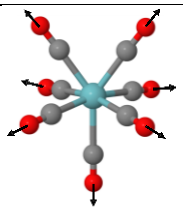	2168 (vw), *2166 (vw)*	A_1, ν_s	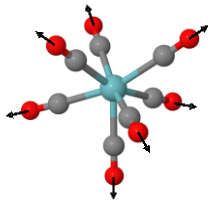
2134 (vw), *2126 (vw)*	A_1, ν_{as}	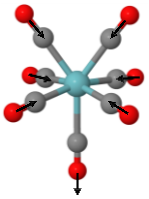	2114 (w), *2104 (m)*	E, ν_{as}	
2093 (vw)*, *2083 (vw)**	A_2, ν_{as}	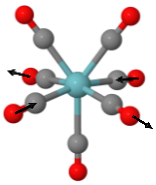	2114 (w), *2104 (m)*	E, ν_{as}	
2087 (m), *2078 (m)*	B_2, ν_{as}	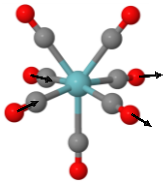	2092 (s), *2083 (s)*	A_1, ν_{as}	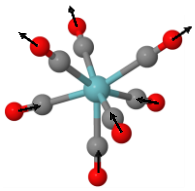
2083 (vs), *2074 (vs)*	B_1, ν_{as}	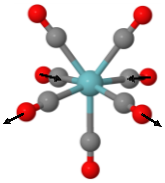	2073 (vs), *2067 (vs)*	E, ν_{as}	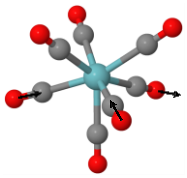
2066 (s), *2062 (s)*	A_1, ν_s	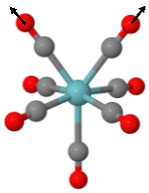	2073 (vs), *2067 (vs)*	E, ν_{as}	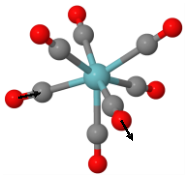
2064 (m), *2060 (m)*	B_2, ν_{as}	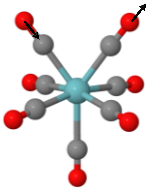	2061 (m), *2057 (m)*	A_1, ν_s	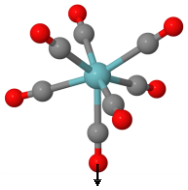

[a] Calculated at the (RI-)B3LYP-D3(BJ)/def2-TZVPP level, scale factor 0.968 [48]

IR and Raman Data of $[(o\text{-dfb})M(CO)_4]^+[Al\{OC(CF_3)_3\}_4]^-$ (M = Nb (**4**), Ta (**5**))

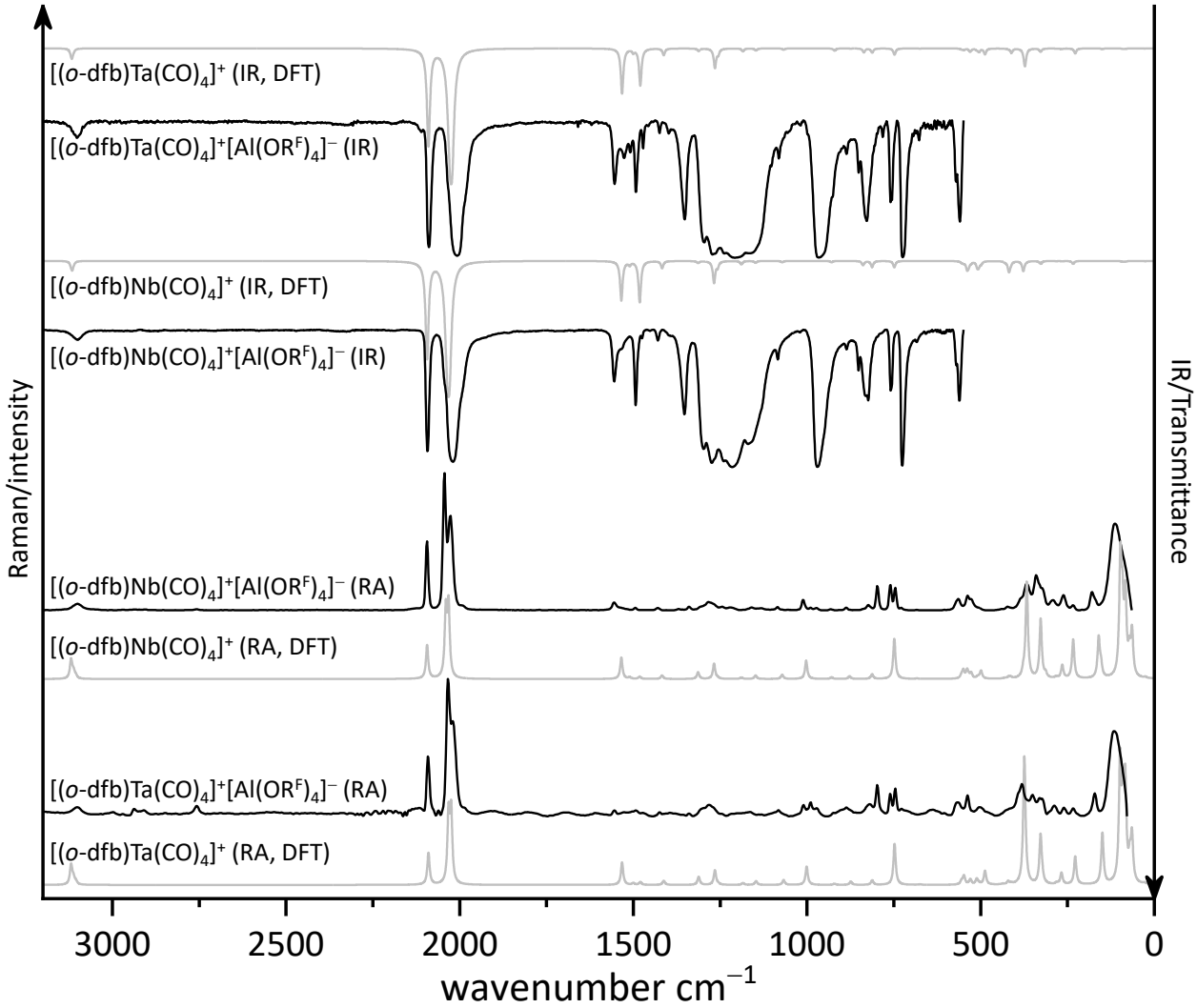

Supplementary Figure 12. Experimental and calculated IR and Raman spectra of **4** and **5**; calculated at the (RI-)B3LYP-D3(BJ)/def2-TZVPP level, scale factor 0.968 [48]. The frequencies and intensities are listed in Supplemental Table 9 as well as given in the section "Detailed Synthesis of Compounds 1, 2, 4, 5 and 6" on p. 8-10.

Supplementary Table 9. Experimental and calculated IR and Raman frequencies ν(CO) [cm^{-1}] of [(*o*-dfb)M(CO)$_4$]$^+$ **4**$^+$ (M = Nb) and **5**$^+$ (M = Ta); v: very, s: strong, m: medium, w: weak. All vibrations are IR and Raman active.

calcd[a]	**IR**	**Raman**	**IR**	**Raman**	**calcd**[a]	**sym**	
***C*$_s$** (M = Nb)	**4**[b]	**4**[b]	**5**[b]	**5**[b, c]	***C*$_s$** (M = Ta)		
2094 (m)	2093 (m)	2094 (m)	2111 (vw)	2091 (m)	2090 (m)	A', ν_s	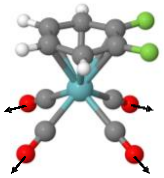
2040 (vw)		2044 (vs)	2089 (vs)	2034 (vs)	2032 (vw)	A'', ν_{as}	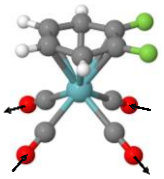
2032 (vs)	2024 (s)	2027 (s)	2007 (vs)	2020 (s)	2025 (vs)	A', ν_{as}	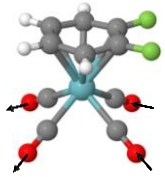
2032 (vs)					2024 (vs)	A'', ν_{as}	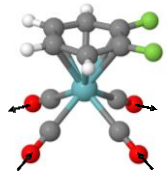

[a] calculated at the (RI-)B3LYP-D3(BJ)/def2-TZVPP level, scale factor 0.968 [48]; IR spectra are ATR corrected [b] condensed phase; [c] individual baseline correction.

Full Raman Data for $Ta_2(CO)_{12}$ (**6**)

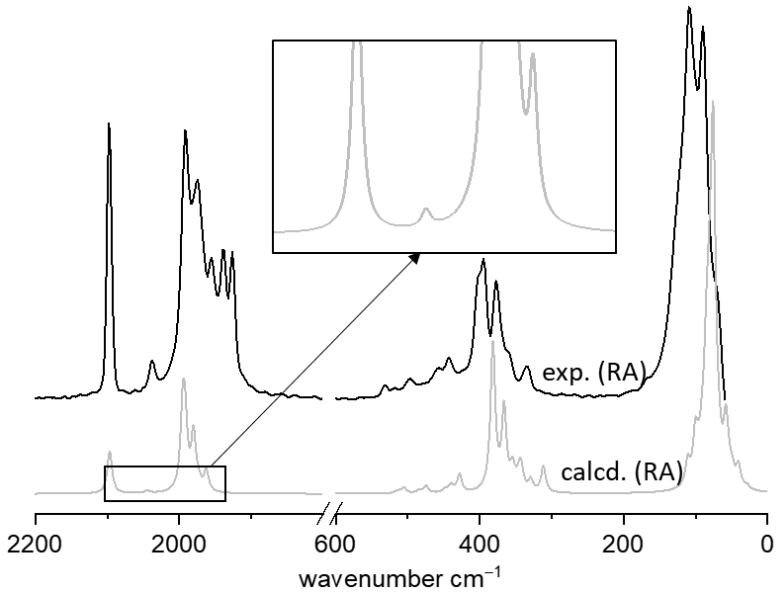

Supplementary Figure 13. Experimental and calculated IR and Raman spectra of **6**; calculated at the (RI-)B3LYP-D3(BJ)/def2-TZVPP level, scale factor 0.968 [48]. A Raman spectrum could be measured from crystals in the reaction flask. It shows two additional bands at 1939 and 1926 cm^{-1} compared with the calculated gas phase spectrum in D_2 symmetry. Apparently, the additional bands occur due to interactions in the solid state or due to the presence of both isomers with slightly differing band patterns in the sample. The frequencies and intensities are listed in Supplemental Table 10 as well as given in the section "Detailed Synthesis of Compounds 1, 2, 4, 5 and 6" on p. 8-10.

Supplementary Table 10. Experimental and calculated Raman frequencies of $Ta_2(CO)_{12}$ (**6**).

6	***D*₂ calcd[a]**	**Sym**	**attribute**	***ν*(CO)**
2097 (s)	2097 (vw)	A	ν_s (CO)	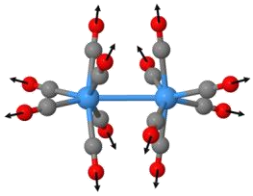
2038 (vw)	2044 (vw)	B_1	ν_{as} (CO)	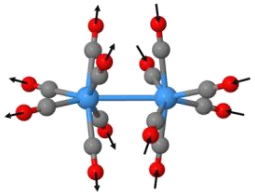

	2016	B_3	ν_{as} (CO)	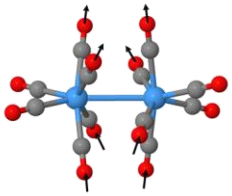
	2004	B_2	ν_{as} (CO)	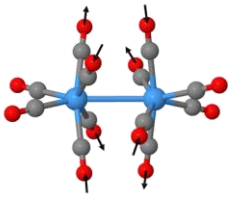
	1995 (w)	A	ν_{as} (CO)	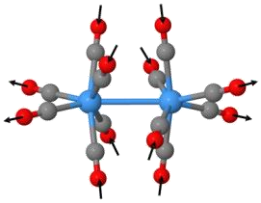
	1992	A	ν_{as} (CO)	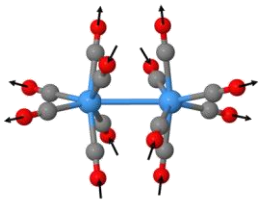
1991 (s)	1991	B_1	ν_{as} (CO)	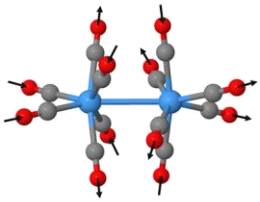
	1980 (vw)	B_2	ν_{as} (CO)	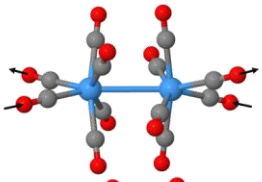
	1980	B_3	ν_{as} (CO)	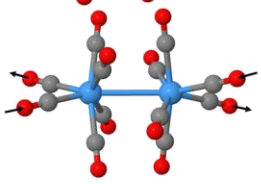
1975 (s)	1973	B_1	ν_{as} (CO)	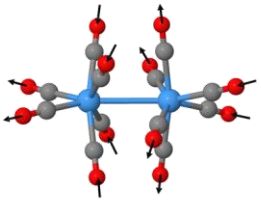

1955 (m)	1969	B_2	ν_{as} (CO)	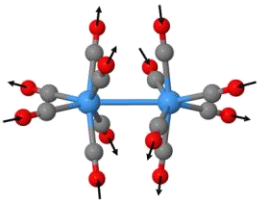
	1962 (vw)	B_3	ν_{as} (CO)	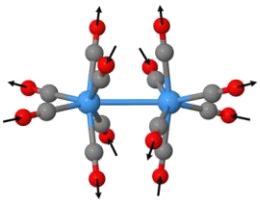
1939 (m)				
1926 (m)				
531 (vw)	519	B_3	δ_{as} (CO)	
	518	B_2	δ_{as} (CO)	
	516	B_3	δ_{as} (CO)	
	515	B_2	δ_{as} (CO)	
	512	A	δ_s (CO)	
	511	B_1	δ_{as} (CO)	
	505 (vw)	A	δ_s (CO)	
497 (vw)	493	B_1	δ_{as} (CO)	
	484 (vw)	A	δ_s (CO)	
	476	B_1	δ_{as} (CO)	
	475 (vw)	B_2	δ_{as} (CO)	
	473	B_3	δ_{as} (CO)	
457 (vw)	448 (sh)	B_2	δ_{as} (CO)	
443 (vw)	443	B_1	δ_{as} (CO)	
	440 (vw)	A	δ_s (CO)	
	428 (vw)	B_3	δ_{as} (CO)	
395 (w)	388	B_2	δ_{as} (CO)	
	386	B_3	δ_{as} (CO)	
	384	B_1	ν_{as} (CO), δ_{as} (CO)	
	382	B_3	δ_{as} (CO)	
	382 (w)	A	ν_s (CO), δ_s (CO)	
377 (w)	378	B_2	δ_{as} (CO)	
	369	B_1	δ_{as} (CO)	
	366 (w)	A	δ_s (CO)	
	364	B_2	ν_{as} (CO), δ_{as} (CO)	
360 (vw)	360	B_3	δ_{as} (CO)	
	355 (vw)	A	δ_s (CO)	
	351	B_1	δ_{as} (CO)	
	347	B_2	ν_{as} (CO), δ_{as} (CO)	
	345	B_3	ν_{as} (CO), δ_{as} (CO)	
	343 (vw)	A	δ_s (CO)	
	342	B_1	δ_{as} (CO)	
335 (vw)	334	B_3	ν_{as} (CO), δ_{as} (CO)	

	329 (vw)	B_2	δ_{as} (CO)
	312 (vw)	A	δ_s (CO)
	303	B_1	δ_{as} (CO)
	111 (vw)	A	δ_s (MC), δ_s (CO)
109 (vs)	111	B_3	δ_s (MC), δ (CO)
	101	A	*v* (MM), δ_s (MC), δ_s (CO)
	99 (vw)	B_2	δ (MC)
	97	B_1	δ (MC)
	96	A	δ (MC)
90 (vs)	91	B_3	δ (MC)
	91	B_1	δ (MC)
	86	B_2	δ (MC)
	84	B_2	δ (MC)
	83 (sh)	B_1	δ (MC)
	80	A	δ (MC)
	78	B_3	δ (MC)
	77	B_1	*v* (MM), δ_{as} (MC)
	75 (vs)	A	*v* (MM), δ_s (MC)
	74	B_2	δ (MC)
	68	B_3	δ (MM/MC)
	59	B_3	δ (MM)
	58 (w)	B_2	δ (MM)
	53	A	δ (MC)
	49	B_3	δ (MC)
	40 (vw)	A	δ (MC)
	36	B_2	δ (MC)
	28 (sh)	B_1	δ (MC)

[a] Calculated at the (RI-)B3LYP-D3(BJ)/def2-TZVPP) level, scaled by 0.968 [48]; [b] intensities from picked bands in calculated Raman spectrum.

6 ^{93}Nb NMR Spectra of the Temperature and CO Pressure Dependent Equilibrium of $[Nb(CO)_7]^+[Al\{OC(CF_3)_3\}_4]^-$ (1) and $[(o\text{-dfb})Nb(CO)_4]^+[Al\{OC(CF_3)_3\}_4]^-$ (4)

For analysis by NMR-spectroscopy, the reaction solution was cannulated into a NMR-tube at –30 °C under a reverse flow of Argon after the silver precipitated and measured several times, while the temperature increased stepwise up to room temperature (Supplementary Figure 14). At –30 °C the main signal at –1431 ppm belongs to the heptacarbonyl cation **1**$^+$ (marked with *), which is in equilibrium with **4**$^+$ (marked with ◊) at –1459 ppm, dependent on temperature and CO pressure until only **4**$^+$ remains (Table S9). The signal shift is due to different measuring temperatures (Table S9). The reversibility of the reaction could be shown by storing the NMR-tube overnight at –30 °C under CO-pressure (3 bar). The next day **1**$^+$ was obtained again. Besides the main products, side products were detected at –1493 and –1512 ppm (298 K, marked with ‡). Further investigation of the solvent suggests that niobium compounds like piano stool complexes resulted from other fluorobenzenes, which could be found as trace impurities in *o*-dfb.

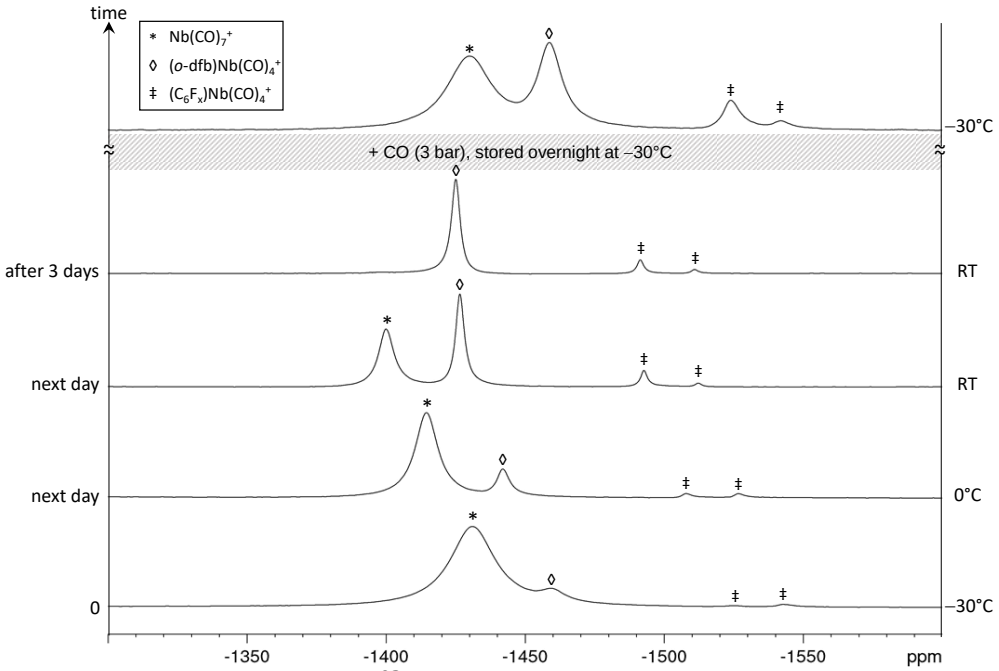

Supplementary Figure 14. Section of ^{93}Nb NMR spectra (97.95 MHz, *o*-dfb) of the temperature and CO pressure dependent equilibrium between **1** and **4**. Signals of **1**$^+$ are marked with *, **4**$^+$ with ◊ and side products probably caused by solvent impurities of fluorobenzenes with ‡. The spectra were recorded, before we developed the method to remove all arene impurities from *o*-DFB by distallation from $Ag[Al(OR^F)_4]$.

Supplementary Table 11. ^{93}Nb NMR chemical shift (97.95 MHz, *o*-dfb) of **1**$^+$ and **4**$^+$ at different temperatures.

Temp. [K]	chemical shift [ppm]	
	1$^+$	**4**$^+$
243	–1431	–1459
273	–1414	–1441
298	–1400	–1427

7 Computational Details on Relaxed Potential Energy Scan Along $C_{3v} \rightarrow C_{2v} \rightarrow C_{3v}$ Path with Varying Point Charges 0 - –0.7 *e*

Gas phase DFT calculations with point charges from 0 to –0.7 e were carried out to simulate solid state effects on the symmetry of the cation. Atom coordinates of the experimentally obtained structure of **2** were used, whereby from the anion only ten fluorine atoms within an O-F distances below 3 Å were included (Table 12). To generate an input file, point charges *q* were placed on the fixed positions of the fluorine atoms. In Supplementary Figure 15 the relative electronic energy of each geometry with different point charges is plotted against the C1-Ta-C4 bond angle. The use of the different basis sets and fuctionals (RI-)BP86&-D3(BJ)/def2-SVP and (RI-)B3LYP-D3(BJ)/def2-TZVPP showed a very small difference in the activation barrier of 2.3 kJ/mol (B3LYP) / 2.6 kJ/mol (BP86) between the C_{3v} and C_{2v} symmetry. The qualitative information of the scan by the curves remains, on the other hand, remains unchanged. IR spectra were simulated for the minimum structure (marked with *) of each scan.

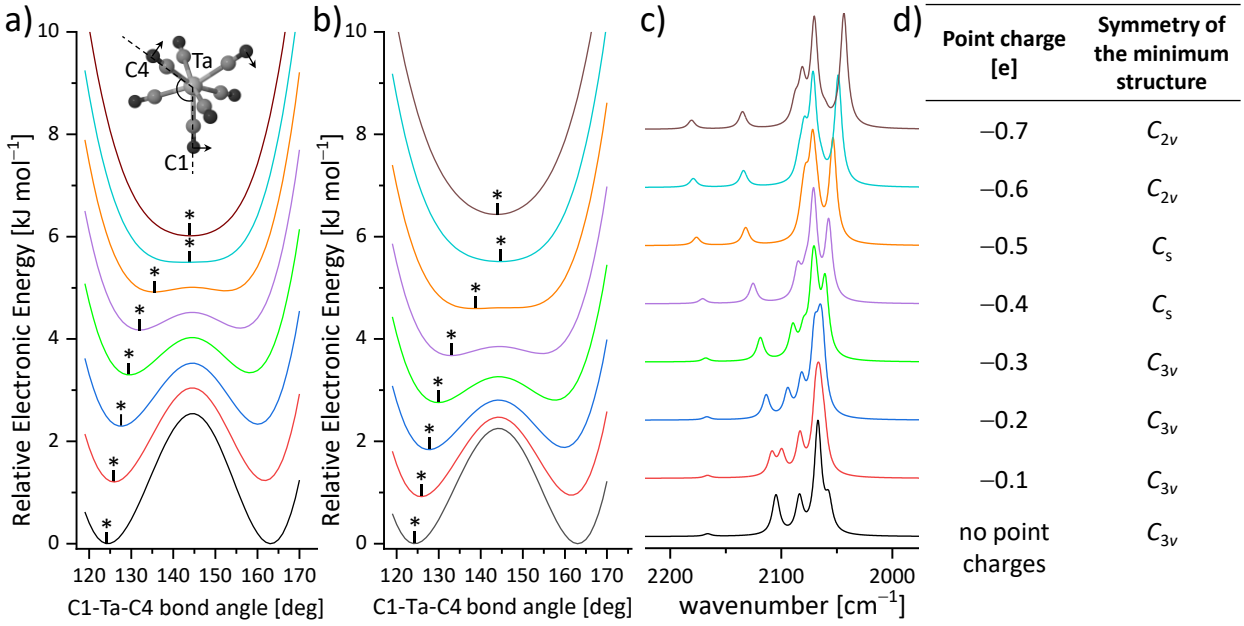

Supplementary Figure 15. Relaxed potential energy scan along $C_{3v} \rightarrow C_{2v} \rightarrow C_{3v}$ path (**a**) with varying point charges 0 - –0.7 *e* (**d**) and corresponding IR spectra (**c**) of the global minimum structure (marked with a "*" in **a** and **b**). The potential energy scan was calculated at the (RI-)BP86-D3(BJ)/def2-SVP (**a**) or (RI-)B3LYP-D3(BJ)/def2-TZVPP (**b**) level. IR spectra were calculated at the (RI-)B3LYP-D3(BJ)/def2-TZVPP level, scaling factor 0.968 (*28*). Positions of the fixed point charges have been selected from the experimental structure considering all fluorine atoms with a O--F distance of or below 3 Å. The scale of the y-axis in the scan plot (**a** and **b**) does not show any relation between the calculations, but allows an estimation of the energy differences.

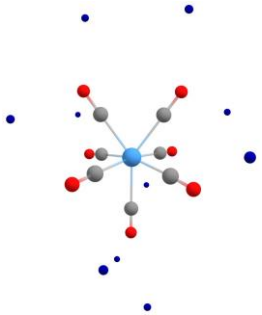

Supplementary Figure 16. Calculated $\mathbf{2}^{+}$ surrounded by 10 point charges shown in dark blue.

Table 12. O-F distances [Å] of **2**. Symmetry generated distances are omitted. Those shown in bold including their symmetry-generated equivalents were considered for the calculation.

d_{O1-F}	d_{O2-F}	d_{O3-F}	d_{O4-F}
2.9842(2)	**2.8889(2)**	**2.9879(1)**	**2.9326(2)**
2.9842(2)	3.0125(2)	3.0125(2)	2.9752(2)
3.0577(1)	3.1398(2)	3.2152(2)	3.0187(2)
3.0577(1)	3.1727(2)	3.2165(2)	3.0476(2)
3.2807(2)	3.1735(2)	3.3571(2)	3.0918(2)
3.2807(2)	3.2386(2)	3.4522(2)	3.1577(2)
3.6128(2)	3.6455(2)	3.5607(2)	3.3962(2)
3.6128(2)	3.7471(2)	3.7829(2)	3.5830(3)
3.9447(3)	3.8331(2)	3.8758(2)	3.8642(2)
3.9447(3)	3.8718(2)	3.9075(2)	4.2665(3)
4.2080(3)	3.8810(2)	4.0022(3)	4.2798(3)
4.2080(3)	4.1063(2)	4.1981(3)	4.3851(2)
4.2291(3)	4.1234(2)	4.2848(3)	4.5197(3)
4.2291(3)	4.2412(2)	4.3456(2)	4.5215(2)
4.7315(3)	4.6415(3)	4.4185(3)	4.6717(3)
4.7315(3)	4.7996(3)	4.8829(3)	4.6909(3)
4.7914(3)		4.9108(2)	4.7169(3)
4.7914(3)		4.9627(3)	4.7369(3)
			4.7846(2)
			4.8813(2)
			4.9166(4)
			4.9493(3)

8 UV/VIS Spectra of 2, 4 and 5

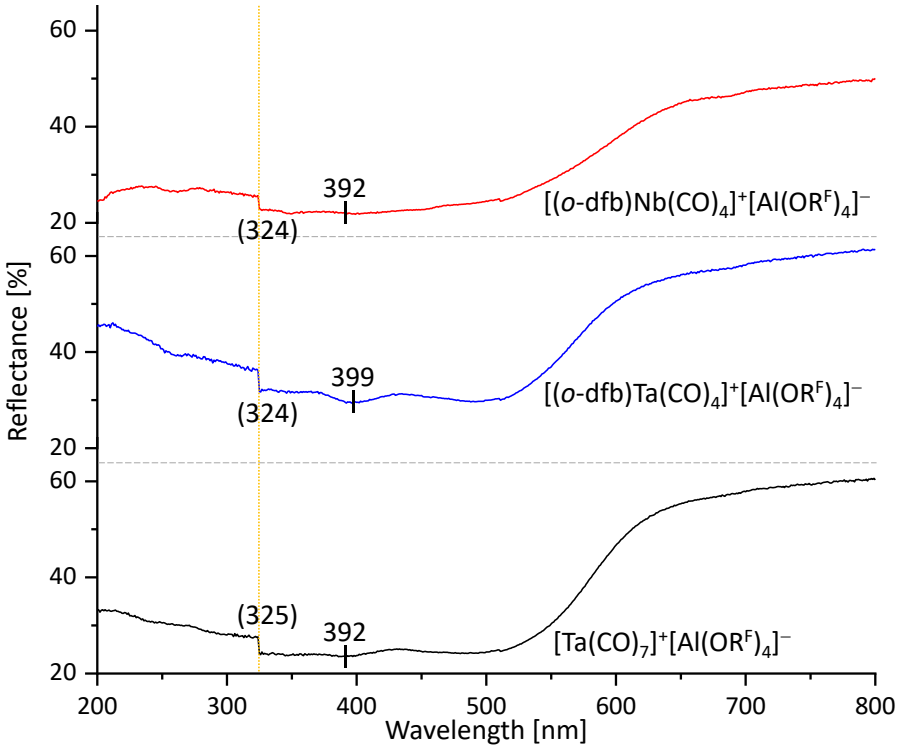

Supplementary Figure 17. Diffuse reflectance spectra of compounds **2** (black), **4** (red) and **5** (blue). Maximum absorption at 392 nm (**2**, **5**) and 399 nm (**4**). The yellow dashed line indicates the change of the lamps. **1** was too sensitive to run a spectrum. The band positions are also given in the section "Detailed Synthesis of Compounds 1, 2, 4, 5 and 6" on p. 8-10.

9 Single-Crystal Diffraction Results for Compounds 1 - 6

Supplementary Table 13. Crystallographic data for complexes **1** – **6**.

	1	**2**	**3a**	**3b**
CCDC	1909275	1909276	1909277	1909279
Empirical formula	$C_{23}AlF_{36}NbO_{11}$	$C_{23}AlF_{36}O_{11}Ta$	$C_{92}H_{24}Ag_6Al_2F_{84}Nb_4O_{32}$	$C_{80}H_8Ag_6Al_2F_{88}Nb_4O_{32}$
Formula weight	1256.12	1344.16	4309.93	4225.68
Temperature/K	100(2)	100(2)	100(2)	100(2)
Crystal system	orthorhombic	orthorhombic	monoclinic	orthorhombic
Space group	$C222_1$	$C222_1$	$P2_1/c$	$Pbca$
a/Å	9.3829(6)	9.3419(7)	30.6389(12)	30.4820(12)
b/Å	20.0929(13)	20.1079(15)	19.1641(8)	21.4374(8)
c/Å	20.1106(13)	20.0816(16)	22.0852(8)	36.6092(14)
α/°	90	90	90	90
β/°	90	90	98.788(2)	90
γ/°	90	90	90	90
Volume/Å^3	3791.4(4)	3772.2(5)	12815.5(9)	23922.5(16)
Z	4	4	4	8
ρ_{calc}g/cm^3	2.201	2.367	2.234	2.347
μ/mm^{-1}	0.573	3.171	1.448	1.553
F(000)	2416.0	2544.0	8240.0	16064.0
Crystal size/mm^3	0.100 × 0.080 × 0.020	0.100 × 0.080 × 0.030	0.080 × 0.050 × 0.050	0.080 × 0.020 × 0.020
Radiation	MoKα (λ = 0.71073)	MoKα (λ = 0.71073)	MoKα (λ = 0.71073)	MoKα (λ = 0.71073)
2Θ range for data collection/°	2.024 to 52.87	2.028 to 52.834	1.344 to 63.834	2.224 to 50.14
Index ranges	-11 ≤ h ≤ 10, -25 ≤ k ≤ 25, -25 ≤ l ≤ 22	-11 ≤ h ≤ 11, -25 ≤ k ≤ 24, -25 ≤ l ≤ 24	-45 ≤ h ≤ 41, -25 ≤ k ≤ 28, -32 ≤ l ≤ 32	-36 ≤ h ≤ 36, -25 ≤ k ≤ 25, -43 ≤ l ≤ 43
Reflections collected	46351	43646	446595	743919
Independent reflections	3895 [R_{int} = 0.0211, R_{sigma} = 0.0106]	3849 [R_{int} = 0.0530, R_{sigma} = 0.0362]	38990 [R_{int} = 0.0585, R_{sigma} = 0.0509]	21232 [R_{int} = 0.0966, R_{sigma} = 0.0312]
Data/restraints/parameters	3895/0/330	3849/0/330	38990/18829/2266	21232/50458/3324
Goodness-of-fit on F^2	1.081	1.030	1.058	1.264
Final R indexes [I>=2σ (I)]	R_1 = 0.0154, wR_2 = 0.0405	R_1 = 0.0219, wR_2 = 0.0423	R_1 = 0.0433, wR_2 = 0.0843	R_1 = 0.0702, wR_2 = 0.1514
Final R indexes [all data]	R_1 = 0.0155, wR_2 = 0.0406	R_1 = 0.0250, wR_2 = 0.0429	R_1 = 0.0752, wR_2 = 0.0950	R_1 = 0.0804, wR_2 = 0.1559
Largest diff. peak/hole / e Å^{-3}	0.23/-0.37	0.97/-1.06	2.77/-0.69	1.46/-1.08

Continued **Supplementary Table 13.**

	4	5	6a	6b
CCDC	1909278	1909449	1909450	1909274
Empirical formula	$C_{26}H_4AlF_{38}NbO_8$	$C_{26}H_4AlF_{38}O_8Ta_{1.08}$	$C_{12}O_{12}Ta_2$	$C_{12}O_{12}Ta_2$
Formula weight	1286.20	1388.70	698.02	698.02
Temperature/K	100(2)	100(2)	100(2)	100(2)
Crystal system	monoclinic	monoclinic	orthorhombic	triclinic
Space group	$P2_1/n$	$P2_1/n$	$Pbca$	$P\bar{1}$
a/Å	13.050(4)	13.0435(6)	13.3988(10)	8.9441(10)
b/Å	18.799(5)	18.7956(8)	15.0804(11)	9.4906(11)
c/Å	16.005(4)	15.9397(7)	16.6239(12)	10.1265(11)
α/°	90	90	90	78.600(3)
β/°	94.187(12)	94.046(2)	90	83.777(3)
γ/°	90	90	90	89.970(3)
Volume/Å^3	3916.0(19)	3898.0(3)	3359.0(4)	837.47(16)
Z	4	4	8	2
ρ_{calc}g/cm^3	2.182	2.366	2.761	2.768
μ/mm^{-1}	0.560	3.296	13.082	13.118
F(000)	2480.0	2631.0	2512.0	628.0
Crystal size/mm^3	0.2 × 0.2 × 0.1	0.2 × 0.1 × 0.08	0.080 × 0.020 × 0.010	0.150 × 0.030 × 0.030
Radiation	MoKα (λ = 0.71073)	MoKα (λ = 0.71073)	MoKα (λ = 0.71073)	MoKα (λ = 0.71073)
2Θ range for data collection/°	3.348 to 59.366	3.356 to 50.2	4.748 to 61.214	4.128 to 66.31
Index ranges	-18 ≤ h ≤ 18, -26 ≤ k ≤ 25, -22 ≤ l ≤ 21	-11 ≤ h ≤ 10, -14 ≤ k ≤ 22, -19 ≤ l ≤ 18	-18 ≤ h ≤ 19, -21 ≤ k ≤ 21, -22 ≤ l ≤ 23	-13 ≤ h ≤ 13, -14 ≤ k ≤ 14, -15 ≤ l ≤ 15
Reflections collected	149377	11830	86652	51350
Independent reflections	10766 [R_{int} = 0.0326, R_{sigma} = 0.0237]	5664 [R_{int} = 0.0192, R_{sigma} = 0.0286]	5092 [R_{int} = 0.1117, R_{sigma} = 0.0672]	6152 [R_{int} = 0.0517, R_{sigma} = 0.0354]
Data/restraints/parameters	10766/20454/1623	5664/16241/1368	5092/0/235	6152/0/235
Goodness-of-fit on F^2	1.028	1.146	1.048	1.045
Final R indexes [I>=2σ (I)]	R_1 = 0.0438, wR_2 = 0.1095	R_1 = 0.0510, wR_2 = 0.1349	R_1 = 0.0509, wR_2 = 0.1087	R_1 = 0.0253, wR_2 = 0.0420
Final R indexes [all data]	R_1 = 0.0607, wR_2 = 0.1197	R_1 = 0.0566, wR_2 = 0.1381	R_1 = 0.0853, wR_2 = 0.1264	R_1 = 0.0390, wR_2 = 0.0451
Largest diff. peak/hole / e Å^{-3}	0.85/-0.54	1.42/-1.74	5.43/-1.77	1.61/-1.57

10 Full Details to the Single-Crystal Structure Determinations

All crystallographic cif-files were checked with the program checkcif. All A and B alerts were explained and answered in the following under the relevant structures. All other alerts can be found in the respective cif-files.

Structure of **1**

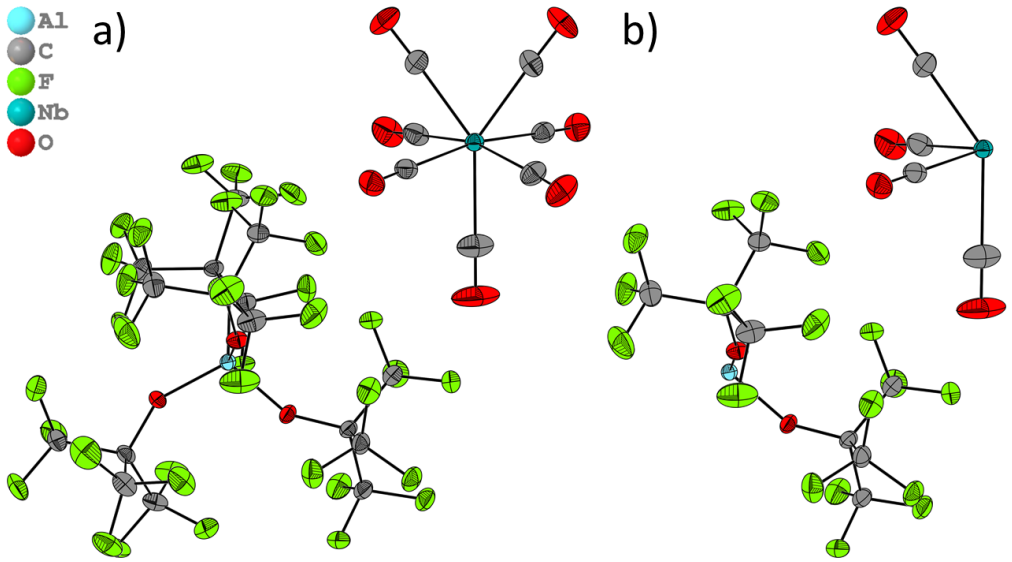

Supplementary Figure 18. Molecular structure (**a**) and asymmetric unit (**b**) of **1**. Thermal ellipsoids are shown at the 50 % probability level.

Structures of **1** and **2** were not disordered. The crystals were twinned by pseudo merohery with a twin law of -1 0 0 0 0 1 0 1 0 with 9% (**1**) and 2% (**2**). Additionally, one of the twin components in **1** is partially twinned by inversion with 94%. In **2** one twin component is partially twinned by inversion with 6%, the other with 48%.

A-, B- and C-level alerts of structure **1** in CheckCIF:

Alert level C

PLAT034_ALERT_1_C _vrf_PLAT034_IK_WU18_2_0m_final

PROBLEM: No Flack Parameter Given. Z > Si, NonCentro .... Please Do !

RESPONSE: The crystal turned out to be twinned by pseudo merohery with a twin law of -1 0 0 0 0 1 0 1 0 with 9%. Additionally, one of the twin components is partially twinned by inversion with 94%.

Structure of **2**

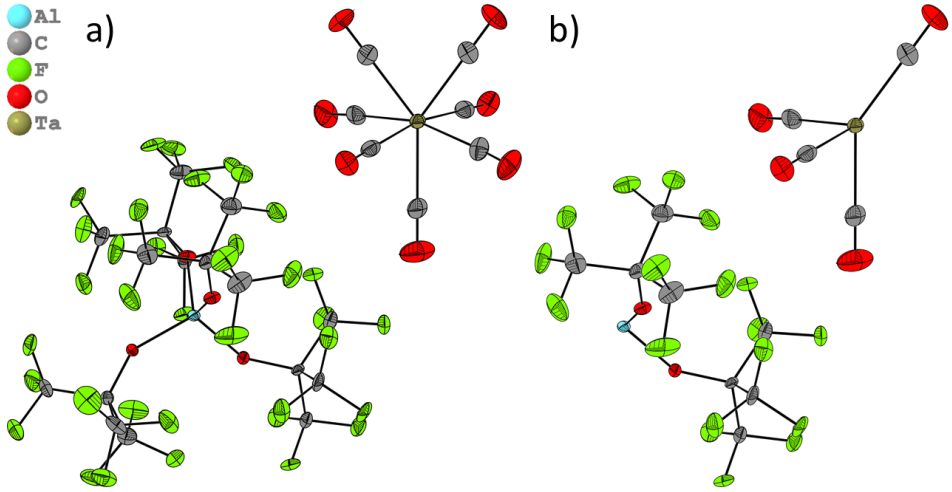

Supplementary Figure 19. Molecular structure (**a**) and asymmetric unit (**b**) of **2**. Thermal ellipsoids are shown at the 50 % probability level.

A-, B- and C-level alerts of structure **2** in CheckCIF:

Alert level C

PLAT034_ALERT_1_C_vrf_PLAT034_c2221_a

PROBLEM: No Flack Parameter Given. Z > Si, NonCentro .... Please Do !

RESPONSE: The crystal turned out to be twinned by pseudo merohery with a twin law of -1 0 0 0 0 1 0 1 0 with 2%. Additionally, one twin component is partially twinned by inversion with 6%, the other with 48%.

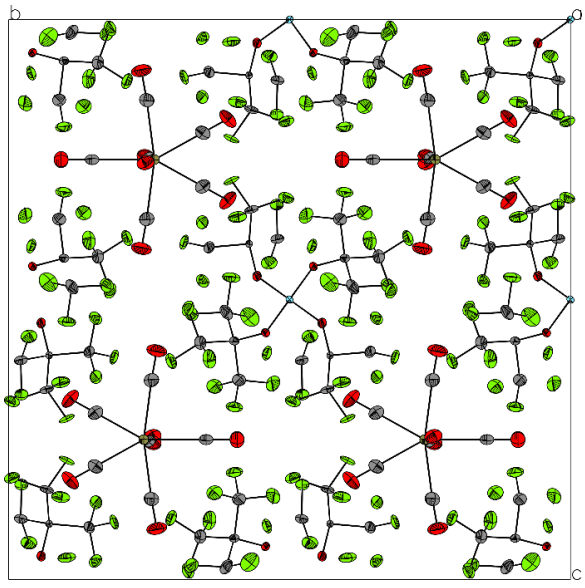

Supplementary Figure 20. Filled unit cell of **2**. Thermal ellipsoids are shown at the 50 % probability level.

Structure of **3a** and **b**

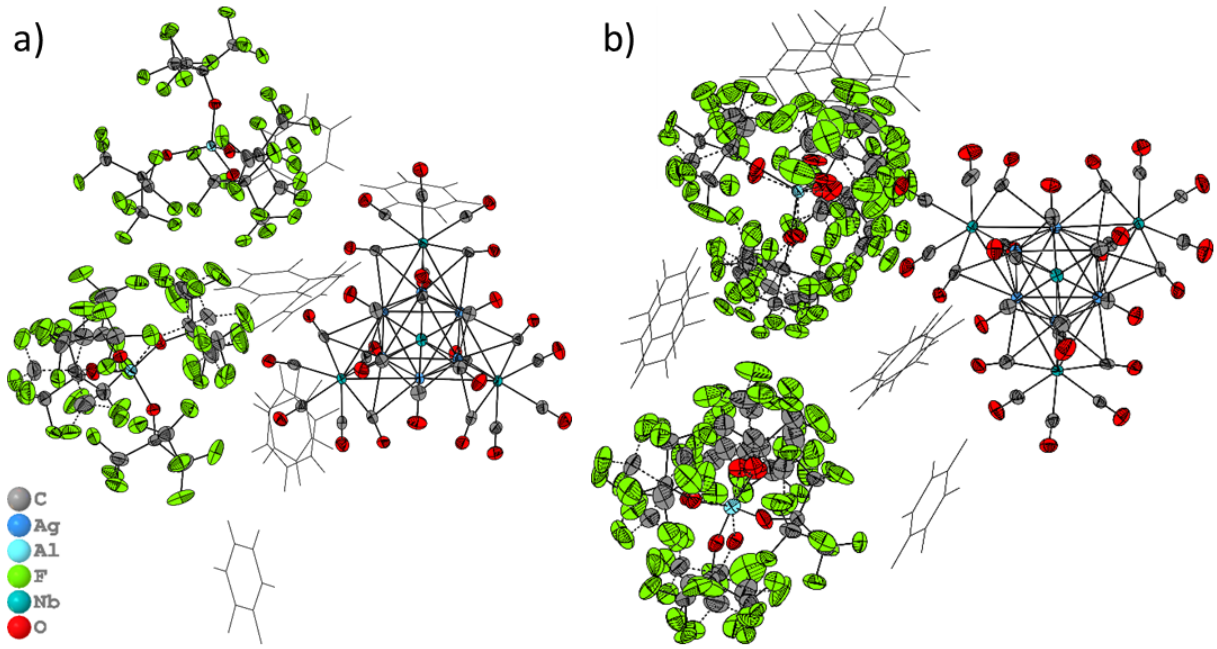

Supplementary Figure 21. Molecular structures of **3a** and **b**. Thermal ellipsoids are shown at the 50 % probability level. Solvent molecules (**a)** *o*-dfb, **b)** 4FB) are displayed as wire frame and were partly disordered twice or three times. Disorders of the anions are included with dashed bonds.

The use of different solvents in the reaction resulted in two structures with different space groups. Six *o*-dfb molecules were found in the monoclinic (*P*21/*c*) structure of **3a** and four 4FB molecules were detected in the orthorhombic (*Pbca*) structure of **3b**.

The positive residual density is caused by absorption in both cases. The six heavy silver and four niobium atoms in the supertetrahedron with their huge electron densities cause large absorption of the x-ray beam that led to positive residual densities observed in the difference fourier maps.

The poor data/parameter ratio in the structure of **3b** is caused by the disorder of both the anion and the solvent molecules, especially of the strongly oscillating fluorine atoms, required the used set of parameters including the use of restraints (SADI and SIMU).

A-level alerts of structure **3a** in CheckCIF (no B-alerts):

Alert level A
PLAT973_ALERT_2_A Check Calcd Positive Resid. Density on Ag6 3.13 eA-3
Author Response: Caused by absorption of the x-ray light by the heavy element Ag
PLAT973_ALERT_2_A Check Calcd Positive Resid. Density on Ag2 2.96 eA-3
Author Response: Caused by absorption of the x-ray light by the heavy element Ag
PLAT973_ALERT_2_A Check Calcd Positive Resid. Density on Ag5 2.93 eA-3
Author Response: Caused by absorption of the x-ray light by the heavy element Ag
PLAT973_ALERT_2_A Check Calcd Positive Resid. Density on Ag4 2.79 eA-3
Author Response: Caused by absorption of the x-ray light by the heavy element Ag

PLAT973_ALERT_2_A Check Calcd Positive Resid. Density on Ag3 2.70 eA-3
Author Response: Caused by absorption of the x-ray light by the heavy element Ag
PLAT973_ALERT_2_A Check Calcd Positive Resid. Density on Ag1 2.55 eA-3
Author Response: Caused by absorption of the x-ray light by the heavy element Ag
PLAT973_ALERT_2_A Check Calcd Positive Resid. Density on Nb4 2.41 eA-3
Author Response: Caused by absorption of the x-ray light by the heavy element Ag
PLAT973_ALERT_2_A Check Calcd Positive Resid. Density on Nb2 2.24 eA-3
Author Response: Caused by absorption of the x-ray light by the heavy element Ag
PLAT973_ALERT_2_A Check Calcd Positive Resid. Density on Nb1 2.11 eA-3
Author Response: Caused by absorption of the x-ray light by the heavy element Ag

B-level alerts of structure **3b**:

The $C(CF_3)_3$ groups of the fluorinated *tert*-butyl rests of the anion $[Al(OR^F)_4]^-$ rotated and fliped around the C-O axes. This flexibility resulted in many atom positions in the structure, which had to be modulated in the structure determinations. The heavy disorder of the both the anion and solvent molecules required the used set of parameters including the use of restraints (SADI and SIMU), resulting in a poor data to parameter ratio.

Alert level B
PLAT088_ALERT_3_B Poor Data / Parameter Ratio ..... 6.39 Note
Author Response: Disorder of both the anion and the solvent molecules, especially of the strongly oscillating fluorine atoms, require the set parameters.
PLAT213_ALERT_2_B Atom F3_21 has ADP max/min Ratio ..... 4.8 prolat
Author Response: Caused by heavy disorder.
PLAT213_ALERT_2_B Atom F7_4 has ADP max/min Ratio ..... 4.8 prolat
Author Response: Caused by heavy disorder.
PLAT250_ALERT_2_B Large U3/U1 Ratio for Average U(i,j) Tensor .... 6.7 Note
Author Response: Caused by heavy disorder.
PLAT250_ALERT_2_B Large U3/U1 Ratio for Average U(i,j) Tensor .... 7.2 Note
Author Response: Caused by heavy disorder.

Structure of **4**

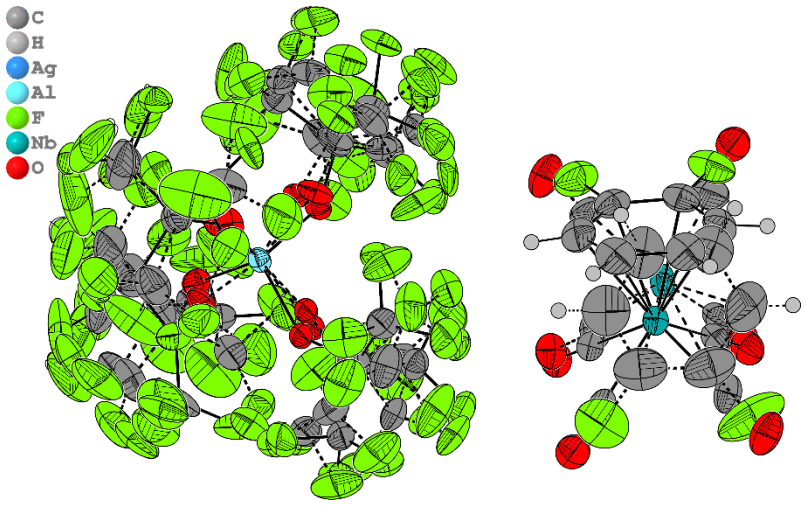

Supplementary Figure 22. Crystal structure of **4**. Thermal ellipsoids are shown at the 50 % probability level. Disorders are included with dashed bonds.

The $C(CF_3)_3$ groups of the fluorinated *tert*-butyl rests of the anion $[Al(OR^F)_4]^-$ rotated and fliped around the C-O axes. This flexibility resulted in many atom positions in the structure, which had to be modulated in the structure determinations. The heavy disorder of the both the anion and solvent molecules required the used set of parameters including the use of restraints (SADI and SIMU), resulting in a poor data to parameter ratio.

Disorder of both the anion and cation, result in a poor data to parameter ratio. The complete cation occupies two positions with an occupancy of 84% and 16% accordingly.

B-level alerts of structure **4**:

_vrf_PLAT088_IK_WU19_0m

PROBLEM: Poor Data / Parameter ratio 6.63 Note

RESPONSE: Disorder of both the anion and the cation, especially of the strongly oscillating fluorine atoms, require the set parameters.

;

_vrf_PLAT220_IK_WU19_0m

PROBLEM: Non-Solvent Resd 1 F Ueq(max)/Ueq(min) Range 6.3 Ratio

RESPONSE: Disorder of both the anion and the cation, especially of the strongly oscillating fluorine atoms, require the set parameters.

Structure of **5**

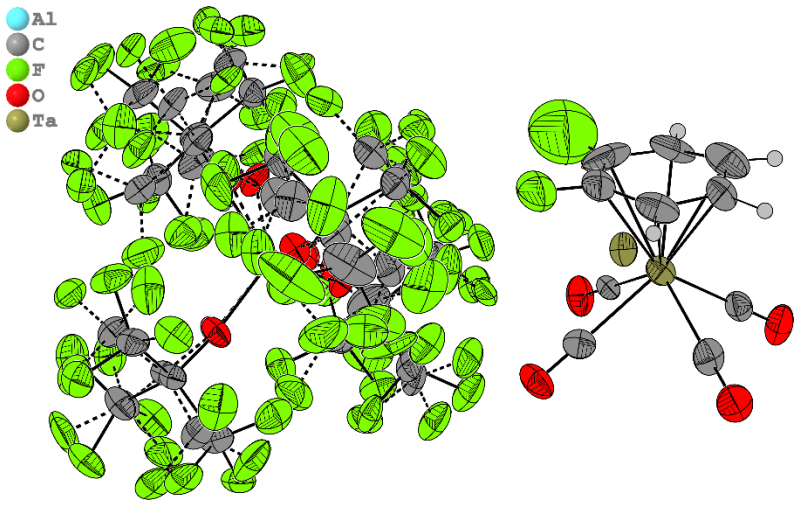

Supplementary Figure 23. Crystal structure of **5**. Thermal ellipsoids are shown at the 50 % probability level. Disorders are included with dashed bonds.

The $C(CF_3)_3$ groups of the fluorinated *tert*-butyl rests of the anion $[Al(OR^F)_4]^-$ rotated and fliped around the C-O axes. This flexibility resulted in many atom positions in the structure, which had to be modulated in the structure determinations. The heavy disorder of the both the anion and solvent molecules required the used set of parameters including the use of restraints (SADI and SIMU), resulting in a poor data to parameter ratio.

The complete cation is disordered. A second orientation of the cation, however, could not be determined clearly. Therefore, only the disordered Tantalum position was introduced into the structure. The size of the one fluorine atom ellipsoid of the *o*-dfb ligand is also caused by unmodelled disorder.

A- and B- level alerts of structure **5**:

Alert level A

PLAT029_ALERT_3_A _diffrn_measured_fraction_theta_full value Low . 0.814 Why?

Author Response: Caused by disorder.

PLAT088_ALERT_3_A Poor Data / Parameter Ratio ..... 4.14 Note

Author Response: The disorder of the anion requires the parameters used to keep the model stable.

PLAT307_ALERT_2_A Isolated Metal Atom found in Structure (Unusual) Ta1B Check

Author Response: The cation is disordered, but only the position of the tantalum atom can be assigned.

Alert level B

PLAT230_ALERT_2_B Hirshfeld Test Diff for F2B --C2A . 11.5 s.u.

Author Response: Caused by disorder.

PLAT911_ALERT_3_B Missing FCF Refl Between Thmin & STh/L= 0.597 637 Report

Author Response: Caused by disorder.

Structure of **6a**

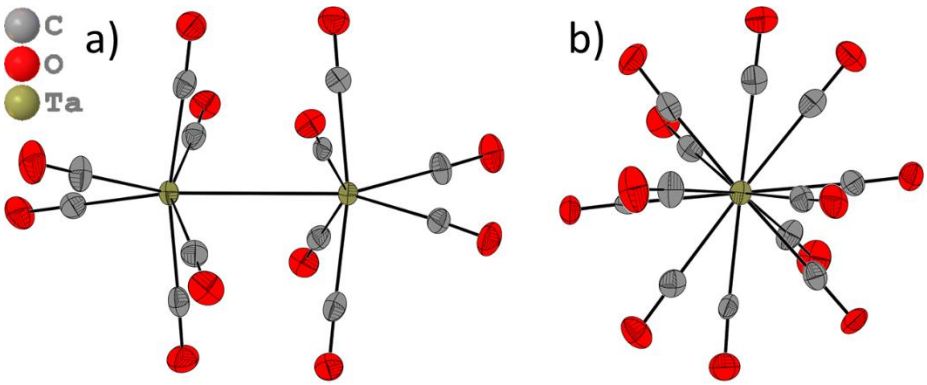

Supplementary Figure 24. Crystal structure of **6a**, side (**a**) and front view along the Ta-Ta bond (**b**). Thermal ellipsoids are shown at the 50 % probability level.

The positive residual density is caused by absorption. The two heavy tantalum atoms with their huge electron densities in the structure else only formed by light atoms (C, O) cause large absorption of the x-ray beam that led to positive residual densities observed in the difference fourier maps. The higher residual density peak in **6a** is caused by absorption. It is located 0.06 Å from Ta2.

A- and B- level alerts of structure **6a**:

Alert level A

PLAT971_ALERT_2_A Check Calcd Resid. Dens. 0.75A From Ta1 3.67 eA-3

Author Response: Caused by absorption of the x-ray light by the heavy element Ta.

PLAT971_ALERT_2_A Check Calcd Resid. Dens. 0.78A From Ta2 3.64 eA-3

Author Response: Caused by absorption of the x-ray light by the heavy element Ta.

PLAT973_ALERT_2_A Check Calcd Positive Resid. Density on Ta2 6.02 eA-3

Author Response: Caused by absorption of the x-ray light by the heavy element Ta.

PLAT973_ALERT_2_A Check Calcd Positive Resid. Density on Ta1 5.26 eA-3

Author Response: Caused by absorption of the x-ray light by the heavy element Ta.

Alert level B

PLAT971_ALERT_2_B Check Calcd Resid. Dens. 0.78A From Ta1 3.26 eA-3

Author Response: Caused by absorption of the x-ray light by the heavy element Ta.

PLAT971_ALERT_2_B Check Calcd Resid. Dens. 0.95A From Ta2 2.99 eA-3

Author Response: Caused by absorption of the x-ray light by the heavy element Ta.

Structure of **6b**

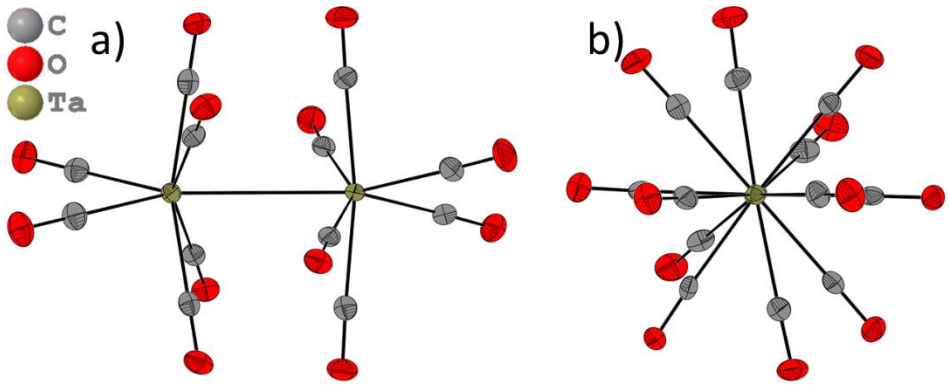

Supplementary Figure 25. Crystal structure of **6b**, side (**a**) and front view along the Ta-Ta bond (**b**). Thermal ellipsoids are shown at the 50 % probability level.

A- and B- level alerts of structure **6b**:

There are only G-level alerts.

Two different crystal structures were obtained including two very similar molecules $Ta_2(CO)_{12}$. Structure of **6a** crystallized in the orthorhombic space group *Pbca* while **6b** was obtained in $P\bar{1}$.

For more information to all structures, see Supplementary Table **13**.

11 Full NMR Characterization of 1, 2, 4, 5

To synthesize the heptacarbonyl cation exclusively, 1,2,3,4-$F_4C_6H_2$ (4FB) was used as solvent. Any coordination could be prevented as evident from the ^{93}Nb-NMR spectrum shown in Supplementary Figure 26 that only includes one signal at −1425 ppm at 243 K. Consequently, the heptacarbonyl cation begins to decompose slowly at about 273 K. As expected, the decomposition was much slower when the spectra were measured under CO pressure slightly above atmospheric pressure. Since no other signals were detected, it was not possible to clarify at which temperature the decomposition began.

All spectra were measured under CO pressure slightly above atmospheric pressure. In a sample of pure 4FB with CO pressure slightly above atmospheric pressure a sharp signal of the free CO was detected in ^{13}C NMR spectrum at 185.8 ppm (100.62 MHz, 298 K). In contrast broad CO signals at δ^{13}C = 207 (FWHM = 360 Hz, 243 K, **1**, Supplementary Figure 30), 203 (FWHM = 205 Hz, 298 K, **2**; Supplementary Figure 34), 206 (FWHM = 205 Hz, 298 K, **4**, Supplementary Figure 39) and 203 ppm (FWHM =376 Hz, 298 K, **5**, Supplementary Figure 43) were detected for compounds **1**, **2**, **4** and **5**. This indicates rapid intermolecular exchange between free CO molecules in solution and CO ligands in the complexes since no sharp signal of free CO was obtained.

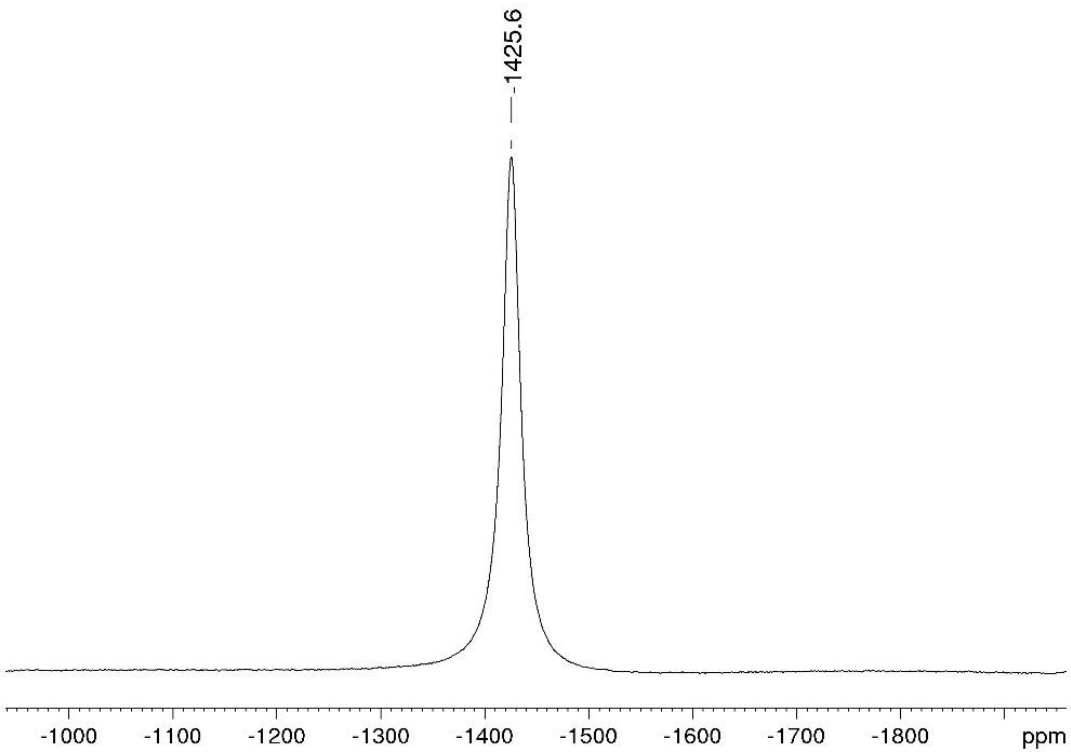

Supplementary Figure 26. ^{93}Nb NMR spectrum (97.95 MHz, $F_4C_6H_2$, 243 K) of **1**. The peak positions of the resonances are also given in the section "Detailed Synthesis of Compounds 1, 2, 4, 5 and 6" on p. 8-10.

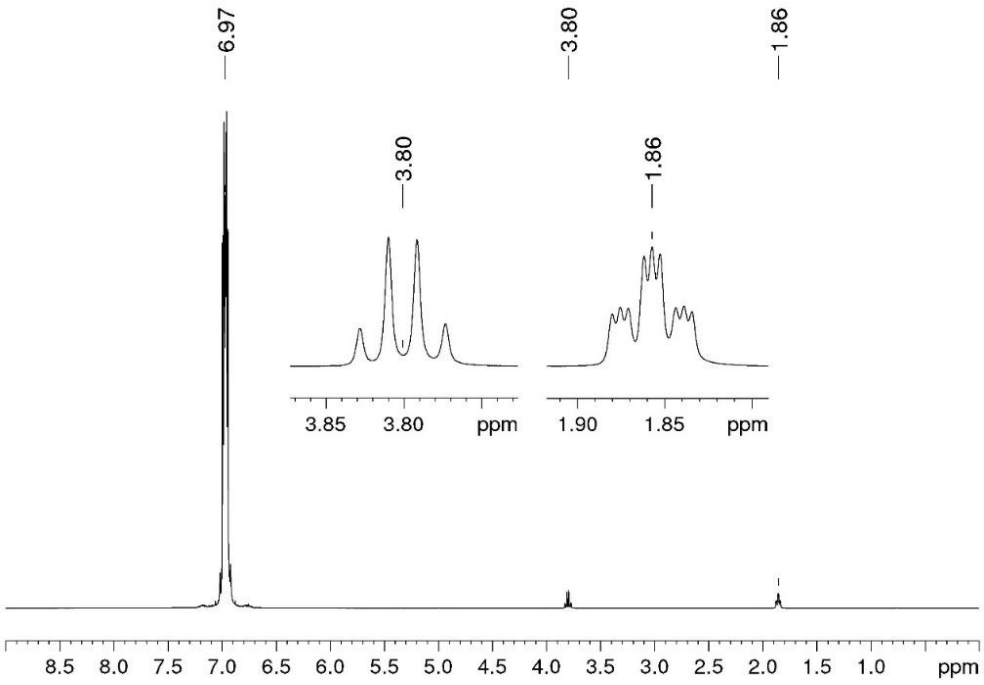

Supplementary Figure 27. Section of the ^{1}H NMR spectrum (400.17 MHz, $F_4C_6H_2$, 243 K) of **1** containing the co-product $[NEt_4]^+[Al(OR^F)_4]^-$. The peak positions of the resonances are also given in the section "Detailed Synthesis of Compounds 1, 2, 4, 5 and 6" on p. 8-10.

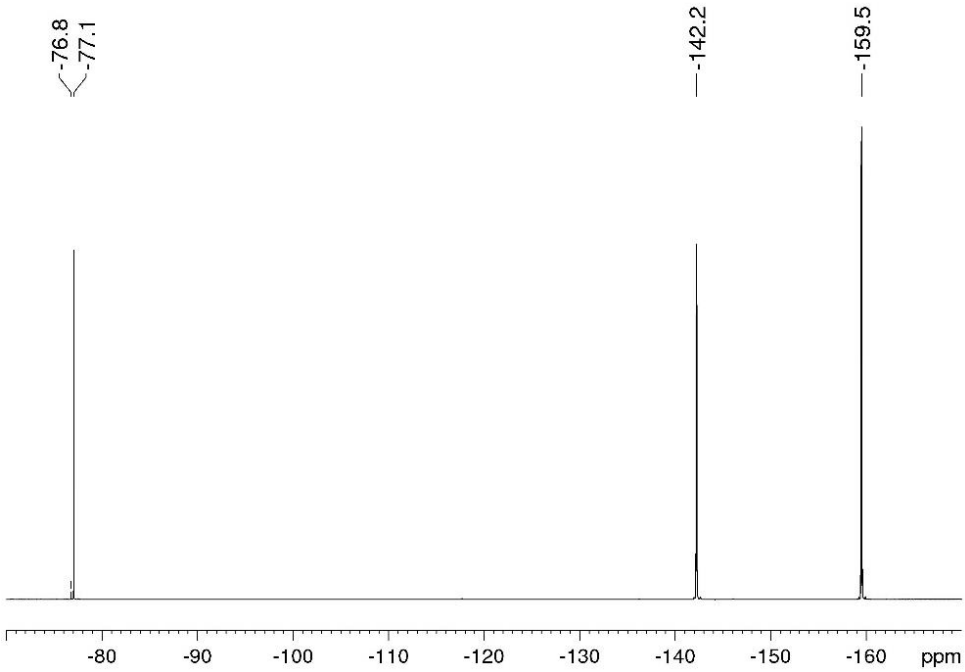

Supplementary Figure 28. Section of the ^{19}F NMR spectrum (376.54 MHz, $F_4C_6H_2$, 243 K) of **1**. The peak positions of the resonances are also given in the section "Detailed Synthesis of Compounds 1, 2, 4, 5 and 6" on p. 8-10.

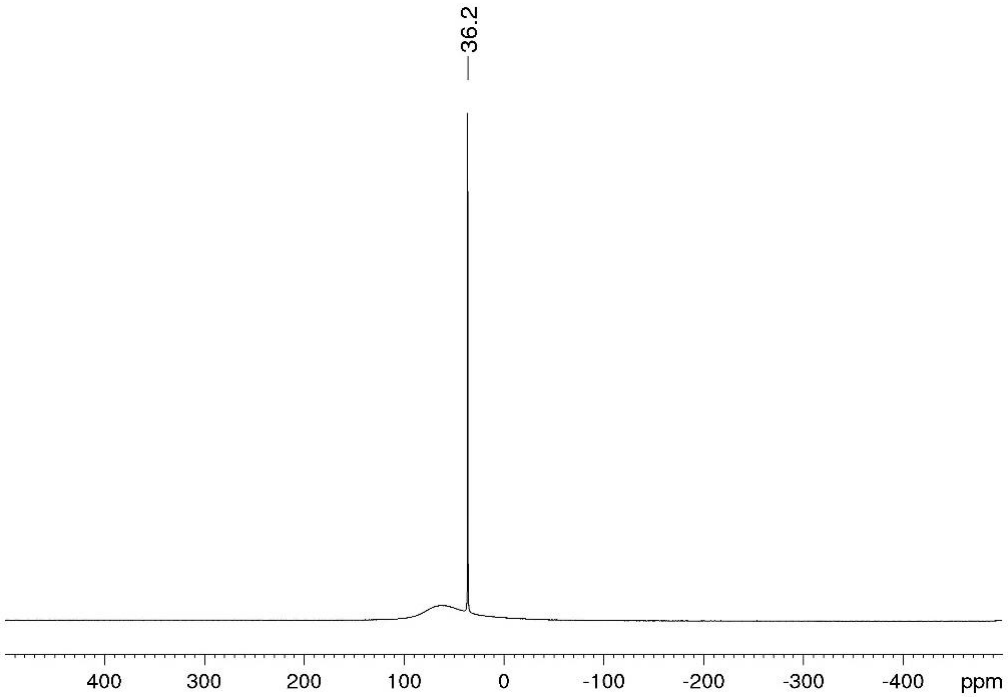

Supplementary Figure 29. ^{27}Al NMR spectrum (104.27 MHz, $F_4C_6H_2$, 243 K) of **1**. The peak positions of the resonances are also given in the section "Detailed Synthesis of Compounds 1, 2, 4, 5 and 6" on p. 8-10.

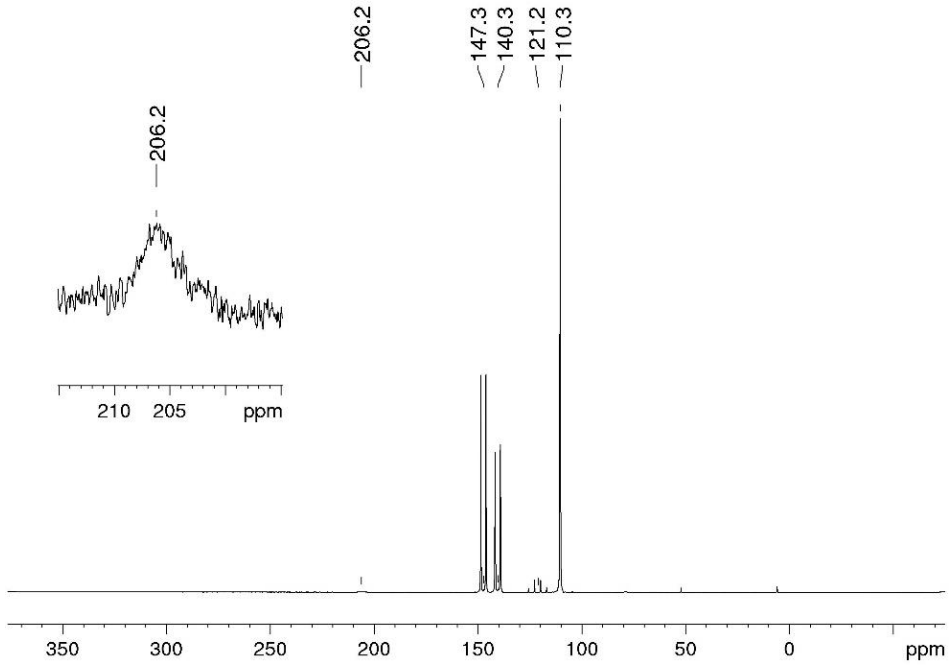

Supplementary Figure 30. ^{13}C NMR spectrum (100.62 MHz, $F_4C_6H_2$, 243 K) of **1** containing the co-product $[NEt_4]^+[Al(OR^F)_4]^-$. The peak positions of the resonances are also given in the section "Detailed Synthesis of Compounds 1, 2, 4, 5 and 6" on p. 8-10.

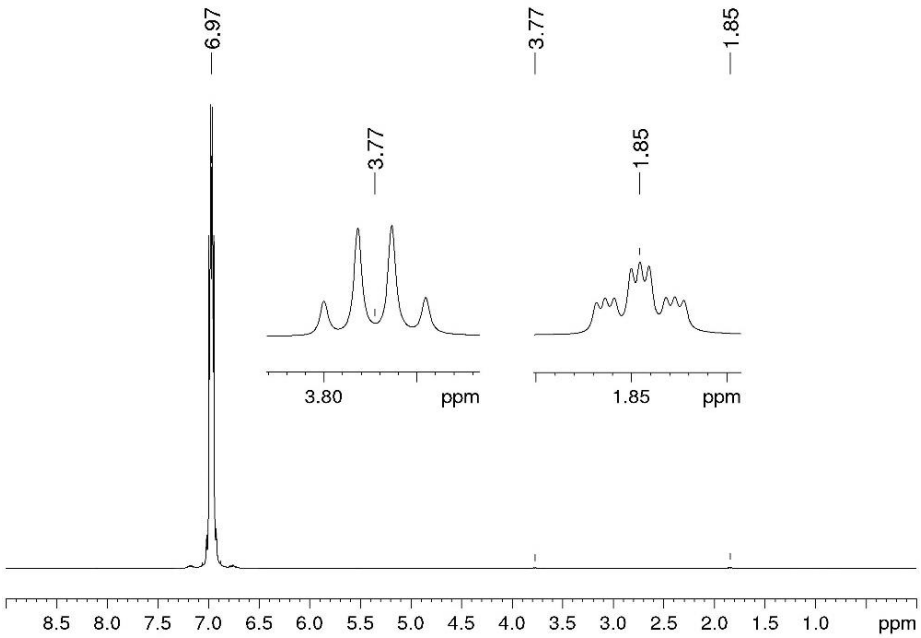

Supplementary Figure 31. Section of ^{1}H NMR spectrum (400.17 MHz, $F_4C_6H_2$, 298 K) of **2** containing the co-product $[NEt_4]^+[Al(OR^F)_4]^-$. The peak positions of the resonances are also given in the section "Detailed Synthesis of Compounds 1, 2, 4, 5 and 6" on p. 8-10.

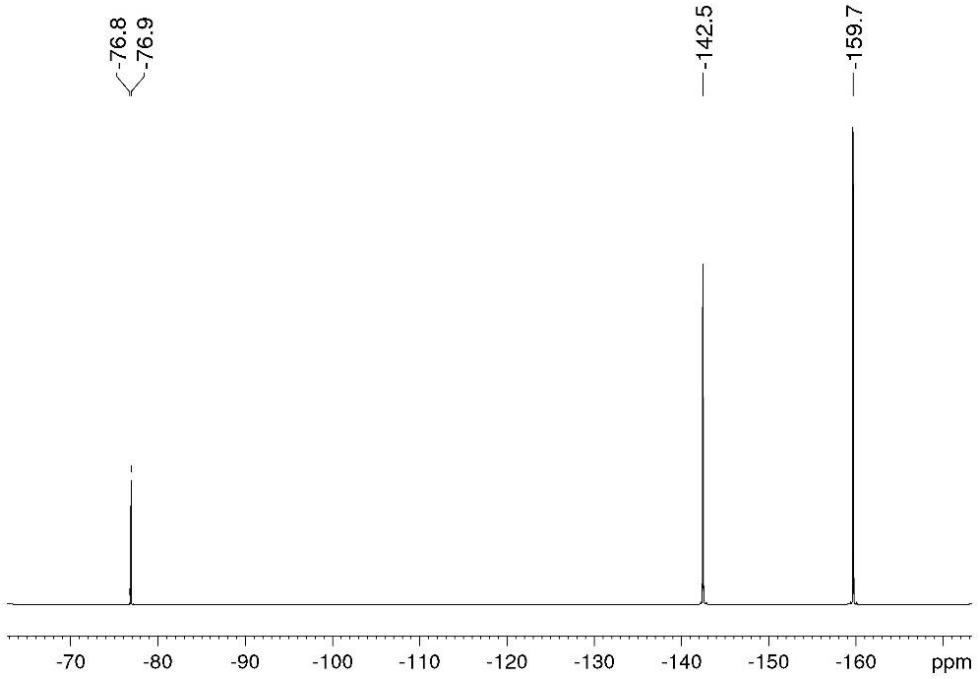

Supplementary Figure 32. ^{19}F NMR spectrum (376.54 MHz, $F_4C_6H_2$, 298 K) of **2**. The peak positions of the resonances are also given in the section "Detailed Synthesis of Compounds 1, 2, 4, 5 and 6" on p. 8-10.

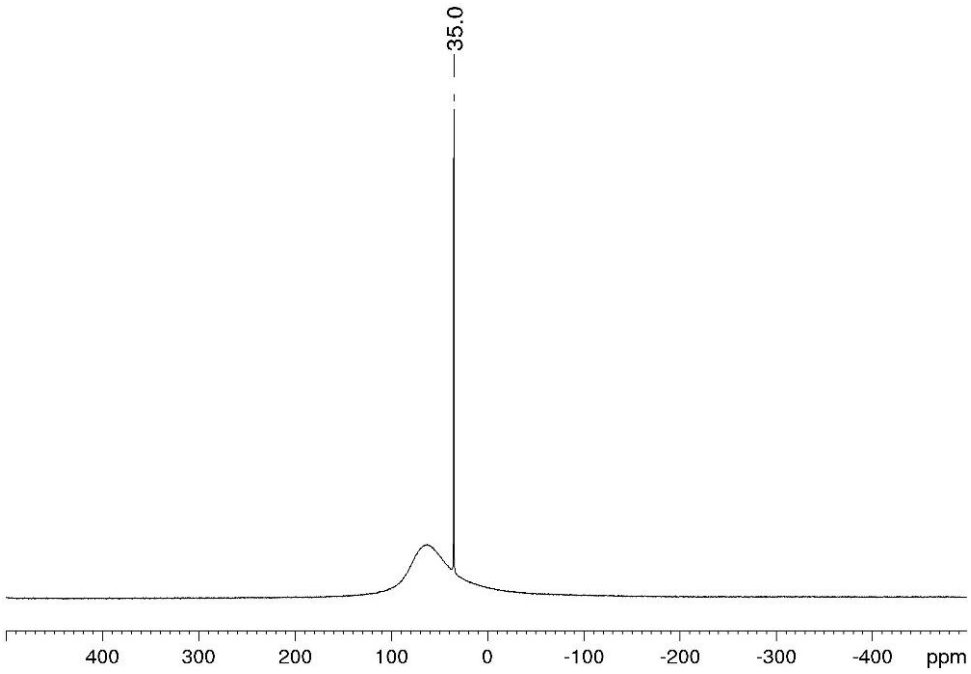

Supplementary Figure 33. ^{27}Al NMR spectrum (104.27 MHz, $F_4C_6H_2$, 298 K) of **2**. The peak positions of the resonances are also given in the section "Detailed Synthesis of Compounds 1, 2, 4, 5 and 6" on p. 8-10.

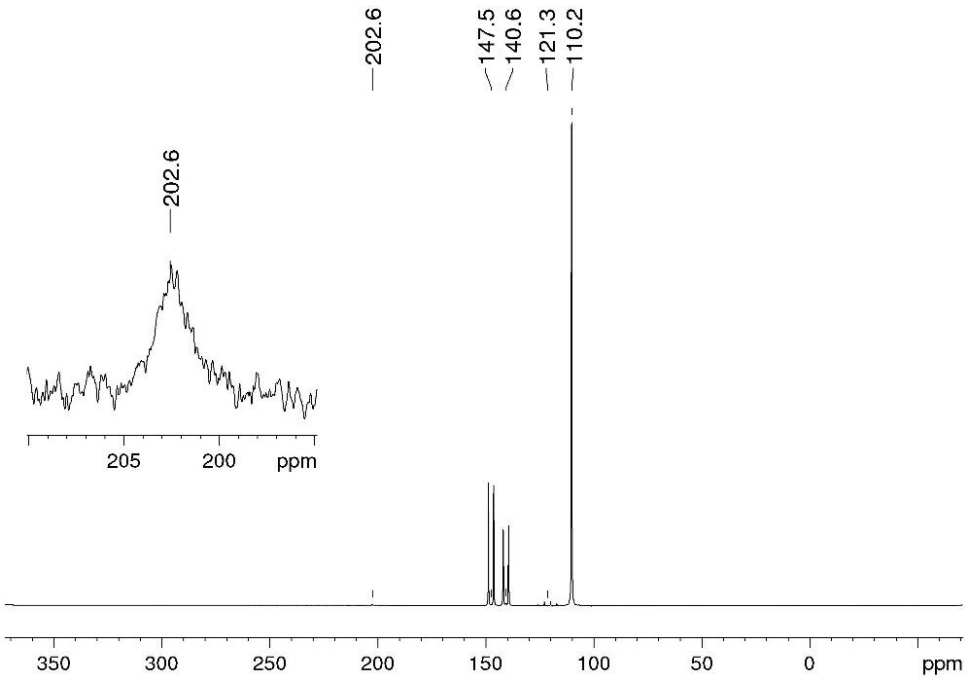

Supplementary Figure 34. Section of the ^{13}C NMR spectrum (100.62 MHz, $F_4C_6H_2$, 298 K) of **2** containing the co-product $[NEt_4]^+[Al(OR^F)_4]^-$. The peak positions of the resonances are also given in the section "Detailed Synthesis of Compounds 1, 2, 4, 5 and 6" on p. 8-10.

Crystals of **4** and the co-product $[NEt_4]^+[Al(OR^F)_4]^-$ were isolated in the glovebox and dissolved in 4FB for the NMR analysis.

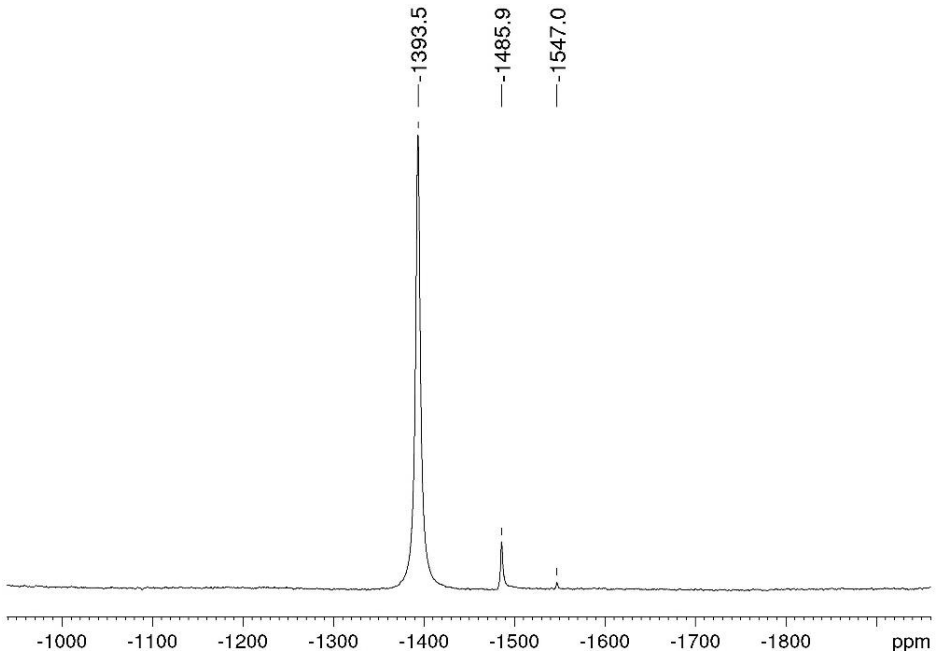

Supplementary Figure 35. ^{93}Nb NMR spectrum (97.95 MHz, $F_4C_6H_2$, 298 K) of **4** with side products, probably caused by minor impurities of *o*-dfb. The peak positions of the resonances are also given in the section "Detailed Synthesis of Compounds 1, 2, 4, 5 and 6" on p. 8-10.

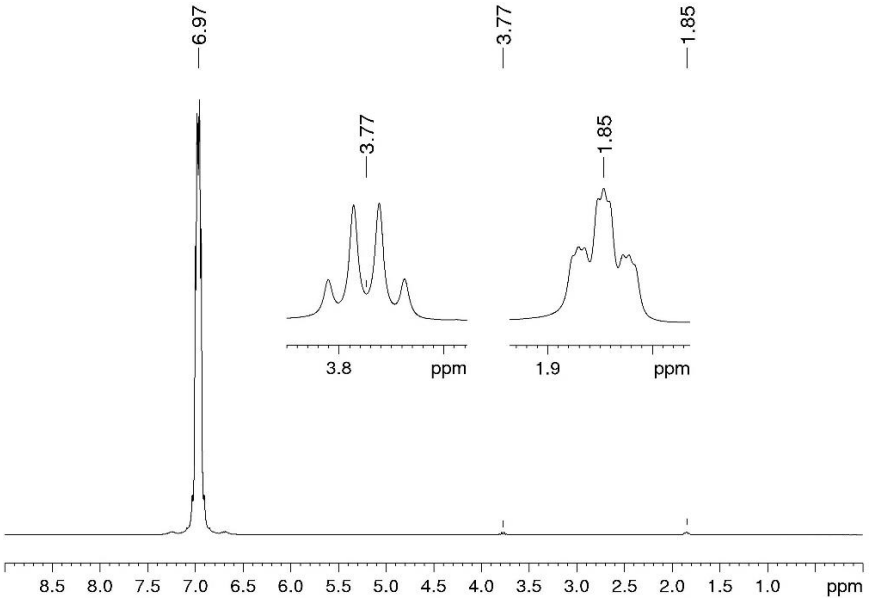

Supplementary Figure 36. Section of ^{1}H NMR spectrum (300.18 MHz, $F_4C_6H_2$, 298 K) of **4** containing the co-product $[NEt_4]^+[Al(OR^F)_4]^-$. The peak positions of the resonances are also given in the section "Detailed Synthesis of Compounds 1, 2, 4, 5 and 6" on p. 8-10.

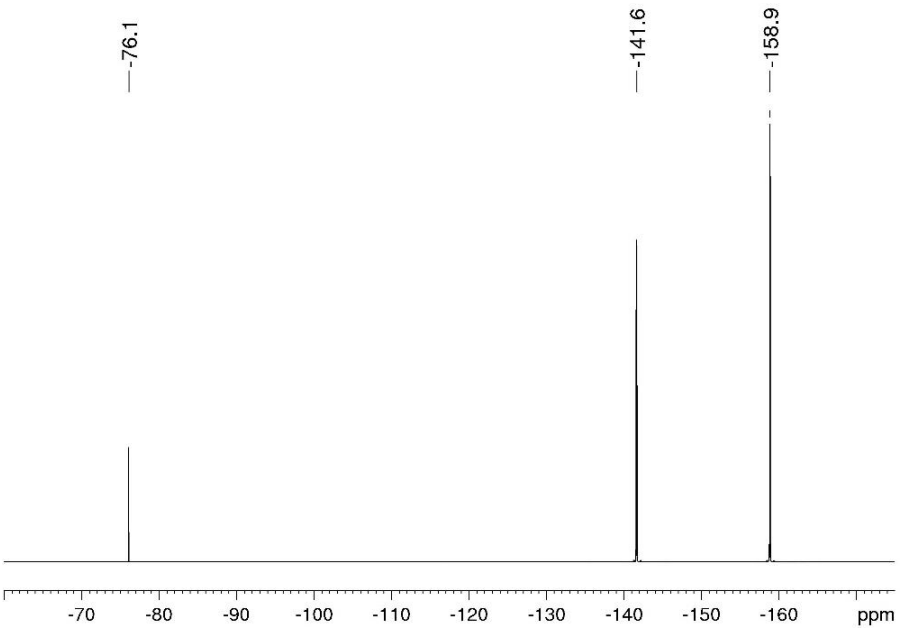

Supplementary Figure 37. ^{19}F NMR spectrum (282.45 MHz, $F_4C_6H_2$, 298 K) of **4**. The peak positions of the resonances are also given in the section "Detailed Synthesis of Compounds 1, 2, 4, 5 and 6" on p. 8-10.

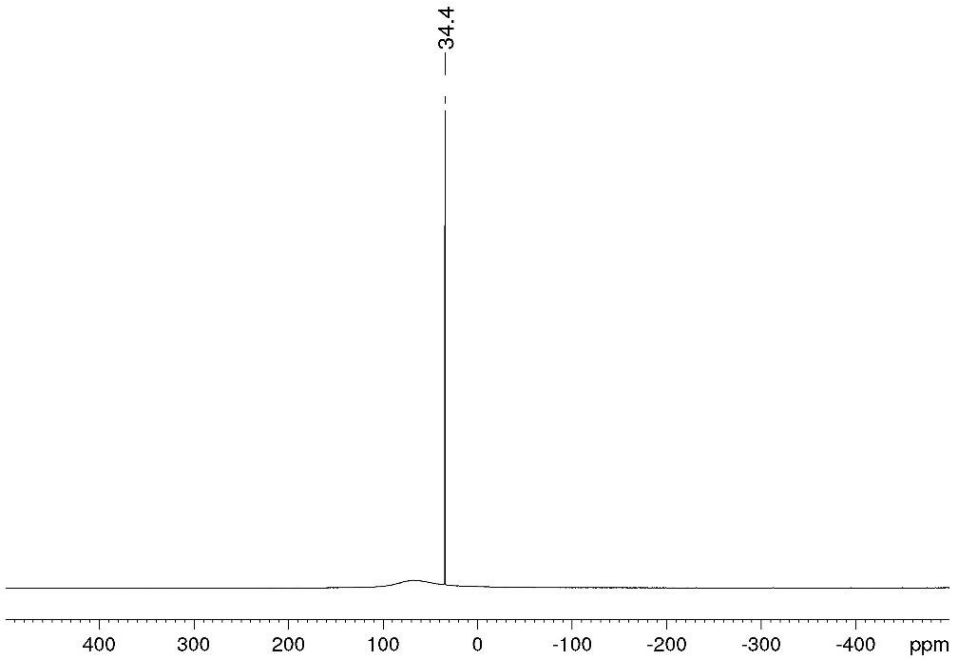

Supplementary Figure 38. ^{27}Al NMR spectrum (78.22 MHz, $F_4C_6H_2$, 298 K) of **4**. The peak positions of the resonances are also given in the section "Detailed Synthesis of Compounds 1, 2, 4, 5 and 6" on p. 8-10.

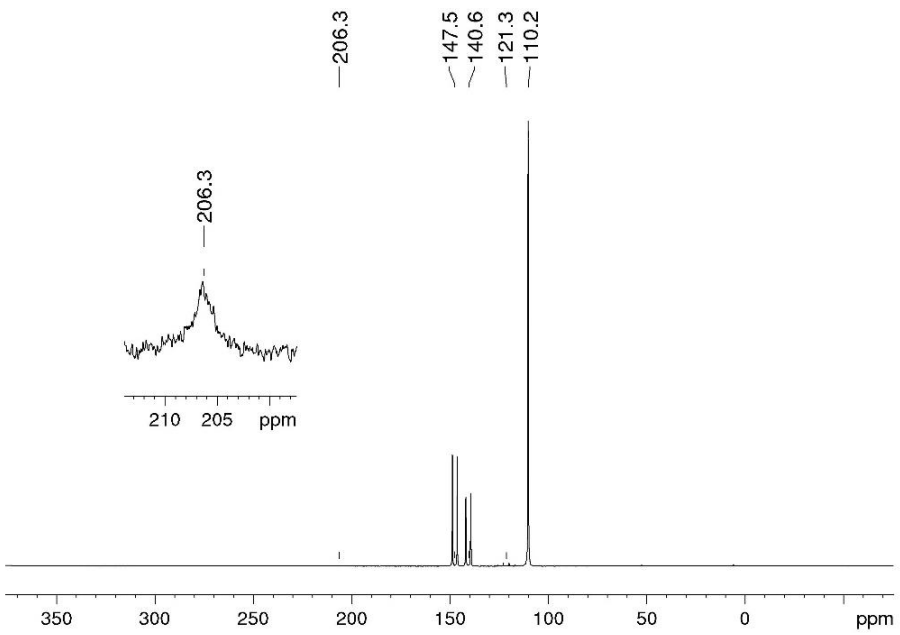

Supplementary Figure 39. ^{13}C NMR spectrum (100.62 MHz, $F_4C_6H_2$, 298 K) of **4** containing the co-product $[NEt_4]^+[Al(OR^F)_4]^-$. The peak positions of the resonances are also given in the section "Detailed Synthesis of Compounds 1, 2, 4, 5 and 6" on p. 8-10.

Crystals of **5** and the co-product $[NEt_4]^+[Al(OR^F)_4]^-$ were isolated in the glovebox and dissolved in 4FB for the NMR analysis.

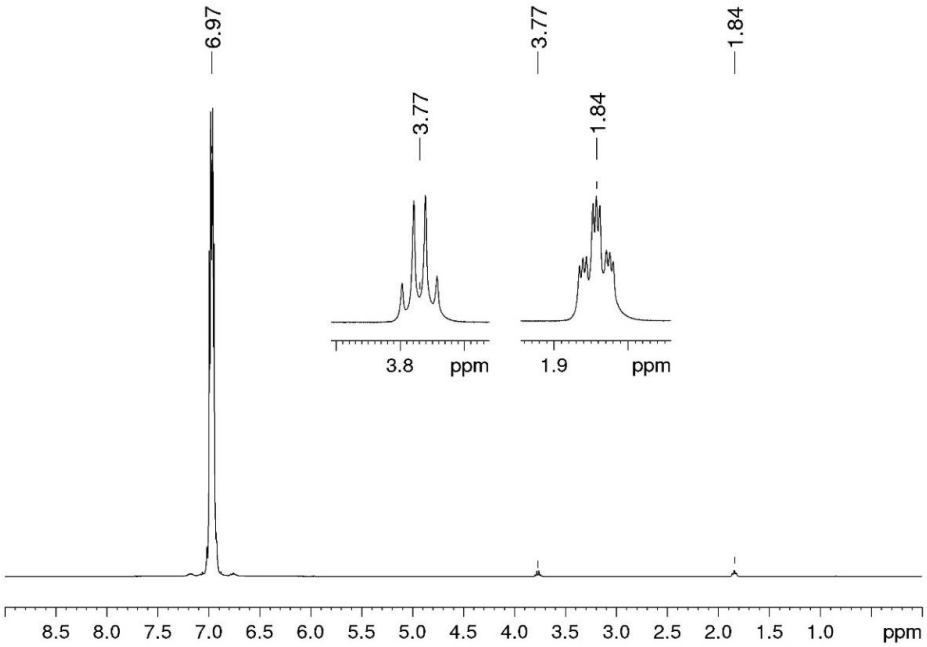

Supplementary Figure 40. Section of ^1H NMR spectrum (400.17 MHz, $F_4C_6H_2$, 298 K) of **5** containing the co-product $[NEt_4]^+[Al(OR^F)_4]^-$. The peak positions of the resonances are also given in the section "Detailed Synthesis of Compounds 1, 2, 4, 5 and 6" on p. 8-10.

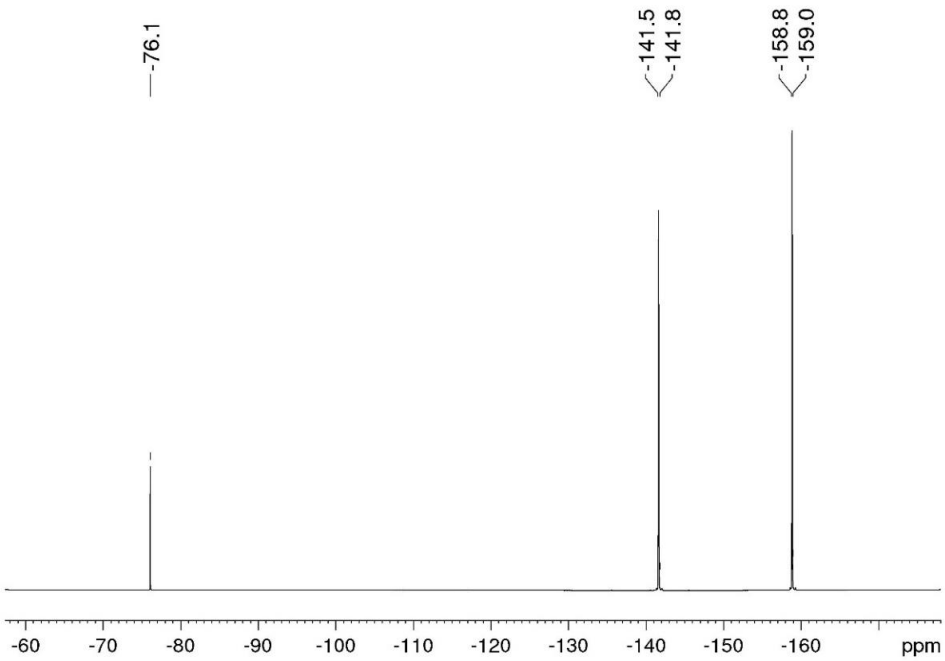

Supplementary Figure 41. ^{19}F NMR spectrum (376.54 MHz, $F_4C_6H_2$, 298 K) of **5**. The peak positions of the resonances are also given in the section "Detailed Synthesis of Compounds 1, 2, 4, 5 and 6" on p. 8-10.

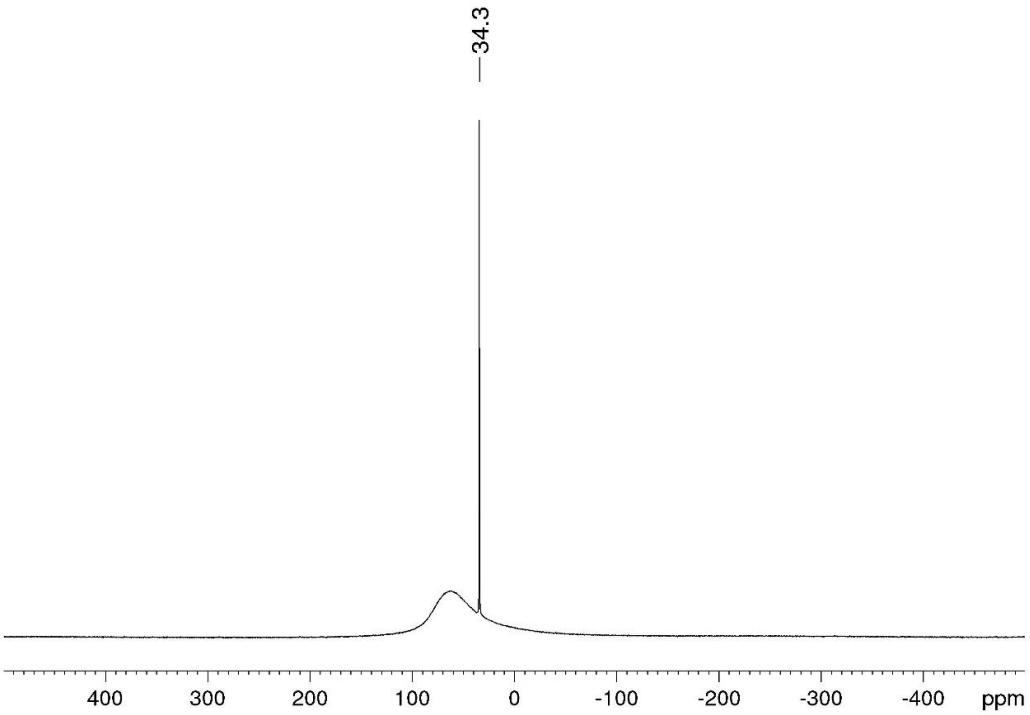

Supplementary Figure 42. ^{27}Al NMR spectrum (104.27 MHz, $F_4C_6H_2$, 298 K) of **5**. The peak positions of the resonances are also given in the section "Detailed Synthesis of Compounds 1, 2, 4, 5 and 6" on p. 8-10.

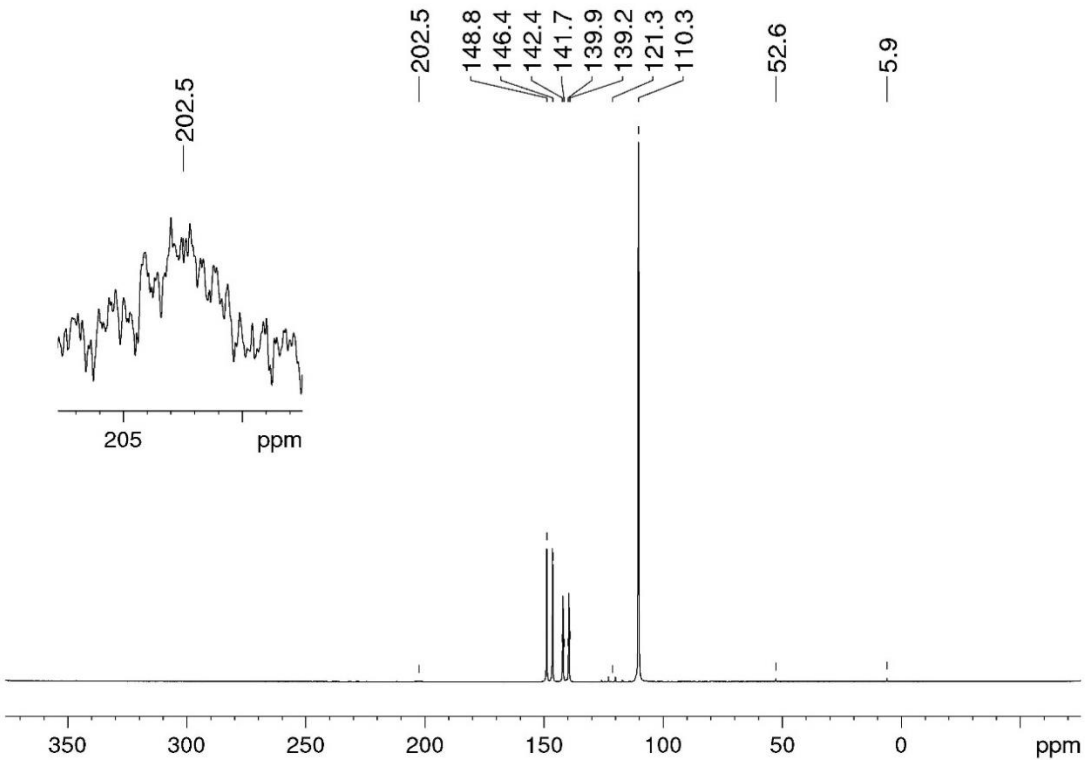

Supplementary Figure 43. Section of the ^{13}C NMR spectrum (100.62 MHz, $F_4C_6H_2$, 298 K) of **5** containing the co-product $[NEt_4]^+[Al(OR^F)_4]^-$. The peak positions of the resonances are also given in the section "Detailed Synthesis of Compounds 1, 2, 4, 5 and 6" on p. 8-10.

12 Computational Details to the Structure Determination

Table 14. Details of quantumchemical calculations of compound **1**.

	B3LYP/def2-TZVPP	Evrt (B3LYP, 0.96)	S0(B3LYP,0.96)	CC/def2-TZVPP	MP2/def2-TZVPP	MP2/def2-QZVPPD
$Nb(CO)_7^+$_C3v	-850.112269	188.62	0.59346	-848.884709	-848.786686	-849.054884
$Nb(CO)_7^+$_C2v	-850.111360	186.05	0.57340	-848.883933	-848.785853	-849.054086
$Nb(CO)_7^+$_D5h	-850.098680	182.69	0.54691	-848.871933	-848.771139	-849.039393
C3v -> C2v	2.39	-2.57	-0.02006	2.04	2.19	2.09
C3v-> D5h	35.68	-5.93	-0.04655	33.54	40.82	40.67

	Eext	H°(g)	G°(g)	T1diag (CCSD/def2-TZVPP)	
$Nb(CO)_7^+$_C3v	-849.152907	-2229259.857418	-2229436.797517	0.0207	
$Nb(CO)_7^+$_C2v	-849.152165	-2229260.480268	-2229431.439478	0.0207	1 imag, b2, 36.40i
$Nb(CO)_7^+$_D5h	-849.140188	-2229232.392780	-2229395.453997	0.0203	imag: e2'', 65.93i
C3v -> C2v	1.95	-0.62	5.36		
C3v-> D5h	33.39	27.46	41.34		

Table 15. Details of quantumchemical calculations of compound **2**.

	B3LYP/def2-TZVPP	Evrt (B3LYP, 0.96)	S0(B3LYP,0.96)	CC/def2-TZVPP	MP2/def2-TZVPP	MP2/def2-QZVPPD
$Ta(CO)_7^+$_C3v	-850.143899	188.38	0.59594	-848.846611	-848.757962	-849.025271
$Ta(CO)_7^+$_C2v	-850.143038	185.81	0.57538	-848.845916	-848.757178	-849.024469
$Ta(CO)_7^+$_D5h	-850.129396	182.44	0.54911	-848.833059	-848.741410	-849.008841
C3v->C2v	2.26	-2.57	-0.02056	1.82	2.06	2.11
C3v->D5h	38.08	-5.94	-0.04683	35.58	43.46	43.14

	Eext	H°(g)	G°(g)	T1diag (CCSD/def2-TZVPP)	
$Ta(CO)_7^+$_C3v	-849.113920	-2229157.735999	-2229335.415510	0.0198	
$Ta(CO)_7^+$_C2v	-849.113206	-2229158.433177	-2229329.982724	0.0198	1 im, b2, 35.59i
Ta(CO)7+_D5h	-849.100490	-2229128.416348	-2229292.133494	0.0195	imag: e2'', 71.76i
C3v->C2v	1.87	-0.70	5.43		
C3v->D5h	35.26	29.32	43.28		

Table 16. Details of quantum chemical calculations of release of one CO ligand of compound **1**.

	B3LYP/def2-TZVPP	Evrt (B3LYP, 0.968)	S0(B3LYP,0.968)	CC/def2-TZVPP	MP2/def2-TZVPP	MP2/def2-QZVPPD
$Nb(CO)_7^+$_C3v	-850.1122637	189.57	0.59173	-848.8846882	-848.7866361	-849.054838
$Nb(CO)_6^+$_t-d3d	-736.7526946	159.49	0.57486	-735.6767606	-735.5743504	-735.8092647
CO_C6v	-113.3110756	19.02	0.19772	-113.1588621	-113.1384829	-113.1700806
$Nb(CO)_7^+$->$Nb(CO)_6^+$ + CO	127.32	-11.06	0.18	128.82	193.77	198.21

	Eext	H°(g)	G°(g)	T1diag (CCSD/def2-TZVPP)	D1diag (CCSD/def2-TZVPP)
$Nb(CO)_7^+$_C3v	-849.15289	-2229258.862817	-2229435.287117	0.0207	0.0648
$Nb(CO)_6^+$_t-d3d	-735.9116749	-1931974.132330	-1932145.526839	0.0291	0.068
CO_C6v	-113.1904599	-297160.052386	-297219.002604	0.0184	0.0356
$Nb(CO)_7^+$->$Nb(CO)_6^+$ + CO	133.26	124.68	70.76		

Table 17. Details of quantum chemical calculations of release of one CO ligand of compound **2**.

	B3LYP/def2-TZVPP	Evrt (B3LYP, 0.968)	S0(B3LYP,0.968)	CC/def2-TZVPP	MP2/def2-TZVPP	MP2/def2-QZVPPD
$Ta(CO)_7^+$_C3v	-850.143894	189.33	0.59411	-848.8465739	-848.7579922	-849.0252928
$Ta(CO)_6^+$_t-d3d	-736.779981	159.49	0.57317	-735.6326516	-735.5405633	-735.7758253
CO_C6v	-113.3110756	19.02	0.19772	-113.1588621	-113.1384829	-113.1700806
$Ta(CO)_7^+$->$Ta(CO)_6^+$ + CO	138.72	-10.82	0.18	144.56	207.27	208.43

	Eext	H°(g)	G°(g)	T1diag (CCSD/def2-TZVPP)	D1diag (CCSD/def2-TZVPP)
$Ta(CO)_7^+$_C3v	-849.1138745	-2229156.667393	-2229333.801289	0.0198	0.0598
$Ta(CO)_6^+$_t-d3d	-735.8679136	-1931859.237103	-1932030.127738	0.0282	0.0597
CO_C6v	-113.1904599	-297160.052386	-297219.002604	0.0184	0.0356
$Ta(CO)_7^+$->$Ta(CO)_6^+$ + CO	145.72	137.38	84.67		

13 Computational Details on Gas Phase DFT Studies

Coordinates of the fixed point charges in Ångström.

Point charges q

q	7.42691	3.63716	-0.31337
q	5.65479	7.36888	3.11261
q	10.26364	10.50980	6.63498
q	8.42016	10.50980	3.40582
q	11.25689	3.63716	10.35417
q	13.02901	7.36888	6.92819
q	5.41788	3.12533	7.26773
q	8.82295	-0.59081	7.03545
q	13.26592	3.12533	2.77307
q	9.86085	-0.59081	3.00535

The following symmetries were optimized at the (RI-)B3LYP-D3(BJ)/def2-TZVPP level of theory. All coordinates are given in Ångström. All structures are minimum structures with the exception of the C_{2v} structures of $M(CO)_7^+$ without point charges, which are transition states with one imaginary frequency each (–36.44 (M = Nb), –35.52 cm^{-1} (M = Ta).

$[Ta(CO)_7]^+$, q = – 0.1

Method: (RI-)B3LYP-D3(BJ)/def2-TZVPP

Ta	9.34117	4.82389	5.02263
C	9.63140	7.01699	4.67597
C	7.13306	5.10951	5.15841
C	11.49960	5.06501	5.23768
C	9.59577	5.11232	7.21609
C	8.74743	5.06726	2.93870
C	10.27235	3.24709	3.91648
C	8.63514	2.93558	5.85631
O	9.77094	8.12054	4.50826
O	6.02053	5.26557	5.23429
O	12.61068	5.22169	5.37333
O	9.71068	5.27972	8.32418
O	8.41794	5.23445	1.87018
O	10.76578	2.41634	3.32672
O	8.23960	1.98490	6.32161

SCF energy GEOOPT = -850.2421044668 H
ZPE = 141.0 kJ/mol
FREEH energy = 189.39 kJ/mol
FREEH entropy = 0.60174 kJ/mol

$vibrational spectrum

# mode	symmetry	wave number cm**(-1)	IR intensity km/mol	selection rules IR	RAMAN
1		0.00	0.00000	-	-
2		0.00	0.00000	-	-
3		0.00	0.00000	-	-
4		0.00	0.00000	-	-
5		0.00	0.00000	-	-

```
     6                    0.00         0.00000       -       -
     7        a          35.11         1.74618     YES     YES
     8        a          40.59         1.39859     YES     YES
     9        a          69.06         0.25981     YES     YES
    10        a          78.92         0.09492     YES     YES
    11        a          82.29         0.75199     YES     YES
    12        a          83.10         0.35419     YES     YES
    13        a          84.46         1.95733     YES     YES
    14        a          85.80         1.31560     YES     YES
    15        a          95.44         1.24550     YES     YES
    16        a         100.36         0.40815     YES     YES
    17        a         104.39         0.48581     YES     YES
    18        a         269.85        27.95605     YES     YES
    19        a         276.25        29.24681     YES     YES
    20        a         303.00        20.33781     YES     YES
    21        a         326.35         0.49023     YES     YES
    22        a         331.09         0.12424     YES     YES
    23        a         332.46        28.68901     YES     YES
    24        a         334.56        27.44099     YES     YES
    25        a         335.88         1.14382     YES     YES
    26        a         341.30         3.66103     YES     YES
    27        a         361.68         5.66805     YES     YES
    28        a         384.92         1.43110     YES     YES
    29        a         388.40         0.90398     YES     YES
    30        a         411.46        21.35469     YES     YES
    31        a         441.07         0.18184     YES     YES
    32        a         442.39         0.44158     YES     YES
    33        a         499.91        23.79394     YES     YES
    34        a         504.23         4.86951     YES     YES
    35        a         510.46        36.02572     YES     YES
    36        a         511.40        31.54715     YES     YES
    37        a         521.38         0.30324     YES     YES
    38        a         522.59         0.59575     YES     YES
    39        a        2129.47       645.00962     YES     YES
    40        a        2133.75      1316.18297     YES     YES
    41        a        2137.29      1279.20823     YES     YES
    42        a        2152.13       794.35672     YES     YES
    43        a        2169.03       469.48324     YES     YES
    44        a        2178.25       456.56718     YES     YES
    45        a        2238.03        54.63366     YES     YES
$end
```

$\underline{[Ta(CO)_7]^+, q = -0.2}$

```
Method: (RI-)B3LYP-D3(BJ)/def2-TZVPP

Ta          9.34279        4.82100        5.02223
C           9.60263        7.03122        4.70996
C           7.13595        5.09920        5.13895
C          11.50468        5.06819        5.21335
C           9.61742        5.10680        7.20698
C           8.76895        5.07325        2.93413
C          10.26467        3.22400        3.93080
C           8.62216        2.94412        5.86848
O           9.72894        8.13732        4.55561
O           6.02182        5.25190        5.20332
O          12.61795        5.22161        5.33338
O           9.73892        5.28269        8.31395
O           8.45515        5.24853        1.86189
O          10.75324        2.38852        3.34481
O           8.21682        2.00252        6.34301
```

```
SCF energy GEOOPT =  -850.3406028417 H
ZPE =   140.9 kJ/mol
FREEH energy =   189.35 kJ/mol
FREEH entropy =   0.60268 kJ/mol

$vibrational spectrum
#  mode     symmetry     wave number   IR intensity    selection rules
#                         cm**(-1)        km/mol          IR     RAMAN
     1                      -0.00         0.00000         -       -
     2                       0.00         0.00000         -       -
     3                       0.00         0.00000         -       -
     4                       0.00         0.00000         -       -
     5                       0.00         0.00000         -       -
     6                       0.00         0.00000         -       -
     7        a             31.20         1.92433       YES     YES
     8        a             42.82         1.09987       YES     YES
     9        a             68.87         0.32174       YES     YES
    10        a             77.48         0.07408       YES     YES
    11        a             80.44         1.40027       YES     YES
    12        a             82.88         0.57443       YES     YES
    13        a             85.39         1.60236       YES     YES
    14        a             86.89         0.88737       YES     YES
    15        a             95.29         1.18448       YES     YES
    16        a             99.89         0.45499       YES     YES
    17        a            105.34         0.44425       YES     YES
    18        a            266.12        26.73659       YES     YES
    19        a            279.69        29.25884       YES     YES
    20        a            303.18        19.81197       YES     YES
    21        a            322.42         0.75734       YES     YES
    22        a            330.29        24.55984       YES     YES
    23        a            332.30         4.50091       YES     YES
    24        a            335.21         4.29301       YES     YES
    25        a            335.59        23.99499       YES     YES
    26        a            342.12         5.02419       YES     YES
    27        a            360.07         5.51024       YES     YES
    28        a            380.19         2.90253       YES     YES
    29        a            389.79         1.08077       YES     YES
    30        a            413.14        19.23948       YES     YES
    31        a            440.12         0.05568       YES     YES
    32        a            442.08         0.55450       YES     YES
    33        a            498.46        24.43150       YES     YES
    34        a            501.84         8.46875       YES     YES
    35        a            509.69        36.13350       YES     YES
    36        a            512.76        28.49016       YES     YES
    37        a            518.99         0.04809       YES     YES
    38        a            521.72         0.74304       YES     YES
    39        a           2131.21      1121.25644       YES     YES
    40        a           2133.76       871.89579       YES     YES
    41        a           2138.60      1350.80658       YES     YES
    42        a           2150.67       669.04281       YES     YES
    43        a           2163.51       499.59179       YES     YES
    44        a           2183.48       451.72144       YES     YES
    45        a           2238.62        58.79373       YES     YES
$end
```

$[Ta(CO)_7]^+$, q = – 0.3

Method: (RI-)B3LYP-D3(BJ)/def2-TZVPP

Ta	9.34411	4.81836	5.02146
C	9.57213	7.04584	4.74590
C	7.13853	5.08878	5.11837
C	11.50959	5.06999	5.18828
C	9.63903	5.10323	7.19739
C	8.79140	5.08023	2.92914
C	10.25506	3.19985	3.94549
C	8.61052	2.95317	5.88113
O	9.68526	8.15426	4.60545
O	6.02275	5.23699	5.17082
O	12.62488	5.21972	5.29280
O	9.76785	5.28796	8.30306
O	8.49458	5.26512	1.85330
O	10.73776	2.35834	3.36440
O	8.19863	2.01901	6.36385

SCF energy GEOOPT = -850.4393938024 H
ZPE = 140.8 kJ/mol
FREEH energy = 189.32 kJ/mol
FREEH entropy = 0.60351 kJ/mol

$vibrational spectrum

# mode	symmetry	wave number cm**(-1)	IR intensity km/mol	selection rules IR	RAMAN
1		-0.00	0.00000	-	-
2		-0.00	0.00000	-	-
3		0.00	0.00000	-	-
4		0.00	0.00000	-	-
5		0.00	0.00000	-	-
6		0.00	0.00000	-	-
7	a	27.19	1.99190	YES	YES
8	a	45.24	0.83869	YES	YES
9	a	68.93	0.41670	YES	YES
10	a	76.20	0.10056	YES	YES
11	a	79.43	1.54810	YES	YES
12	a	83.37	0.52175	YES	YES
13	a	85.66	1.39408	YES	YES
14	a	88.90	0.91965	YES	YES
15	a	95.23	1.10882	YES	YES
16	a	99.99	0.54120	YES	YES
17	a	105.40	0.33126	YES	YES
18	a	262.78	25.17494	YES	YES
19	a	283.82	29.47304	YES	YES
20	a	302.77	18.89708	YES	YES
21	a	317.56	1.24753	YES	YES
22	a	328.11	24.20465	YES	YES
23	a	332.93	4.73503	YES	YES
24	a	336.08	4.47476	YES	YES
25	a	336.55	23.06856	YES	YES
26	a	343.18	6.58541	YES	YES
27	a	358.74	5.16443	YES	YES
28	a	375.30	4.99128	YES	YES
29	a	391.39	1.17226	YES	YES
30	a	416.66	16.84816	YES	YES
31	a	439.03	0.09673	YES	YES
32	a	442.18	0.67702	YES	YES
33	a	496.83	25.12646	YES	YES
34	a	499.50	10.65826	YES	YES

```
    35        a             509.25        36.24099       YES     YES
    36        a             514.40        23.53943       YES     YES
    37        a             516.88         2.87560       YES     YES
    38        a             520.68         1.14689       YES     YES
    39        a            2128.56      1352.76382       YES     YES
    40        a            2136.87       725.82053       YES     YES
    41        a            2139.83      1457.63238       YES     YES
    42        a            2148.79       410.93705       YES     YES
    43        a            2158.74       572.10537       YES     YES
    44        a            2188.87       436.31138       YES     YES
    45        a            2239.75        68.42710       YES     YES
$end
```

$[Ta(CO)_7]^+$, q = – 0.4

```
Method: (RI-)B3LYP-D3(BJ)/def2-TZVPP

Ta          9.34707        4.81352        5.01765
C           9.52183        7.06480        4.80666
C           7.14507        5.07464        5.08331
C          11.51802        5.06918        5.14896
C           9.67169        5.10167        7.18098
C           8.82746        5.08862        2.91784
C          10.23800        3.16196        3.96491
C           8.59437        2.97056        5.90241
O           9.60995        8.17774        4.69728
O           6.02722        5.21763        5.11682
O          12.63561        5.21453        5.23151
O           9.81477        5.29973        8.28365
O           8.55575        5.28568        1.83720
O          10.71207        2.31152        3.39095
O           8.17320        2.04906        6.40072

SCF energy GEOOPT =  -850.5384829159 H
ZPE =   140.7 kJ/mol
FREEH energy =   189.29 kJ/mol
FREEH entropy =   0.60529 kJ/mol

$vibrational spectrum
#  mode     symmetry     wave number   IR intensity    selection rules
#                         cm**(-1)        km/mol          IR     RAMAN
     1                      -0.00         0.00000         -       -
     2                      -0.00         0.00000         -       -
     3                      -0.00         0.00000         -       -
     4                       0.00         0.00000         -       -
     5                       0.00         0.00000         -       -
     6                       0.00         0.00000         -       -
     7        a             21.37         1.90215       YES     YES
     8        a             47.76         0.51350       YES     YES
     9        a             69.09         0.56229       YES     YES
    10        a             74.25         0.17563       YES     YES
    11        a             78.37         1.63147       YES     YES
    12        a             84.28         0.59979       YES     YES
    13        a             86.28         1.09546       YES     YES
    14        a             91.09         0.86935       YES     YES
    15        a             94.49         0.97482       YES     YES
    16        a            100.01         0.66179       YES     YES
    17        a            106.33         0.27800       YES     YES
    18        a            259.08        21.66660       YES     YES
    19        a            289.98        29.61340       YES     YES
```

```
    20        a             299.21        14.93328       YES     YES
    21        a             312.18         5.29825       YES     YES
    22        a             324.16        22.35113       YES     YES
    23        a             332.42         5.70515       YES     YES
    24        a             337.91        17.78477       YES     YES
    25        a             338.58         8.71920       YES     YES
    26        a             344.33         9.61629       YES     YES
    27        a             356.83         3.42011       YES     YES
    28        a             369.32         7.74713       YES     YES
    29        a             393.54         0.97827       YES     YES
    30        a             422.47        13.78637       YES     YES
    31        a             437.26         0.47857       YES     YES
    32        a             442.19         1.14616       YES     YES
    33        a             494.15        26.41743       YES     YES
    34        a             497.35        12.36553       YES     YES
    35        a             509.05        36.12112       YES     YES
    36        a             512.16         4.55695       YES     YES
    37        a             517.73        16.22928       YES     YES
    38        a             519.60         5.97150       YES     YES
    39        a            2125.32      1505.33954       YES     YES
    40        a            2138.77      1098.56668       YES     YES
    41        a            2140.13      1020.74924       YES     YES
    42        a            2146.74       346.66956       YES     YES
    43        a            2154.17       583.14647       YES     YES
    44        a            2195.69       383.64820       YES     YES
    45        a            2242.58        93.66993       YES     YES
$end
```

$\underline{[Ta(CO)_7]^+, q = -0.5}$

```
Method: (RI-)B3LYP-D3(BJ)/def2-TZVPP

Ta          9.35400        4.80791        5.00761
C           9.42612        7.08816        4.91741
C           7.15942        5.06249        5.02019
C          11.53380        5.06920        5.07908
C           9.73186        5.09750        7.15066
C           8.89184        5.09530        2.89256
C          10.20904        3.09813        4.00103
C           8.56498        3.01077        5.93760
O           9.46277        8.20686        4.86978
O           6.03954        5.20122        5.02209
O          12.65338        5.21209        5.12572
O           9.90507        5.30688        8.24829
O           8.66220        5.30424        1.80425
O          10.66911        2.22994        3.44392
O           8.12896        2.11016        6.46065

SCF energy GEOOPT =  -850.6378831026 H
ZPE =   140.6 kJ/mol
FREEH energy =   189.26 kJ/mol
FREEH entropy =   0.61050 kJ/mol

$vibrational spectrum
#  mode     symmetry     wave number   IR intensity    selection rules
#                         cm**(-1)        km/mol         IR     RAMAN
     1                       -0.00         0.00000        -       -
     2                       -0.00         0.00000        -       -
     3                       -0.00         0.00000        -       -
     4                       -0.00         0.00000        -       -
     5                        0.00         0.00000        -       -
```

```
     6                    0.00          0.00000        -       -
     7        a          11.96          1.29387      YES     YES
     8        a          49.65          0.11170      YES     YES
     9        a          68.31          0.56230      YES     YES
    10        a          72.00          0.47474      YES     YES
    11        a          77.19          1.63539      YES     YES
    12        a          85.68          0.87433      YES     YES
    13        a          87.63          0.63369      YES     YES
    14        a          91.58          0.77950      YES     YES
    15        a          92.81          0.84641      YES     YES
    16        a          99.35          0.77566      YES     YES
    17        a         105.88          0.13340      YES     YES
    18        a         258.56         14.58473      YES     YES
    19        a         283.98         12.02199      YES     YES
    20        a         300.57         32.04822      YES     YES
    21        a         310.85          9.84409      YES     YES
    22        a         316.77         19.29767      YES     YES
    23        a         331.88          7.53359      YES     YES
    24        a         340.63          7.82859      YES     YES
    25        a         341.18         15.43252      YES     YES
    26        a         345.71         14.36163      YES     YES
    27        a         355.36          1.37572      YES     YES
    28        a         362.19         11.31238      YES     YES
    29        a         397.07          0.40421      YES     YES
    30        a         431.47          8.24833      YES     YES
    31        a         435.52          2.21699      YES     YES
    32        a         440.99          2.82613      YES     YES
    33        a         491.29         29.38515      YES     YES
    34        a         496.42         13.40312      YES     YES
    35        a         507.08          2.26567      YES     YES
    36        a         509.61         35.97182      YES     YES
    37        a         517.27          0.76025      YES     YES
    38        a         520.90         22.40609      YES     YES
    39        a        2121.31       1706.94427      YES     YES
    40        a        2136.24        420.40842      YES     YES
    41        a        2140.30       1445.04226      YES     YES
    42        a        2147.06        740.54928      YES     YES
    43        a        2150.47        289.88211      YES     YES
    44        a        2202.57        288.66853      YES     YES
    45        a        2248.32        134.54494      YES     YES
$end
```

$[Ta(CO)_7]^+$, q = – 0.6

```
Method: (RI-)B3LYP-D3(BJ)/def2-TZVPP

Ta          9.34190        4.80502        5.02040
C           9.34190        7.09420        5.02040
C           7.15407        5.06304        4.99416
C          11.52973        5.06304        5.04664
C           9.76079        5.09951        7.14679
C           8.92301        5.09951        2.89401
C          10.16587        3.04809        4.05151
C           8.51793        3.04809        5.98929
O           9.34190        8.21393        5.02040
O           6.03344        5.20065        4.97512
O          12.65036        5.20065        5.06568
O           9.95560        5.31835        8.24009
O           8.72820        5.31835        1.80071
O          10.61326        2.16433        3.51015
O           8.07053        2.16433        6.53065
```

```
SCF energy GEOOPT =  -850.7375863527 H
ZPE =   140.5 kJ/mol
FREEH energy =   189.22 kJ/mol
FREEH entropy =   0.60938 kJ/mol

$vibrational spectrum
#  mode     symmetry     wave number   IR intensity    selection rules
#                         cm**(-1)        km/mol          IR     RAMAN
     1                      -0.00         0.00000         -       -
     2                      -0.00         0.00000         -       -
     3                      -0.00         0.00000         -       -
     4                       0.00         0.00000         -       -
     5                       0.00         0.00000         -       -
     6                       0.00         0.00000         -       -
     7        a             14.78         0.89184       YES     YES
     8        a             49.32         0.00427       YES     YES
     9        a             66.72         0.69498       YES     YES
    10        a             71.38         0.67501       YES     YES
    11        a             76.26         1.74980       YES     YES
    12        a             85.81         0.83393       YES     YES
    13        a             88.71         0.37670       YES     YES
    14        a             89.80         0.83344       YES     YES
    15        a             93.30         0.85063       YES     YES
    16        a             99.21         0.79469       YES     YES
    17        a            105.88         0.08691       YES     YES
    18        a            261.88        11.09967       YES     YES
    19        a            275.96        14.25654       YES     YES
    20        a            305.28        38.24264       YES     YES
    21        a            311.04         0.08208       YES     YES
    22        a            312.59        21.00216       YES     YES
    23        a            331.38         7.89629       YES     YES
    24        a            340.71        21.34519       YES     YES
    25        a            341.40         0.94186       YES     YES
    26        a            344.85        17.11655       YES     YES
    27        a            354.72         0.62144       YES     YES
    28        a            359.62        11.88656       YES     YES
    29        a            397.90         0.27872       YES     YES
    30        a            432.48         3.68508       YES     YES
    31        a            438.40         3.29955       YES     YES
    32        a            438.75         4.91970       YES     YES
    33        a            489.96        30.05706       YES     YES
    34        a            495.20        13.71899       YES     YES
    35        a            505.07         1.27377       YES     YES
    36        a            509.18        36.73133       YES     YES
    37        a            515.77         0.25803       YES     YES
    38        a            521.92        23.61337       YES     YES
    39        a           2116.46      1789.74065       YES     YES
    40        a           2132.50       173.11299       YES     YES
    41        a           2139.80      1677.27040       YES     YES
    42        a           2148.15       700.38853       YES     YES
    43        a           2152.88       291.40132       YES     YES
    44        a           2204.57       264.84305       YES     YES
    45        a           2251.28       142.22764       YES     YES
$end
```

$[Ta(CO)_7]^+$, q = – 0.7

Method: (RI-)B3LYP-D3(BJ)/def2-TZVPP

Ta	9.35965	4.80257	4.99944
C	9.35393	7.09424	4.99998
C	7.16946	5.05331	4.97848
C	11.54673	5.06835	5.02472
C	9.77319	5.10157	7.12506
C	8.93953	5.10530	2.87725
C	10.19366	3.05006	4.02355
C	8.54114	3.03629	5.96378
O	9.35081	8.21367	4.99995
O	6.04782	5.18324	4.96356
O	12.66743	5.20764	5.04048
O	9.95795	5.32911	8.21883
O	8.75104	5.33562	1.78442
O	10.64209	2.16997	3.47816
O	8.09766	2.14994	6.50320

SCF energy GEOOPT = -850.8375526094 H
ZPE = 140.5 kJ/mol
FREEH energy = 189.17 kJ/mol
FREEH entropy = 0.60754 kJ/mol

$vibrational spectrum

# mode	symmetry	wave number cm**(-1)	IR intensity km/mol	selection rules IR	RAMAN
1		-0.00	0.00000	-	-
2		-0.00	0.00000	-	-
3		0.00	0.00000	-	-
4		0.00	0.00000	-	-
5		0.00	0.00000	-	-
6		0.00	0.00000	-	-
7	a	19.90	0.68063	YES	YES
8	a	48.34	0.00863	YES	YES
9	a	66.16	0.84380	YES	YES
10	a	71.24	0.82262	YES	YES
11	a	75.63	1.89863	YES	YES
12	a	85.69	0.66612	YES	YES
13	a	87.89	0.29413	YES	YES
14	a	88.83	0.67329	YES	YES
15	a	93.34	0.98044	YES	YES
16	a	99.74	0.73311	YES	YES
17	a	105.41	0.03884	YES	YES
18	a	264.21	11.08350	YES	YES
19	a	274.02	14.52051	YES	YES
20	a	304.80	33.48711	YES	YES
21	a	310.64	0.35404	YES	YES
22	a	312.92	21.85371	YES	YES
23	a	331.14	7.27178	YES	YES
24	a	339.15	22.18595	YES	YES
25	a	341.40	0.20684	YES	YES
26	a	343.20	18.22743	YES	YES
27	a	354.58	0.20485	YES	YES
28	a	358.55	11.55897	YES	YES
29	a	397.60	0.38956	YES	YES
30	a	432.06	3.66522	YES	YES
31	a	438.39	2.95909	YES	YES
32	a	439.66	4.06719	YES	YES
33	a	489.03	29.48799	YES	YES
34	a	493.30	13.56477	YES	YES

```
    35        a             504.24         1.51957       YES     YES
    36        a             508.47        37.28517       YES     YES
    37        a             514.33         0.69424       YES     YES
    38        a             522.47        24.19864       YES     YES
    39        a            2111.17      1813.16692       YES     YES
    40        a            2128.77       134.06912       YES     YES
    41        a            2138.72      1664.69267       YES     YES
    42        a            2149.97       705.85164       YES     YES
    43        a            2156.54       334.15812       YES     YES
    44        a            2205.47       268.70316       YES     YES
    45        a            2252.90       140.00838       YES     YES
$end
```

$[Nb(CO)_7]^+$ (C_{3v})

```
Symmetry: c3v (minimum structure)
Method: (RI-)B3LYP-D3(BJ)/def2-TZVPP

Nb        -0.00000        0.00000        0.05556
C          1.03806       -1.79797       -0.60622
C         -0.93066       -1.61195        1.30578
C          1.86132        0.00000        1.30578
C         -0.93066        1.61195        1.30578
C          1.03806        1.79797       -0.60622
C         -2.07612        0.00000       -0.60622
O         -1.39363       -2.41383        1.94406
O         -3.16529        0.00000       -0.90475
O          2.78725        0.00000        1.94406
O         -1.39363        2.41383        1.94406
O          1.58264        2.74122       -0.90475
O          1.58264       -2.74122       -0.90475
C          0.00000        0.00000       -2.07033
O          0.00000        0.00000       -3.20240


SCF energy GEOOPT =  -850.1122641903 H
ZPE =   140.9 kJ/mol
FREEH energy =   189.58 kJ/mol
FREEH entropy =   0.59170 kJ/mol

$vibrational spectrum
#  mode     symmetry     wave number   IR intensity    selection rules
#                         cm**(-1)        km/mol          IR     RAMAN
     1                      -0.00         0.00000         -       -
     2                      -0.00         0.00000         -       -
     3                      -0.00         0.00000         -       -
     4                      -0.00         0.00000         -       -
     5                       0.00         0.00000         -       -
     6                       0.00         0.00000         -       -
     7        e             37.29         1.50688       YES     YES
     8        e             37.29         1.50688       YES     YES
     9        a1            68.49         0.33210       YES     YES
    10        a2            77.21         0.00000       NO      NO
    11        e             80.46         0.01644       YES     YES
    12        e             80.46         0.01644       YES     YES
    13        e             85.87         3.43981       YES     YES
    14        e             85.87         3.43981       YES     YES
    15        a1            95.90         2.39126       YES     YES
    16        e            100.40         0.85465       YES     YES
    17        e            100.40         0.85465       YES     YES
    18        e            264.72        17.09278       YES     YES
```

```
    19        e             264.72        17.09278       YES     YES
    20        a1            297.89        11.60163       YES     YES
    21        e             315.79         0.05518       YES     YES
    22        e             315.79         0.05518       YES     YES
    23        a2            321.58         0.00000       NO      NO
    24        a1            327.56         0.22760       YES     YES
    25        e             337.38        27.51912       YES     YES
    26        e             337.38        27.51912       YES     YES
    27        a1            355.89         2.23135       YES     YES
    28        e             382.62         0.14133       YES     YES
    29        e             382.62         0.14133       YES     YES
    30        a1            412.49        21.96791       YES     YES
    31        e             439.24         0.00291       YES     YES
    32        e             439.24         0.00291       YES     YES
    33        a2            495.94         0.00000       NO      NO
    34        a1            516.87        48.03037       YES     YES
    35        e             517.74        15.23333       YES     YES
    36        e             517.74        15.23333       YES     YES
    37        e             533.90        39.87449       YES     YES
    38        e             533.90        39.87449       YES     YES
    39        a1           2128.79       657.79528       YES     YES
    40        e            2141.93      1166.03976       YES     YES
    41        e            2141.93      1166.03976       YES     YES
    42        a1           2160.88       709.46718       YES     YES
    43        e            2184.04       430.39044       YES     YES
    44        e            2184.04       430.39044       YES     YES
    45        a1           2239.24        63.45465       YES     YES
$end
```

$\underline{[Nb(CO)_7]^+ (C_{2v})}$

```
Symmetry: c2v (transition state)
Method: (RI-)B3LYP-D3(BJ)/def2-TZVPP

Nb          0.00000        0.00000        0.05819
O           2.58823        2.05833        0.45637
O           0.00000        1.94328       -2.57580
O           0.00000        0.00000        3.47167
C           1.70598        1.37281        0.30470
C           1.70598       -1.37281        0.30470
C           0.00000        0.00000        2.35061
C           0.00000        1.24633       -1.68472
O           2.58823       -2.05833        0.45637
O          -2.58823       -2.05833        0.45637
O           0.00000       -1.94328       -2.57580
C          -1.70598       -1.37281        0.30470
C          -1.70598        1.37281        0.30470
C           0.00000       -1.24633       -1.68472
O          -2.58823        2.05833        0.45637

SCF energy GEOOPT = -850.1113594509 H
ZPE =   140.5 kJ/mol
FREEH energy =   187.00 kJ/mol
FREEH entropy =   0.57164 kJ/mol
```

$vibrational spectrum

# mode	symmetry	wave number cm**(-1)	IR intensity km/mol	selection rules IR	RAMAN
1	b2	-36.44	0.00000	YES	YES
2		0.00	0.00000	-	-
3		0.00	0.00000	-	-
4		0.00	0.00000	-	-
5		0.00	0.00000	-	-
6		0.00	0.00000	-	-
7		0.00	0.00000	-	-
8	a2	50.43	0.00000	NO	YES
9	b1	66.90	0.04320	YES	YES
10	b2	70.49	0.29262	YES	YES
11	a1	77.63	0.63145	YES	YES
12	b1	84.61	2.21075	YES	YES
13	a1	89.28	2.08741	YES	YES
14	a2	89.29	0.00000	NO	YES
15	b2	91.44	2.55246	YES	YES
16	b1	93.57	2.41678	YES	YES
17	a1	103.42	0.72243	YES	YES
18	b2	238.01	5.95944	YES	YES
19	a1	275.48	4.87889	YES	YES
20	a2	298.28	0.00000	NO	YES
21	b1	305.30	24.24696	YES	YES
22	b2	305.82	10.75007	YES	YES
23	b1	324.29	24.60909	YES	YES
24	a2	325.01	0.00000	NO	YES
25	a1	330.78	3.41114	YES	YES
26	b2	343.05	3.48237	YES	YES
27	a1	358.15	12.37074	YES	YES
28	b2	376.33	11.58924	YES	YES
29	a2	388.10	0.00000	NO	YES
30	b2	421.39	13.30675	YES	YES
31	b1	432.49	2.47676	YES	YES
32	a1	439.03	2.93242	YES	YES
33	a2	499.02	0.00000	NO	YES
34	b1	505.49	0.06047	YES	YES
35	a1	508.40	45.54771	YES	YES
36	b2	526.70	57.14531	YES	YES
37	a1	530.62	8.81707	YES	YES
38	b1	536.86	51.68336	YES	YES
39	b2	2132.40	699.21187	YES	YES
40	a1	2134.46	1033.63248	YES	YES
41	b1	2151.50	1653.86917	YES	YES
42	b2	2156.06	854.04126	YES	YES
43	a2	2161.71	0.00000	NO	YES
44	a1	2204.80	229.84959	YES	YES
45	a1	2244.44	141.61752	YES	YES

$end

$[Ta(CO)_7]^+$ (C_{3v})

```
Symmetry: c3v (minimum structure)
Method: (RI-)B3LYP-D3(BJ)/def2-TZVPP

Ta        -0.00000        0.00000        0.04764
C          1.04073       -1.80259       -0.60427
C         -0.92264       -1.59807        1.30597
C          1.84529        0.00000        1.30597
C         -0.92264        1.59807        1.30597
C          1.04073        1.80259       -0.60427
C         -2.08146        0.00000       -0.60427
O         -1.38408       -2.39730        1.95052
O         -3.17283        0.00000       -0.89825
O          2.76817        0.00000        1.95052
O         -1.38408        2.39730        1.95052
O          1.58642        2.74775       -0.89825
O          1.58642       -2.74775       -0.89825
C          0.00000        0.00000       -2.08845
O          0.00000        0.00000       -3.22106

SCF energy GEOOPT =  -850.1438968605 H
ZPE =   140.8 kJ/mol
FREEH energy =   189.33 kJ/mol
FREEH entropy =   0.59410 kJ/mol

$vibrational spectrum
#  mode     symmetry     wave number   IR intensity    selection rules
#                         cm**(-1)        km/mol          IR     RAMAN
     1                      -0.00         0.00000         -       -
     2                      -0.00         0.00000         -       -
     3                      -0.00         0.00000         -       -
     4                      -0.00         0.00000         -       -
     5                       0.00         0.00000         -       -
     6                       0.00         0.00000         -       -
     7        e             37.07         1.55363       YES     YES
     8        e             37.07         1.55363       YES     YES
     9        a1            68.79         0.22307       YES     YES
    10        a2            78.63         0.00000       NO      NO
    11        e             82.15         0.24818       YES     YES
    12        e             82.15         0.24818       YES     YES
    13        e             83.20         1.95325       YES     YES
    14        e             83.20         1.95325       YES     YES
    15        a1            93.20         1.31061       YES     YES
    16        e            100.24         0.38695       YES     YES
    17        e            100.24         0.38695       YES     YES
    18        e            272.52        28.41869       YES     YES
    19        e            272.52        28.41869       YES     YES
    20        a1           302.53        20.55272       YES     YES
    21        e            327.73         1.01658       YES     YES
    22        e            327.73         1.01658       YES     YES
    23        e            333.53        27.12914       YES     YES
    24        e            333.53        27.12914       YES     YES
    25        a2           334.05         0.00000       NO      NO
    26        a1           340.33         2.78272       YES     YES
    27        a1           363.61         5.23897       YES     YES
    28        e            386.36         0.67159       YES     YES
    29        e            386.36         0.67159       YES     YES
    30        a1           410.48        24.08437       YES     YES
    31        e            441.11         0.30061       YES     YES
    32        e            441.11         0.30061       YES     YES
    33        a1           500.61        23.54860       YES     YES
```

```
    34        a2            504.72          0.00000       NO      NO
    35        e             509.89         36.08138       YES     YES
    36        e             509.89         36.08138       YES     YES
    37        e             523.56          0.53141       YES     YES
    38        e             523.56          0.53141       YES     YES
    39        a1           2125.15        667.29220       YES     YES
    40        e            2135.06       1255.01911       YES     YES
    41        e            2135.06       1255.01911       YES     YES
    42        a1           2152.05        821.24737       YES     YES
    43        e            2173.68        467.21224       YES     YES
    44        e            2173.68        467.21224       YES     YES
    45        a1           2237.32         55.34699       YES     YES
$end
```

$[Ta(CO)_7]^+$ (C_{2v})

```
Symmetry: c2v (transition state)
Method: (RI-)B3LYP-D3(BJ)/def2-TZVPP

Ta          0.00000        0.00000        0.02692
O           2.58349        2.05775        0.44472
O           0.00000        1.95742       -2.60763
O           0.00000        0.00000        3.42643
C           1.70282        1.37015        0.28521
C           1.70282       -1.37015        0.28521
C           0.00000        0.00000        2.30443
C           0.00000        1.25731       -1.71824
O           2.58349       -2.05775        0.44472
O          -2.58349       -2.05775        0.44472
O           0.00000       -1.95742       -2.60763
C          -1.70282       -1.37015        0.28521
C          -1.70282        1.37015        0.28521
C           0.00000       -1.25731       -1.71824
O          -2.58349        2.05775        0.44472

SCF energy GEOOPT =  -850.1430385989 H
ZPE =   140.4 kJ/mol
FREEH energy =   186.76 kJ/mol
FREEH entropy =   0.57364 kJ/mol

$vibrational spectrum
#  mode     symmetry     wave number   IR intensity    selection rules
#                         cm**(-1)        km/mol          IR     RAMAN
     1        b2            -35.52         0.00000       YES     YES
     2                      -0.00         0.00000         -       -
     3                      -0.00         0.00000         -       -
     4                       0.00         0.00000         -       -
     5                       0.00         0.00000         -       -
     6                       0.00         0.00000         -       -
     7                       0.00         0.00000         -       -
     8        a2            50.81         0.00000       NO      YES
     9        b1            69.03         0.06300       YES     YES
    10        b2            70.51         0.21731       YES     YES
    11        a1            77.84         0.75371       YES     YES
    12        b1            83.28         1.94403       YES     YES
    13        a1            87.72         1.01969       YES     YES
    14        b2            89.91         1.36020       YES     YES
    15        a2            90.11         0.00000       NO      YES
    16        b1            93.19         0.92785       YES     YES
    17        a1           102.65         0.30632       YES     YES
    18        b2           250.77         8.98400       YES     YES
```

```
    19        a1            284.92        12.40125       YES     YES
    20        b1            303.17        51.62960       YES     YES
    21        b2            309.68        19.03791       YES     YES
    22        a2            309.82         0.00000       NO      YES
    23        b1            330.80         8.41550       YES     YES
    24        a2            337.85         0.00000       NO      YES
    25        a1            341.78        13.13920       YES     YES
    26        b2            350.43         8.36102       YES     YES
    27        a1            361.17         8.77935       YES     YES
    28        b2            366.43        11.26904       YES     YES
    29        a2            397.07         0.00000       NO      YES
    30        b2            431.81        13.19801       YES     YES
    31        b1            434.73         0.95793       YES     YES
    32        a1            435.51         6.91113       YES     YES
    33        a1            492.14        30.64027       YES     YES
    34        b1            504.54        12.55754       YES     YES
    35        a2            507.40         0.00000       NO      YES
    36        b2            511.75        33.89141       YES     YES
    37        b1            518.33        22.22829       YES     YES
    38        a1            526.14         0.11461       YES     YES
    39        b2           2128.22       742.93334       YES     YES
    40        a1           2129.65      1098.65591       YES     YES
    41        b1           2142.60      1783.21672       YES     YES
    42        b2           2146.48       921.24890       YES     YES
    43        a2           2152.31         0.00000       NO      YES
    44        a1           2195.90       307.63799       YES     YES
    45        a1           2241.22       118.89295       YES     YES
$end
```

[(*o*-dfb)Nb(CO)$_4$]$^+$ (C$_s$)

```
Symmetry: cs (minimum structure)
Method: (RI-)B3LYP-D3(BJ)/def2-TZVPP

C          0.00674        1.87777        0.70061
C          0.00674        1.87777       -0.70061
C          0.89352        1.04421       -1.41182
H          0.87968        1.06959       -2.49159
C          1.87227        0.31820       -0.69787
H          2.60796       -0.25742       -1.24033
C          1.87227        0.31820        0.69787
H          2.60796       -0.25742        1.24033
C          0.89352        1.04421        1.41182
H          0.87968        1.06959        2.49159
F         -0.82497        2.66606        1.34883
F         -0.82497        2.66606       -1.34883
Nb        -0.39626       -0.55046        0.00000
O         -2.98978       -0.54494        1.96139
O          0.00057       -3.10724        1.96667
O         -2.98978       -0.54494       -1.96139
O          0.00057       -3.10724       -1.96667
C         -0.15582       -2.22339        1.27268
C         -2.09205       -0.56761        1.26877
C         -2.09205       -0.56761       -1.26877
C         -0.15582       -2.22339       -1.27268

SCF energy GEOOPT =  -940.8297511964 H
ZPE =   301.7 kJ/mol
FREEH energy =   347.43 kJ/mol
FREEH entropy =   0.57112 kJ/mol
```

$vibrational spectrum

# mode	symmetry	wave number cm**(-1)	IR intensity km/mol	selection rules IR	RAMAN
1		-0.00	0.00000	-	-
2		-0.00	0.00000	-	-
3		-0.00	0.00000	-	-
4		0.00	0.00000	-	-
5		0.00	0.00000	-	-
6		0.00	0.00000	-	-
7	a"	26.84	1.02698	YES	YES
8	a"	65.97	0.00083	YES	YES
9	a'	67.19	0.28831	YES	YES
10	a"	74.25	0.00737	YES	YES
11	a'	85.99	2.76486	YES	YES
12	a"	94.70	1.36679	YES	YES
13	a'	94.77	1.93211	YES	YES
14	a'	101.00	0.00037	YES	YES
15	a"	158.61	0.74918	YES	YES
16	a'	165.51	0.16726	YES	YES
17	a'	241.41	11.10881	YES	YES
18	a"	273.84	1.58927	YES	YES
19	a'	291.62	0.90670	YES	YES
20	a"	323.32	0.00486	YES	YES
21	a'	338.07	11.23037	YES	YES
22	a'	379.40	0.82759	YES	YES
23	a"	380.60	0.01198	YES	YES
24	a"	389.31	22.44786	YES	YES
25	a'	390.13	18.48613	YES	YES
26	a"	426.72	6.83344	YES	YES
27	a"	431.39	16.69752	YES	YES
28	a'	432.87	27.93564	YES	YES
29	a"	444.36	3.14034	YES	YES
30	a'	515.50	10.07230	YES	YES
31	a"	522.24	15.02994	YES	YES
32	a'	526.26	22.91215	YES	YES
33	a'	544.71	4.47084	YES	YES
34	a"	552.51	16.18176	YES	YES
35	a'	556.84	29.72735	YES	YES
36	a'	568.06	6.39555	YES	YES
37	a"	573.73	3.81258	YES	YES
38	a"	706.07	0.66322	YES	YES
39	a'	773.42	25.17142	YES	YES
40	a'	839.55	23.32806	YES	YES
41	a"	866.43	16.66703	YES	YES
42	a"	906.34	0.37108	YES	YES
43	a'	960.17	5.23403	YES	YES
44	a"	1025.92	0.19671	YES	YES
45	a'	1035.64	0.32995	YES	YES
46	a"	1106.90	5.46811	YES	YES
47	a'	1185.93	7.12272	YES	YES
48	a"	1228.31	13.02379	YES	YES
49	a"	1298.95	20.69882	YES	YES
50	a'	1309.61	91.09288	YES	YES
51	a'	1357.09	7.73774	YES	YES
52	a"	1464.15	28.34371	YES	YES
53	a'	1530.70	188.13161	YES	YES
54	a"	1560.73	12.92875	YES	YES
55	a'	1585.34	178.30326	YES	YES
56	a"	2098.97	1162.46765	YES	YES
57	a'	2099.65	1261.23323	YES	YES
58	a"	2107.58	75.38414	YES	YES
59	a'	2163.13	657.61598	YES	YES
60	a"	3207.83	0.01627	YES	YES

```
    61        a'           3214.23         4.06125       YES     YES
    62        a"           3218.76        31.62663       YES     YES
    63        a'           3222.46        10.02868       YES     YES
$end
```

[(*o*-dfb)Ta(CO)$_4$]$^+$ (C_s)

```
Symmetry: cs (minimum structure)
Method: (RI-)B3LYP-D3(BJ)/def2-TZVPP

C         -1.29036        1.36316       -0.70009
C         -1.29036        1.36316        0.70009
C         -1.35175        0.14502        1.41319
C         -1.57906       -1.05452        0.69742
C         -1.57906       -1.05452       -0.69742
C         -1.35175        0.14502       -1.41319
F         -1.22960        2.50599       -1.34970
F         -1.22960        2.50599        1.34970
Ta         0.66213       -0.12947        0.00000
O          2.54655        1.65796        1.96197
O          2.11239       -2.27055       -1.97420
O          2.11239       -2.27055        1.97420
O          2.54655        1.65796       -1.96197
C          1.63000       -1.51635       -1.27522
C          1.91073        1.02279       -1.26826
C          1.63000       -1.51635        1.27522
C          1.91073        1.02279        1.26826
H         -1.72105       -1.97789        1.23984
H         -1.72105       -1.97789       -1.23984
H         -1.35854        0.17310       -2.49280
H         -1.35854        0.17310        2.49280

SCF energy GEOOPT =  -940.8542230427 H
ZPE =   300.9 kJ/mol
FREEH energy =   346.75 kJ/mol
FREEH entropy =   0.57504 kJ/mol

$vibrational spectrum
#  mode     symmetry     wave number   IR intensity    selection rules
#                         cm**(-1)        km/mol          IR     RAMAN
     1                      -0.00         0.00000        -       -
     2                      -0.00         0.00000        -       -
     3                       0.00         0.00000        -       -
     4                       0.00         0.00000        -       -
     5                       0.00         0.00000        -       -
     6                       0.00         0.00000        -       -
     7        a"            28.44         0.88524       YES     YES
     8        a'            66.45         0.23336       YES     YES
     9        a"            66.56         0.00285       YES     YES
    10        a"            73.15         0.14692       YES     YES
    11        a'            86.53         2.38301       YES     YES
    12        a"            93.63         0.79862       YES     YES
    13        a'            93.95         1.15936       YES     YES
    14        a'           101.96         0.00370       YES     YES
    15        a'           154.23         1.06332       YES     YES
    16        a"           155.02         1.82695       YES     YES
    17        a'           235.39        20.85456       YES     YES
    18        a"           276.12         3.13579       YES     YES
    19        a'           290.79         1.16476       YES     YES
    20        a"           333.71         0.01330       YES     YES
    21        a'           338.44        13.76958       YES     YES
```

```
    22        a"            384.11        41.61233       YES     YES
    23        a'            385.61        33.28673       YES     YES
    24        a'            386.85         7.08794       YES     YES
    25        a"            390.47         0.02977       YES     YES
    26        a"            424.71         6.90668       YES     YES
    27        a'            425.28        10.58428       YES     YES
    28        a"            434.55         1.67086       YES     YES
    29        a"            451.12         0.39266       YES     YES
    30        a'            503.67        24.36858       YES     YES
    31        a"            520.67         4.83690       YES     YES
    32        a'            522.03         8.37938       YES     YES
    33        a'            528.27         4.69396       YES     YES
    34        a'            546.83         4.44387       YES     YES
    35        a"            548.38         9.40849       YES     YES
    36        a'            566.23         5.28736       YES     YES
    37        a"            573.45         3.61776       YES     YES
    38        a"            697.36         1.13987       YES     YES
    39        a'            772.66        26.45705       YES     YES
    40        a'            839.30        17.75478       YES     YES
    41        a"            864.06        16.00482       YES     YES
    42        a"            903.03         0.89156       YES     YES
    43        a'            951.37         9.61802       YES     YES
    44        a"           1023.27         0.23098       YES     YES
    45        a'           1034.16         0.14602       YES     YES
    46        a"           1102.59         5.47453       YES     YES
    47        a'           1184.85         8.59891       YES     YES
    48        a"           1223.74        12.11355       YES     YES
    49        a"           1297.03        20.79064       YES     YES
    50        a'           1307.03        84.33124       YES     YES
    51        a'           1355.38        10.74240       YES     YES
    52        a"           1459.30        27.91112       YES     YES
    53        a'           1528.97       175.91435       YES     YES
    54        a"           1549.78        13.96770       YES     YES
    55        a'           1583.21       221.84884       YES     YES
    56        a"           2091.29      1219.68948       YES     YES
    57        a'           2091.90      1338.72264       YES     YES
    58        a"           2099.37        86.28846       YES     YES
    59        a'           2159.07       692.73587       YES     YES
    60        a"           3207.63         0.10022       YES     YES
    61        a'           3214.73         5.56972       YES     YES
    62        a"           3219.71        34.80041       YES     YES
    63        a'           3222.47        11.16646       YES     YES
$end
```

$Ta_2(CO)_{12}(D_2)$

```
Symmetry: d2 (minimum structure)
Method: (RI-)B3LYP-D3(BJ)/def2-TZVPP

Ta          0.00000        0.00000       -1.69629
O          -1.51454       -2.83889       -0.94814
C          -0.96006       -1.86950       -1.17990
Ta          0.00000        0.00000        1.69629
O          -3.16353        0.86643       -1.33510
C          -2.07071        0.56979       -1.46067
C           0.36956       -1.20318       -3.39827
O           0.59379       -1.84269       -4.31799
O          -0.59379        1.84269       -4.31799
C          -0.36956        1.20318       -3.39827
C           0.96006        1.86950       -1.17990
O           1.51454        2.83889       -0.94814
```

O	3.16353	-0.86643	-1.33510
C	2.07071	-0.56979	-1.46067
O	-3.16353	-0.86643	1.33510
C	-2.07071	-0.56979	1.46067
C	0.36956	1.20318	3.39827
O	0.59379	1.84269	4.31799
C	-0.36956	-1.20318	3.39827
O	-0.59379	-1.84269	4.31799
C	2.07071	0.56979	1.46067
O	3.16353	0.86643	1.33510
C	-0.96006	1.86950	1.17990
O	-1.51454	2.83889	0.94814
C	0.96006	-1.86950	1.17990
O	1.51454	-2.83889	0.94814

SCF energy GEOOPT = -1474.154357504 H
ZPE = 243.5 kJ/mol
FREEH energy = 328.84 kJ/mol
FREEH entropy = 0.88358 kJ/mol

$vibrational spectrum

# mode	symmetry	wave number cm**(-1)	IR intensity km/mol	selection rules IR	RAMAN
1		-0.00	0.00000	-	-
2		-0.00	0.00000	-	-
3		0.00	0.00000	-	-
4		0.00	0.00000	-	-
5		0.00	0.00000	-	-
6		0.00	0.00000	-	-
7	b1	29.34	2.64620	YES	YES
8	b2	36.98	0.45294	YES	YES
9	a	41.83	0.00000	NO	YES
10	b3	50.80	0.01504	YES	YES
11	a	55.21	0.00000	NO	YES
12	b2	59.61	0.05449	YES	YES
13	b3	60.93	0.01295	YES	YES
14	b3	69.98	0.01738	YES	YES
15	b2	76.28	1.48016	YES	YES
16	a	77.92	0.00000	NO	YES
17	b1	79.07	1.15581	YES	YES
18	b3	80.45	2.94422	YES	YES
19	a	82.43	0.00000	NO	YES
20	b1	85.40	0.07405	YES	YES
21	b2	86.35	0.17893	YES	YES
22	b2	88.35	0.20723	YES	YES
23	b1	93.67	0.00044	YES	YES
24	b3	93.82	0.00040	YES	YES
25	a	99.29	0.00000	NO	YES
26	b1	99.86	1.03132	YES	YES
27	b2	102.59	0.19453	YES	YES
28	a	103.91	0.00000	NO	YES
29	b3	114.22	0.12982	YES	YES
30	a	114.72	0.00000	NO	YES
31	b1	313.09	28.99354	YES	YES
32	a	321.88	0.00000	NO	YES
33	b2	340.12	7.44296	YES	YES
34	b3	345.25	25.23491	YES	YES
35	b1	353.57	0.34238	YES	YES
36	a	354.75	0.00000	NO	YES
37	b3	356.44	16.89290	YES	YES
38	b2	358.91	37.68565	YES	YES
39	b1	363.04	2.62463	YES	YES
40	a	366.25	0.00000	NO	YES

```
    41        b3           371.58         4.10647       YES     YES
    42        b2           376.36        20.23833       YES     YES
    43        a            378.50         0.00000       NO      YES
    44        b1           381.56         8.15120       YES     YES
    45        b2           390.43         2.48144       YES     YES
    46        a            394.34         0.00000       NO      YES
    47        b3           394.83         4.12813       YES     YES
    48        b1           396.21        19.94043       YES     YES
    49        b3           398.90         0.19609       YES     YES
    50        b2           400.70         5.14044       YES     YES
    51        b3           442.46         5.81352       YES     YES
    52        a            454.17         0.00000       NO      YES
    53        b1           458.01        20.79788       YES     YES
    54        b2           463.20         2.08450       YES     YES
    55        b3           488.94        15.71830       YES     YES
    56        b2           490.54        16.66200       YES     YES
    57        b1           492.03       146.38378       YES     YES
    58        a            500.19         0.00000       NO      YES
    59        b1           509.27        53.11905       YES     YES
    60        a            521.79         0.00000       NO      YES
    61        b1           528.27         2.44685       YES     YES
    62        a            528.56         0.00000       NO      YES
    63        b2           532.35        24.72483       YES     YES
    64        b3           533.32        19.78719       YES     YES
    65        b2           534.83        18.49154       YES     YES
    66        b3           535.87         0.00442       YES     YES
    67        b3          2027.27        11.37526       YES     YES
    68        b2          2033.86       179.62684       YES     YES
    69        b1          2038.69      1333.35403       YES     YES
    70        b2          2045.02       998.82756       YES     YES
    71        b3          2045.83       105.23241       YES     YES
    72        b1          2057.32       253.76583       YES     YES
    73        a           2058.04         0.00000       NO      YES
    74        a           2061.07         0.00000       NO      YES
    75        b2          2070.61      2459.90455       YES     YES
    76        b3          2082.51      3084.64659       YES     YES
    77        b1          2111.62      1681.67608       YES     YES
    78        a           2166.05         0.00000       NO      YES
$end
```

Optimized at the (RI-)BP86-D3BJ/def-SV(P) level of theory.

$[Ag_6\{Nb(CO)_6\}_4]^{2+}$ (T)

```
Symmetry: t (minimum structure)
Method: (RI-)bp86-D3(BJ)/def-SV(P)

Ag          0.00000        2.07198       -0.00000
Ag         -0.00000        0.00000        2.07198
Ag          0.00000       -0.00000       -2.07198
Ag         -2.07198        0.00000        0.00000
Ag          2.07198       -0.00000       -0.00000
Ag         -0.00000       -2.07198        0.00000
Nb         -2.09597        2.09597       -2.09597
Nb          2.09597       -2.09597       -2.09597
Nb          2.09597        2.09597        2.09597
O           0.89635       -2.65534        3.35720
Nb         -2.09597       -2.09597        2.09597
O          -1.94410       -5.37044        2.60784
O          -3.35720        0.89635        2.65534
```

O	-2.65534	-3.35720	-0.89635
O	5.37044	-2.60784	-1.94410
O	2.65534	-3.35720	0.89635
O	0.89635	2.65534	-3.35720
O	-3.35720	-0.89635	-2.65534
O	-2.60784	1.94410	-5.37044
O	-2.65534	3.35720	0.89635
O	-5.37044	2.60784	-1.94410
O	-0.89635	-2.65534	-3.35720
O	-5.37044	-2.60784	1.94410
O	3.35720	0.89635	-2.65534
O	1.94410	5.37044	2.60784
O	2.60784	-1.94410	-5.37044
O	-2.60784	-1.94410	5.37044
O	2.60784	1.94410	5.37044
O	-0.89635	2.65534	3.35720
O	1.94410	-5.37044	-2.60784
O	2.65534	3.35720	-0.89635
O	3.35720	-0.89635	2.65534
O	5.37044	2.60784	1.94410
O	-1.94410	5.37044	-2.60784
C	-0.07108	2.31664	-2.80127
C	-2.42367	-1.98889	4.23983
C	-4.23983	2.42367	-1.98889
C	4.23983	-2.42367	-1.98889
C	2.80127	-0.07108	-2.31664
C	-2.31664	2.80127	-0.07108
C	0.07108	-2.31664	-2.80127
C	-2.80127	0.07108	-2.31664
C	-2.80127	-0.07108	2.31664
C	-2.42367	1.98889	-4.23983
C	-4.23983	-2.42367	1.98889
C	-0.07108	-2.31664	2.80127
C	1.98889	4.23983	2.42367
C	2.80127	0.07108	2.31664
C	2.31664	-2.80127	-0.07108
C	-2.31664	-2.80127	0.07108
C	2.42367	-1.98889	-4.23983
C	0.07108	2.31664	2.80127
C	-1.98889	4.23983	-2.42367
C	1.98889	-4.23983	-2.42367
C	2.31664	2.80127	0.07108
C	2.42367	1.98889	4.23983
C	4.23983	2.42367	1.98889
C	-1.98889	-4.23983	2.42367

SCF energy GEOOPT = -3829.451095701 H
ZPE = 490.7 kJ/mol
FREEH energy = 703.17 kJ/mol
FREEH entropy = 1.87815 kJ/mol

$vibrational spectrum

# mode	symmetry	wave number cm**(-1)	IR intensity km/mol	selection rules IR	RAMAN
1		-0.00	0.00000	-	-
2		-0.00	0.00000	-	-
3		0.00	0.00000	-	-
4		0.00	0.00000	-	-
5		0.00	0.00000	-	-
6		0.00	0.00000	-	-
7	e	23.16	0.00000	NO	YES
8	e	23.16	0.00000	NO	YES
9	t	26.67	0.05788	YES	YES

10	t	26.67	0.05786	YES	YES
11	t	26.67	0.05785	YES	YES
12	e	28.38	0.00000	NO	YES
13	t	33.28	0.00811	YES	YES
14	t	33.28	0.00810	YES	YES
15	t	33.28	0.00807	YES	YES
16	t	36.58	0.04753	YES	YES
17	t	36.58	0.04754	YES	YES
18	t	36.58	0.04751	YES	YES
19	t	48.42	0.01260	YES	YES
20	t	48.42	0.01259	YES	YES
21	t	48.42	0.01258	YES	YES
22	e	48.57	0.00000	NO	YES
23	e	48.57	0.00000	NO	YES
24	t	53.82	0.42885	YES	YES
25	t	53.82	0.42888	YES	YES
26	t	53.82	0.42885	YES	YES
27	e	56.12	0.00000	NO	YES
28	e	56.12	0.00000	NO	YES
29	t	62.72	0.45028	YES	YES
30	t	62.72	0.45021	YES	YES
31	t	62.72	0.45020	YES	YES
32	e	70.26	0.00000	NO	YES
33	t	74.69	0.00334	YES	YES
34	t	74.69	0.00334	YES	YES
35	t	74.69	0.00335	YES	YES
36	e	75.13	0.00000	NO	YES
37	e	77.34	0.00000	NO	YES
38	e	77.34	0.00000	NO	YES
39	t	77.98	0.05014	YES	YES
40	t	77.98	0.05016	YES	YES
41	t	77.98	0.05018	YES	YES
42	t	80.85	0.00028	YES	YES
43	t	80.85	0.00029	YES	YES
44	t	80.85	0.00029	YES	YES
45	t	86.32	1.11109	YES	YES
46	t	86.32	1.11133	YES	YES
47	t	86.32	1.11128	YES	YES
48	t	91.78	0.65241	YES	YES
49	t	91.78	0.65260	YES	YES
50	t	91.78	0.65237	YES	YES
51	e	95.35	0.00000	NO	YES
52	e	95.35	0.00000	NO	YES
53	t	99.01	0.22585	YES	YES
54	t	99.01	0.22586	YES	YES
55	t	99.01	0.22579	YES	YES
56	t	99.86	0.04735	YES	YES
57	t	99.86	0.04731	YES	YES
58	t	99.86	0.04727	YES	YES
59	e	115.84	0.00000	NO	YES
60	t	116.96	0.04743	YES	YES
61	t	116.96	0.04744	YES	YES
62	t	116.96	0.04743	YES	YES
63	e	123.87	0.00000	NO	YES
64	e	129.04	0.00000	NO	YES
65	e	129.04	0.00000	NO	YES
66	t	132.18	0.13585	YES	YES
67	t	132.18	0.13591	YES	YES
68	t	132.18	0.13589	YES	YES
69	t	138.63	0.35018	YES	YES
70	t	138.63	0.35021	YES	YES
71	t	138.63	0.35024	YES	YES
72	t	149.55	0.00223	YES	YES

73	t	149.55	0.00224	YES	YES
74	t	149.55	0.00223	YES	YES
75	e	150.01	0.00000	NO	YES
76	t	167.08	0.60798	YES	YES
77	t	167.08	0.60798	YES	YES
78	t	167.08	0.60798	YES	YES
79	e	320.12	0.00000	NO	YES
80	e	320.12	0.00000	NO	YES
81	t	320.53	0.00160	YES	YES
82	t	320.53	0.00158	YES	YES
83	t	320.53	0.00161	YES	YES
84	t	322.20	0.70057	YES	YES
85	t	322.20	0.70070	YES	YES
86	t	322.20	0.70075	YES	YES
87	t	337.39	0.06469	YES	YES
88	t	337.39	0.06454	YES	YES
89	t	337.39	0.06455	YES	YES
90	e	337.93	0.00000	NO	YES
91	t	338.05	0.00038	YES	YES
92	t	338.05	0.00044	YES	YES
93	t	338.05	0.00039	YES	YES
94	t	338.85	1.06172	YES	YES
95	t	338.85	1.06074	YES	YES
96	t	338.85	1.06047	YES	YES
97	e	339.01	0.00000	NO	YES
98	e	339.48	0.00000	NO	YES
99	e	339.48	0.00000	NO	YES
100	t	339.95	31.33306	YES	YES
101	t	339.95	31.33238	YES	YES
102	t	339.95	31.33188	YES	YES
103	t	376.76	75.84350	YES	YES
104	t	376.76	75.84388	YES	YES
105	t	376.76	75.84412	YES	YES
106	e	381.46	0.00000	NO	YES
107	e	386.49	0.00000	NO	YES
108	e	386.49	0.00000	NO	YES
109	t	388.07	3.93404	YES	YES
110	t	388.07	3.93748	YES	YES
111	t	388.07	3.93492	YES	YES
112	t	393.10	13.82224	YES	YES
113	t	393.10	13.82037	YES	YES
114	t	393.10	13.82423	YES	YES
115	t	438.27	0.48831	YES	YES
116	t	438.27	0.48878	YES	YES
117	t	438.27	0.48851	YES	YES
118	t	440.14	8.22334	YES	YES
119	t	440.14	8.22283	YES	YES
120	t	440.14	8.22351	YES	YES
121	e	440.54	0.00000	NO	YES
122	e	440.54	0.00000	NO	YES
123	t	451.89	4.39435	YES	YES
124	t	451.89	4.39412	YES	YES
125	t	451.89	4.39441	YES	YES
126	e	455.03	0.00000	NO	YES
127	t	460.77	0.01554	YES	YES
128	t	460.77	0.01545	YES	YES
129	t	460.77	0.01563	YES	YES
130	e	465.10	0.00000	NO	YES
131	e	465.10	0.00000	NO	YES
132	e	465.50	0.00000	NO	YES
133	t	465.77	3.22244	YES	YES
134	t	465.77	3.22373	YES	YES
135	t	465.77	3.22083	YES	YES

```
     136        t             466.93        15.63359       YES     YES
     137        t             466.93        15.63431       YES     YES
     138        t             466.93        15.63328       YES     YES
     139        t             527.05       288.41019       YES     YES
     140        t             527.05       288.43480       YES     YES
     141        t             527.05       288.43999       YES     YES
     142        t             533.40         2.45691       YES     YES
     143        t             533.40         2.45502       YES     YES
     144        t             533.40         2.45703       YES     YES
     145        e             534.88         0.00000       NO      YES
     146        e             534.88         0.00000       NO      YES
     147        t             536.55       102.39177       YES     YES
     148        t             536.55       102.37067       YES     YES
     149        t             536.55       102.36449       YES     YES
     150        e             537.89         0.00000       NO      YES
     151        t            1935.03        27.55850       YES     YES
     152        t            1935.03        27.55810       YES     YES
     153        t            1935.03        27.55814       YES     YES
     154        e            1935.16         0.00000       NO      YES
     155        e            1935.16         0.00000       NO      YES
     156        t            1955.41       394.83511       YES     YES
     157        t            1955.41       394.82841       YES     YES
     158        t            1955.41       394.82993       YES     YES
     159        t            1974.84       737.65181       YES     YES
     160        t            1974.84       737.64996       YES     YES
     161        t            1974.84       737.64476       YES     YES
     162        a            1979.72         0.00000       NO      YES
     163        t            2090.91         5.29112       YES     YES
     164        t            2090.91         5.29115       YES     YES
     165        t            2090.91         5.29113       YES     YES
     166        t            2094.63      1029.80607       YES     YES
     167        t            2094.63      1029.80581       YES     YES
     168        t            2094.63      1029.80587       YES     YES
     169        e            2094.89         0.00000       NO      YES
     170        e            2094.89         0.00000       NO      YES
     171        t            2117.46      3023.55447       YES     YES
     172        t            2117.46      3023.55432       YES     YES
     173        t            2117.46      3023.55509       YES     YES
     174        a            2139.97         0.00000       NO      YES
 $end
```

14 References to the Supporting Materials

56. Meier, S. C. *et al.* From an Easily Accessible Pentacarbonylcobalt(I) Salt to Piano-Stool Cations (arene)$Co(CO)_2$. *Chem. Eur. J.* **23,** 14658–14664 (2017).
57. Krossing, I. & Reisinger, A. Chemistry with weakly-coordinating fluorinated alkoxyaluminate anions. Gas phase cations in condensed phases? *Coord. Chem. Rev.* **250,** 2721–2744 (2006).
58. Herrmann, W. A. ed. *Synthetic methods of organometallic and inorganic chemistry. Transition Metals* (Thieme, Stuttgart [u.a.], 2000).
59. Sheldrick, G. M. SHELXT - integrated space-group and crystal-structure determination. *Acta Cryst. A* **71,** 3–8 (2015).
60. Sheldrick, G. M. A short history of SHELX. *Acta Cryst. A* **64,** 112–122 (2008).
61. Sheldrick, G. M. Crystal structure refinement with SHELXL. *Acta crystallographica. Section C, Structural chemistry* **71,** 3–8 (2015).
62. Hübschle, C. B., Sheldrick, G. M. & Dittrich, B. ShelXle. A Qt graphical user interface for SHELXL. *J. Appl. Crystallogr.* **44,** 1281–1284 (2011).
63. Krause, L., Herbst-Irmer, R., Sheldrick, G. M. & Stalke, D. Comparison of silver and molybdenum microfocus X-ray sources for single-crystal structure determination. *J. Appl. Crystallogr.* **48,** 3–10 (2015).
64. Kratzert, D., Holstein, J. J. & Krossing, I. DSR. Enhanced modelling and refinement of disordered structures with SHELXL. *J. Appl. Crystallogr.* **48,** 933–938 (2015).
65. Kratzert, D. & Krossing, I. Recent improvements in DSR. *J. Appl. Crystallogr.* **51,** 928–934 (2018).
66. Dolomanov, O. V., Bourhis, L. J., Gildea, R. J., Howard, J. A. K. & Puschmann, H. OLEX2. A complete structure solution, refinement and analysis program. *J. Appl. Crystallogr.* **42,** 339–341 (2009).
67. Treutler, O. & Ahlrichs, R. Efficient molecular numerical integration schemes. *J. Chem. Phys.* **102,** 346–354 (1995).
68. Arnim, M. von & Ahlrichs, R. Performance of parallel TURBOMOLE for density functional calculations. *J. Comput. Chem.* **19,** 1746–1757 (1998).
69. Neese, F. The ORCA program system. *WIREs Comput Mol Sci* **2,** 73–78 (2012).
70. Becke, A. D. A new mixing of Hartree–Fock and local density-functional theories. *J. Chem. Phys.* **98,** 1372–1377 (1993).
71. Becke, A. D. Density-functional thermochemistry. III. The role of exact exchange. *J. Chem. Phys.* **98,** 5648–5652 (1993).
72. Lee, C., Yang, W. & Parr, R. G. Development of the Colle-Salvetti correlation-energy formula into a functional of the electron density. *Phys. Rev. B* **37,** 785–789 (1988).
73. Ahlrichs, R. Efficient evaluation of three-center two-electron integrals over Gaussian functions. *Phys. Chem. Chem. Phys.* **6,** 5119 (2004).

74. Sierka, M., Hogekamp, A. & Ahlrichs, R. Fast evaluation of the Coulomb potential for electron densities using multipole accelerated resolution of identity approximation. *J. Chem. Phys.* **118,** 9136–9148 (2003).

75. Weigend, F. Accurate Coulomb-fitting basis sets for H to Rn. *Phys. Chem. Chem. Phys.* **8,** 1057–1065 (2006).

76. Weigend, F. & Ahlrichs, R. Balanced basis sets of split valence, triple zeta valence and quadruple zeta valence quality for H to Rn. Design and assessment of accuracy. *Phys. Chem. Chem. Phys.* **7,** 3297–3305 (2005).

77. Grimme, S., Ehrlich, S. & Goerigk, L. Effect of the damping function in dispersion corrected density functional theory. *J. Comput. Chem.* **32,** 1456–1465 (2011).

78. Grimme, S., Antony, J., Ehrlich, S. & Krieg, H. A consistent and accurate ab initio parametrization of density functional dispersion correction (DFT-D) for the 94 elements H-Pu. *J. Chem. Phys.* **132,** 154104 (2010).

79. Deglmann, P., Furche, F. & Ahlrichs, R. An efficient implementation of second analytical derivatives for density functional methods. *Chem. Phys. Lett.* **362,** 511–518 (2002).

80. Andrae, D., Huermann, U., Dolg, M., Stoll, H. & Preu, H. Energy-adjusted *ab initio* pseudopotentials for the second and third row transition elements. *Theoret. Chim. Acta* **77,** 123–141 (1990).

81. Klopper, W. & Luthi, H. P. The MP2 limit correction applied to coupled cluster calculations of the electronic dissociation energies of the hydrogen fluoride and water dimers. *Mol. Phys.* **96,** 559–570 (1999).

82. Boese, A. D., Martin, J. M. L. & Klopper, W. Basis set limit coupled cluster study of h-bonded systems and assessment of more approximate methods. *J. Phys. Chem. A* **111,** 11122–11133 (2007).

83. Rappoport, D. & Furche, F. Lagrangian approach to molecular vibrational Raman intensities using time-dependent hybrid density functional theory. *J. Chem. Phys.* **126,** 201104 (2007).

84. Furche, F. & Rappoport, D. Density functional methods for excited states. Equilibrium structure and electronic spectra. *Theor. Comput. Chem.,* 93–128 (2005).

85. Perdew, J. P. Density-functional approximation for the correlation energy of the inhomogeneous electron gas. *Phys. Rev. B* **33,** 8822–8824 (1986).

86. Perdew, J. P. Erratum. Density-functional approximation for the correlation energy of the inhomogeneous electron gas. *Phys. Rev. B* **34,** 7406 (1986).

87. Bondi, A. van der Waals Volumes and Radii. *J. Phys. Chem.* **68,** 441–451 (1964).